University of South-Eastern Norway

www.usn.no

FMH606 Master's Thesis 2022

Masters in Process technology

Evaluate the fire suppression parameters using FDS

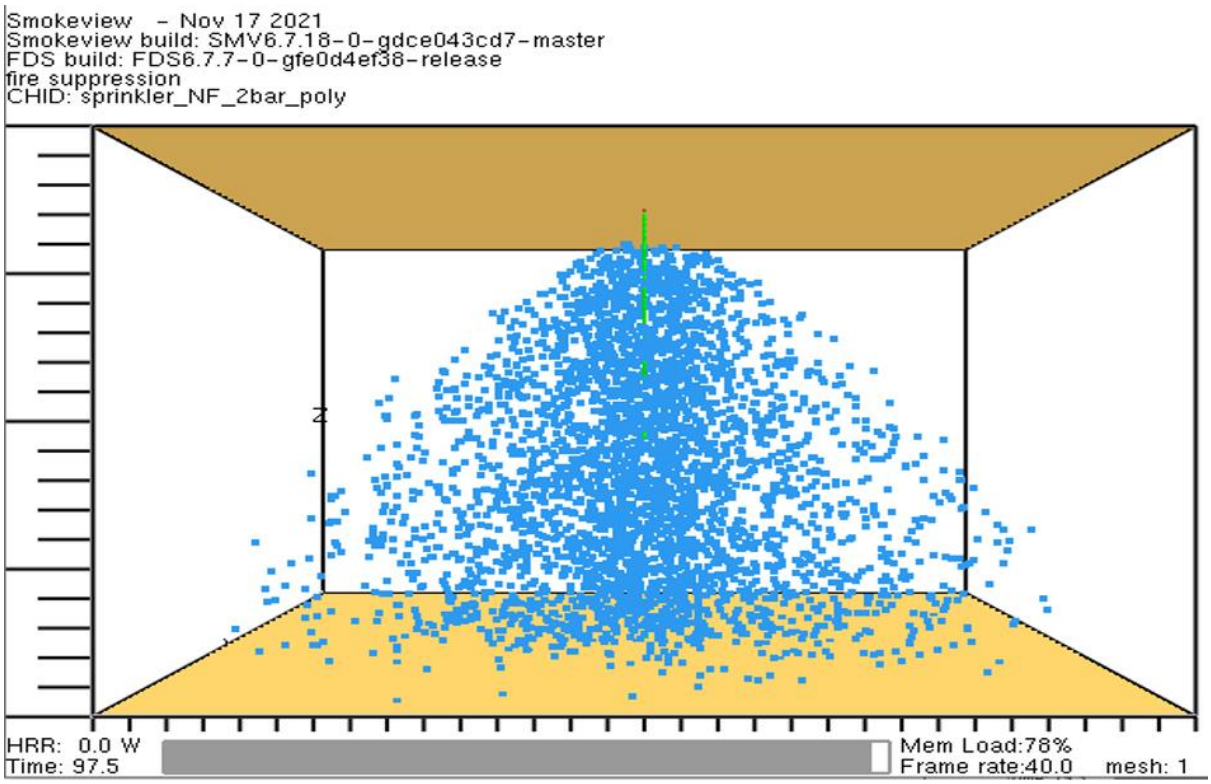

Rajath Ramachandran

University of South-Eastern Norway

www.usn.no

Course: FMH606 Master's Thesis, 2022

Title: Evaluate the spray models using Fire Dynamic Simulator (FDS)

Number of pages: 77

Keywords: CFD, FDS, Droplet Size Distribution, Velocity Distribution, Droplet Number Concentration, Spray pattern, Monodisperse, Polydisperse

Student: Rajath Ramachandran

Supervisor: Dr. Joachim Lundberg

External partner: Danfoss Fire Safety A/S

Summary:

It takes money, time, and energy to construct a fire and spray experimental rig. Due to advancement in technological development, it is easy to illustrate the experiment in computer simulation, especially by coding. The mist spray nozzle and sprinkler spray deluge nozzle are being coded and simulated using Fire Dynamic Simulator, (FDS) developed by National Institute of standards in technology (NIST). FDS is a Large Eddy Simulation (LES) model to represent turbulence. The liquid droplets are being injected into the spray nozzle using Lagrangian particles. The scenario is simulated under, presence and absence of fire and compare monodisperse with polydisperse spray under uniform spray condition. The simulations are simulated under 2 bar, 5 bar and 8 bar of pressure for deluge. 100 bar pressure for mist nozzle is simulated under presence and absence of fire. This study provides the study of suppression parameters such as number concentration, droplet diameter and velocity distribution. A grid sensitivity analysis is performed for improving the results. So, 10 cm and 5 cm has been chosen for this analysis and few scenarios were investigated to show the result comparison and accuracy. The modified geometry is modelled, and simulation was run to see improvements. The main difference was spotted that SMD gave 63 % in the simulation having default particles droplets per second & coarse grid. 100% diameter size distribution is achieved in the modified geometry. Upon analyzing the behavior, the user can get a sound idea on suppression parameters and use the fire suppression system according to the applications.

Acknowledgements

I would like to express my profound gratitude to Associate Professor Dr. Joachim Lundberg for his guidance, commitment, and dedication for making this project come to a conclusive end. Though I had personal issues at the time of my thesis, Dr. Lundberg supported me morally for which I am unforgettable and thankful for his support.

USN, IT supported me well by providing an individual desktop for running my simulations.

I would like to express my sincere appreciation to Miss. Kumarawela & Mr. Wijesekara and to guide me in FDS to support me for this project. Finally, I would like to thank FDS forum scholars and users who gave me right logical advice to arrive the result.

Dedicated to my beloved family.

Contents

Preface

This master thesis topic has been carried out to fulfil the partial requirement for master study program in Process technology at University of South-Eastern Norway. This is a novel topic to understand the behavior of suppression parameters under presence and absence of fire conditions. An intensive literature study has been performed for this thesis. Learning new software FDS was a quite challenge but still it is promising. Grid sensitivity analysis has been performed to show the difference in results from coarse grid. The report structure follows the USN standard template. Results and further works have been expressed in this master thesis.

Porsgrunn, 08/05/2022

Rajath Ramachandran

Contents

Contents

Contents

Nomenclature

Acronyms

CFD – Computational Fluid Dynamics

NIST– National Institute of Standard in Technology

FDS – Fire Dynamics Simulator

PIV – Particle Image Velocimetry

PDA– Phase Doppler Anemometry

PDPA– Phase Doppler Particle Analysis

PMMA– Polymethyl Methacrylate

EDC– Eddy Dissipation Concept

LES– Large Eddy Simulation

DSD– Droplet Size Distribution

CNF– Cumulative Number Fraction

CVF– Cumulative Volume Fraction

CDF– Cumulative Distribution Function

HRRPUA– Heat Release Rate Per Unit Area

HRRPUV– Heat Release Rate Per Unit Volume

MPF– Multiple Pool Fire

VMD– Volume Median Diameter

SMD– Sauter Mean Diameter

SPF– Single Pool Fire

WMFSS– Water Mist Fire Suppression System

DSD– Droplet Size Distribution

Dimensionless Numbers

Re – Reynolds Number

We – Weber number

Latin Characters	**Units**
g – Gravitational acceleration	$\mathrm{m/s^2}$
Q – Water Flux	$\mathrm{kg/m^2.min}$
u – Velocity vector	$\mathrm{m/s}$
u – Particle velocity	$\mathrm{m/s}$

$p-$ Pressure	bar
$\rho-$ Density	kg/m^3
$\tau-$ viscosity	$N.s/m^2$
$Z-$ mixture fraction	[-]
$\dot{q}'''_F-$ Heat release rate per unit volume	$KW/m^3\backslash$
$\dot{q}''_F-$ Heat release rate per unit volume	KW/m^2
$A_{p,s}-$ Area of liquid droplet	m^2
C_d- drag coefficient	[-]
$\theta-$ Spray Angle	degrees
$\mu(T)-$ Dynamic viscosity with refence to the temperature	$kg/m.s$

1 Introduction

1.1 Background to the thesis

In the field of firefighting, safety industry the halon was widely used as a fire suppression agent. This agent was banned due to its unfriendly nature to the environment. Thus, water was introduced as a fire suppression agent. Water mist and deluge (sprinkler) systems are vital and economical to use in industry, offshore sites, domestic buildings, and other general commercial structures. The effectiveness of these fire suppression system is the major topic of discussion in the field.

The effectiveness of the fire suppression systems can be done by conducting experiments. But conducting real time experiments demands more funds, time, risk, and manpower as well. To mitigate these factors Computational Fluid Dynamics (CFD) analyst started to use Fire Dynamic Simulator (FDS) by NIST. FDS was designed to simulate thermally driven flows within the buildings and uses the simplest rectilinear numerical grid. FDS is a Large Eddy Simulation (LES) model and prefers uniform meshing. In FDS the water is represented by Lagrangian particles. In this thesis, the sprinkler and mist suppression systems have been used through FDS to calculate the suppression parameters like droplet size distribution, number concentration distribution and velocity distribution.

The thesis explains the physics of the droplets in the gas phase. The spray is described by orifice diameter of the spray nozzle or sprinkler and spray angle. The flow properties of the spray are also one of the major fire suppression efficiency influencers. The small droplets follow the gas flow, evaporate quickly cool the fire gases [1].

1.1 Research objectives

1) Literature study on spray suppression using sprinkler spray and mist.
2) Develop a setup for a general fire in FDS using input from Danfoss.
3) Evaluate suppression parameters from simplified parameters.
4) Evaluate suppression parameters from detailed characteristics provided by Danfoss or USN.

These objectives are set to be achieved in the order they are presented in. This project is based on both deluge and mist suppression system. The approaches used in this thesis to study the simulation results upon suppression parameters like number concentration distributed radially, droplet size distribution and mean diameter of droplet, there are still some shortcomings in the research which will be discussed in the later chapters.

The water medium velocity deluge nozzle Tyco MV34-110 and HNMP-5-1.19-00 water nozzle properties were used in FDS, and simulations were performed using digitally simulated Phase Doppler Particle Analyzer (PDPA) used to measure the required quantities as output.

1.2 Approach to the task

An intensive literature review has been carried out for this thesis. And several simulations have been carried to reach to an optimized solution and comparison. The simulations have been performed using the software, Fire Dynamic Simulator (FDS) which was built by NIST. The list of simulations has been mentioned below. Lundberg et al [2] has used the gauge pressure as 2 bar (g), 5bar (g) and 8bar (g) for his experiments. But for simplification in this thesis gauge pressure were assumed as absolute pressure respectively.

1) Simulation of monodisperse water mist spray with 100 bar pressure with and without fire.
2) Simulation of polydisperse water mist spray with 100 bar pressures with and without fire.
3) Simulations of monodisperse water deluge spray with 2 bar, 5 bar and 8 bar having no fire.
4) Simulations of monodisperse water deluge spray with 2 bar, 5 bar and 8 bar having fire.
5) Simulation for grid sensitivity analysis for both water mist and sprinkler deluge spray.

The outcome of these simulations gives an overview of the measurement of droplet size distribution, velocity of the particles and number concentration of droplets using PDPA Phase Doppler Particle Analysis in various scenario. The HRRPUA value is 4000 KW/m^2 taken as an assumption for fire scenario.

2 Previous research works

There have been several studies regarding the sprinkler and mist studies for measuring the droplet size distribution, water flux and droplet velocity for assessing the fire suppression. A brief empirical review is mentioned in this chapter. This chapter consist of measurement techniques for measuring the velocity and droplet size. There are several techniques available for measuring particle size of water droplets using both optical and mechanical methods. However, due to complexness nature of mechanical methods researchers are now using optical methods for measuring the parameters. Husted [10] used Particle Image Velocimetry (PIV), Phase Doppler Anemometry (PDA) and a high steed camera for measuring on two high pressure water mist nozzles. After several research PDA is considered as suitable measurement technique. Lundberg [1] has conducted full scale experiment on measuring velocity and droplet size in water spray using laser-based shadow-imaging technique by a high-speed camera with a help of laser. The outcome of research provided experimental data of droplet size and velocity distribution for fire nozzle. The main parameter for measuring the suppression parameter is "K – factor".

2.1 Some previous experimental works

Using PDPA Fu, Sojka, and Sivathanu [3] mapped velocity and size of the droplet using varied mass flow rate to analyze the buoyancy and evaporation on droplet trajectory. The line diagram of this experiment is mentioned in the Figure 2.1

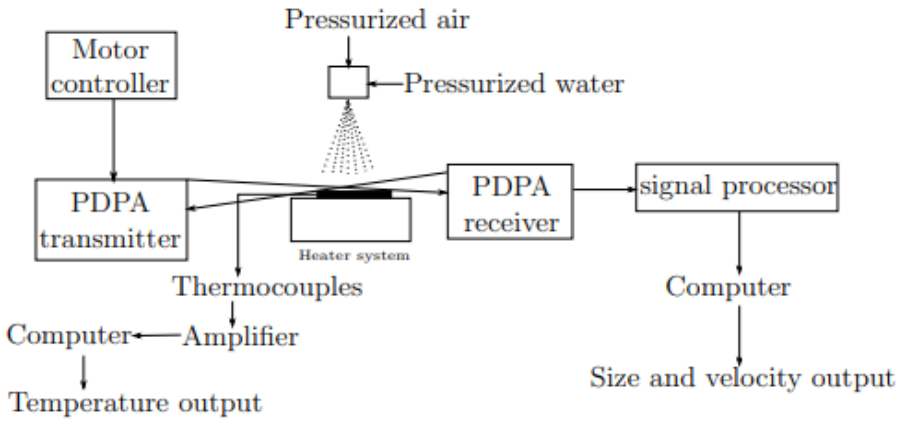

Figure 2.1 Experimental apparatus by Fu, Sojka, and Sivathanu [3]

Further ahead Wijesekere [4] validated the experimental model of Fu et al.[3] using FDS version 6.7.5 with minor adjustment by using Cu plate of a round shaped plate similar to the experiment. The monodispersed spray simulations were simulated using spray nozzle and then compared with experimental results where the temperature profiles were like the experimental results.

R.Sijs, S.Kooji and H.J Holterman [5] conducted and experimental analysis to measure the drop size using 4 different equipment. Figure 2.2 and 2.3 describes the principles of experimental apparatus and depicts the experimental setups.

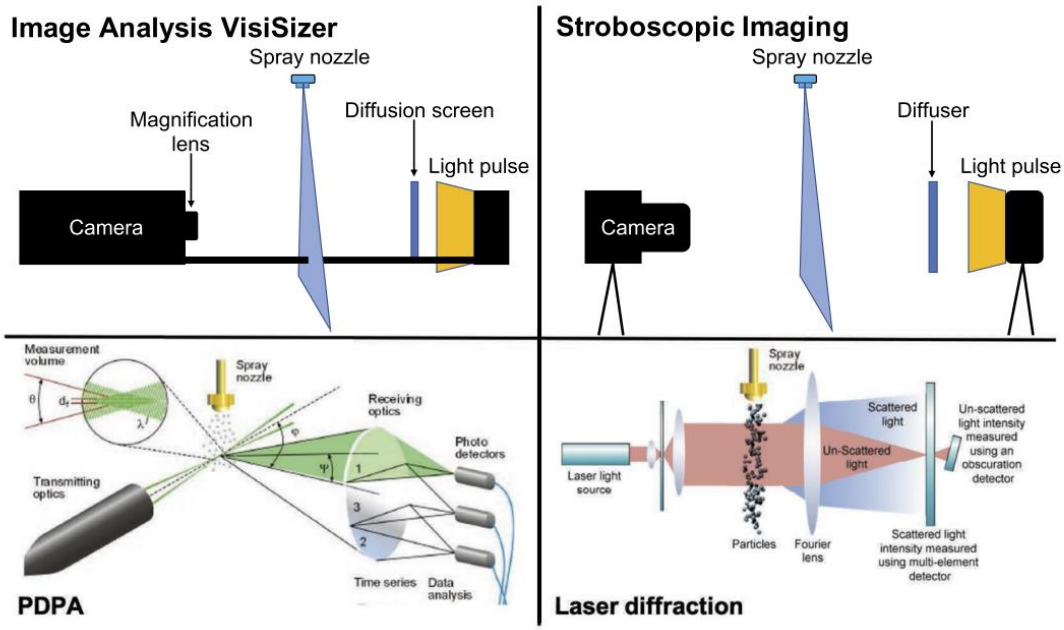

Figure 2.2 Working principle of 4 different apparatus droplet size measurement techniques [5]

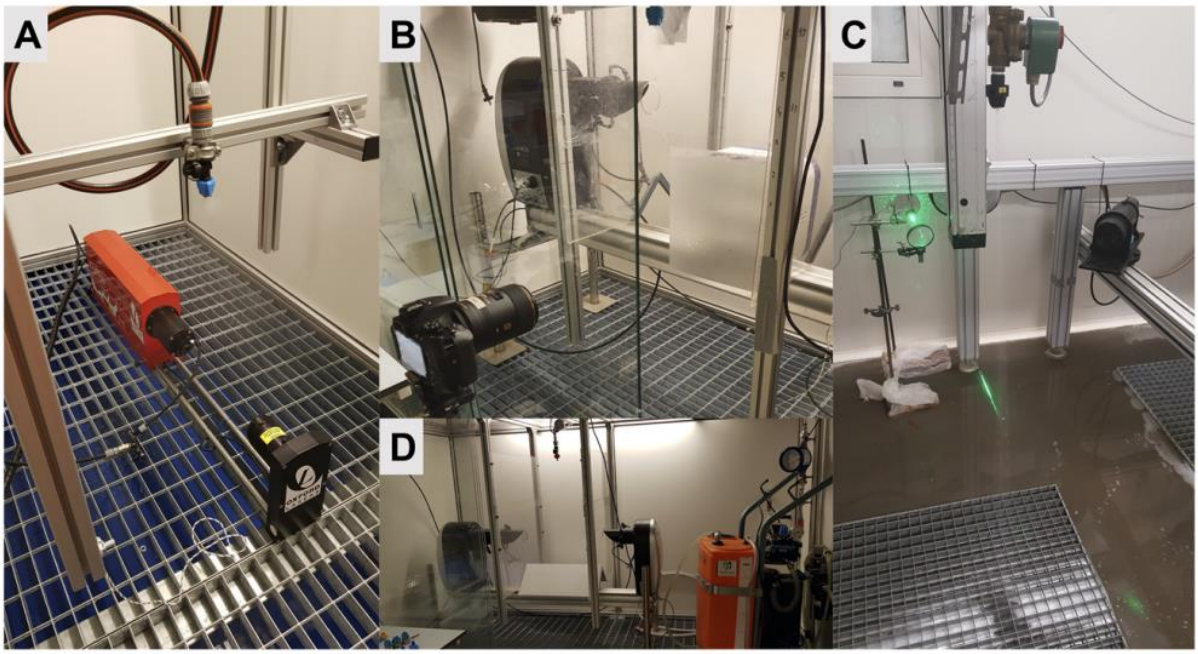

Figure 2.3 Experimental Setups of the Image Analysis VisiSizer technique (a), Stroboscopic imaging technique developed in house (b), PDPA technique (c),laser diffraction technique (d) [5]

The experimental outcome depicts the output of PDPA when compared with other apparatus on volume mean diameter, for PDPA technique, the droplets need to be homogenous,

transparent, and spherical for easy capture of results. Non-spherical drops may be interpreted as slightly smaller drops, resulting in a finer drop size spectrum. Different droplets characteristics due to the presence of air bubbles resulted in PDPA misinterpreting them as smaller droplets, shifting the distribution to smaller sizes. The PDPA technique is mostly suitable for the droplet that are homogenous, transparent, and spherical in shape. PDPA misinterprets the inhomogeneous droplets as smaller droplets shifting the distribution into smaller sizes which will have a chance to overestimate the results [5]. The Figure 2.4 shows how PDPA is plotting the droplets size distribution of water using medium spray nozzle.

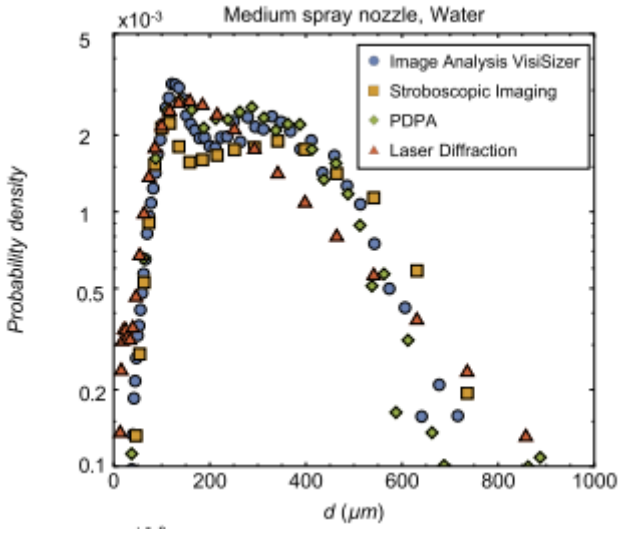

Figure 2.4 Water droplet size distributions for sprays produced by four types of nozzles as determined by the four imaging/analysis methods. The VisiSizer data correspond to the raw data [5].

The PDPA is also called Phase Doppler Anemometry (PDA), in which Sæbø and Wighus [6] have used PDPA for their research in measuring the droplet size from deluge nozzles like HVK44 which is high velocity nozzle and MVK41 medium velocity nozzle. The measurement was done by 2 different techniques. The methods are PDA and photographic technique using Oxford Laser. The PDA methods is suitable for assessing smaller droplets and image processing methods is suitable for assessing large droplets. Henceforth, it gives the larger VMD's (Volume Median Diameter) in sprays where larger droplet than 1200 μm are present. In the medium velocity nozzle, the largest droplet was 3700 μm. The same technique gave 600 to 1300 μm for VMD as output. But PDPA gave VMD from 550 to 750 μm. The findings in this research were that PDA technique gives VMD from 400 to 770 μm at various location in the medium velocity nozzle spray pattern. The VMD values for the HVK44 nozzle measured along the radial position using imaging technique and PDA technique shows that PDA results are stable when compared with PDA technique. The Figure 2.5 describes the VMD results using image method and PDA method.

But in this present thesis, using PDPA in FDS the measurement of droplet size distribution, velocity distribution and number of concentrations has been measured. The method was simulating monodisperse and polydisperse spray and comparing both with and without fire scenarios.

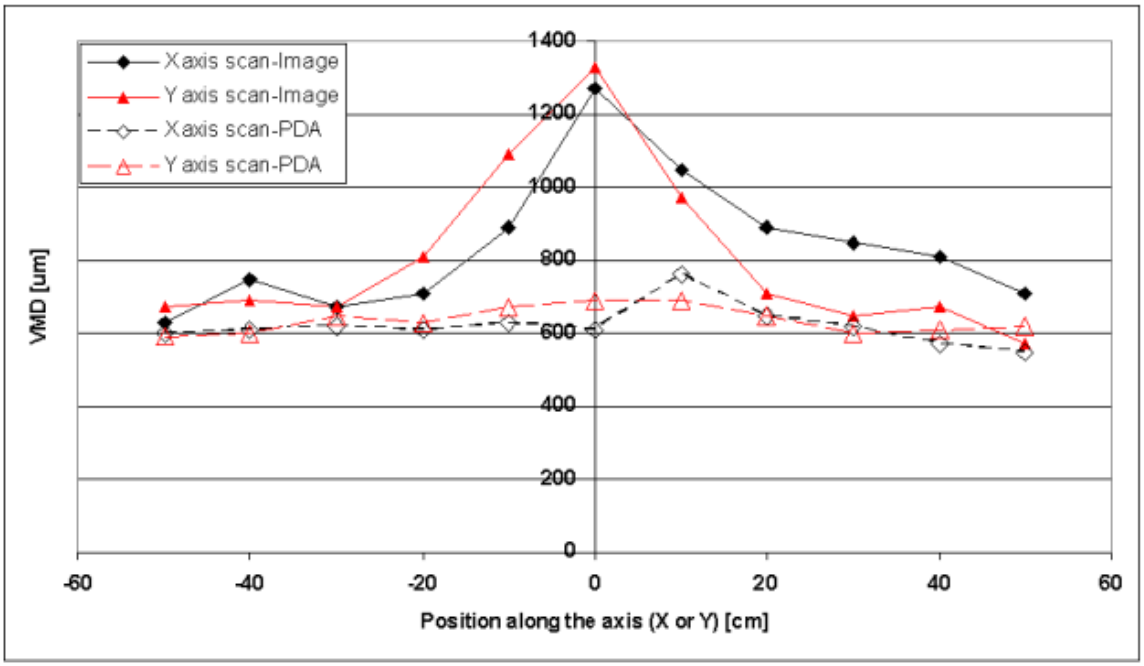

Figure 2.5 VMD values for high velocity nozzle HVK44 comparison with PDA and imaging technique [6]

From the literature of Gupta et al,.[7] an investigation of twin fluid water was carried out. Experimental evaluation of fire suppression characteristics was carried out in $1m^3$ chamber on suppression of n-heptane pool fires using median diameter D_{v50}~$23\ \mu m$ generated through twin fluid nozzle. Suppression factors like fire suppression time, water requirement for fire suppression and temperature in the chambers were measured. Fire suppression performance index (FSPI) was optimized as indicative measure of the fire suppression effectiveness. Larger fire size absorbs $25-30\%$ of combustion heat absorbed by mist, indicating important contribution to fire suppression by other process by two factors like dilution of oxygen and inerting due to water vapor. A detailed experimental setup and spray angle is depicted in the Figure 2.6 (a) and (b).

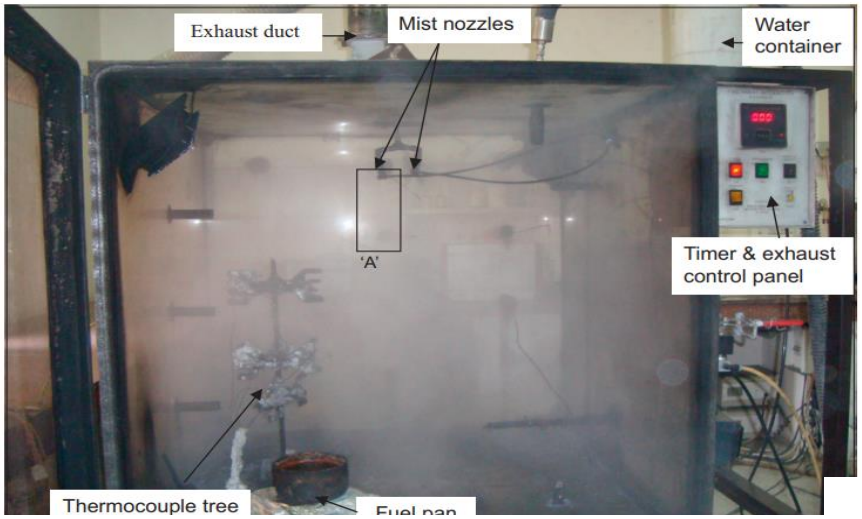

Figure 2.6 (a) Experimental setup

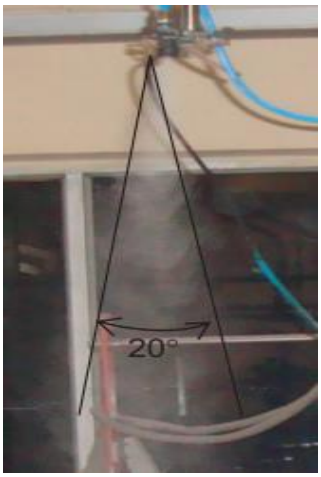

Figure 2.6 (b) Spray angle

2.2 Previous numerical simulation methods

In sub section 2.1 few PDPA related experiments were explained, how PDPA were used to measure the suppression parameters such as droplet size distribution, and velocity distribution. But in this chapter, previous numerical based simulation using FDS based on CFD is explained. CFD based simulation using FDS will be time saving, less expense and gives a validation for an experiment.

In early 20's researcher Desjardin et al., [8] computationally modeled the effect of the water spray suppression on large scale pool fires using spray sub-model using fire simulator VULCAN. This software is based on KAMELEON – fire code and uses RANS model with $k-\varepsilon$ turbulence model, EDC combustion model, soot model and a radiation model. A SIMPLE algorithm with 2nd order upwind scheme is used to solve gas phase conservation equation. A detailed study of VULCAN software model is found in this paper [8]. This study indicated with 3 observations that, firstly there were temperature rise with turbulence mixing before the cooling of evaporation occurs at a large drop size ($D_{v,50} > 150\ \mu m$). Secondly, an optimal drop size allows for maximum decrease of temperature in gas-phase for a spray configuration. Finally, in comparison with single high-pressure nozzle, low pressure spray with more nozzles gave a better suppression.

In the study of Kim and Ryou [9] investigated the interactions between the water mist with fire and investigate how burning rate is influenced by WMFSS of pool fires. An experimental observation was reported having various fuel burning rate in interaction with and without increase in discharge rate of water. FDS version 3.0 have used for simulating the burning rates with WMFSS. Considering water mists on burning rates, better predictions can be made for suppression times and ceiling temperatures than experiments. An experimental validation of Rosin-Rammler is denoted here when the Eulerian-Lagrangian method was used to simulate the pool fires with water mist. Figure 2.7 shows the (CVF) Cumulative Volume Fraction of the

droplet in the function of droplet size. The overall research concluded three points (1) the burning rate is influenced by the effect of water mist and fire plume (2) FDS considers the breakup of water droplets and varied input of HRRPUA when given as input gives a predicted output of mean ceiling temperature (3) two fire suppression mechanisms are used in this present study, and found that, spray momentum overcomes the buoyant force resulting from the fire source. And also, it shows that penetration of water drops from mist spray system, to the plume fire, oxygen displacement becomes more dominant than cooling of fire sources [9].

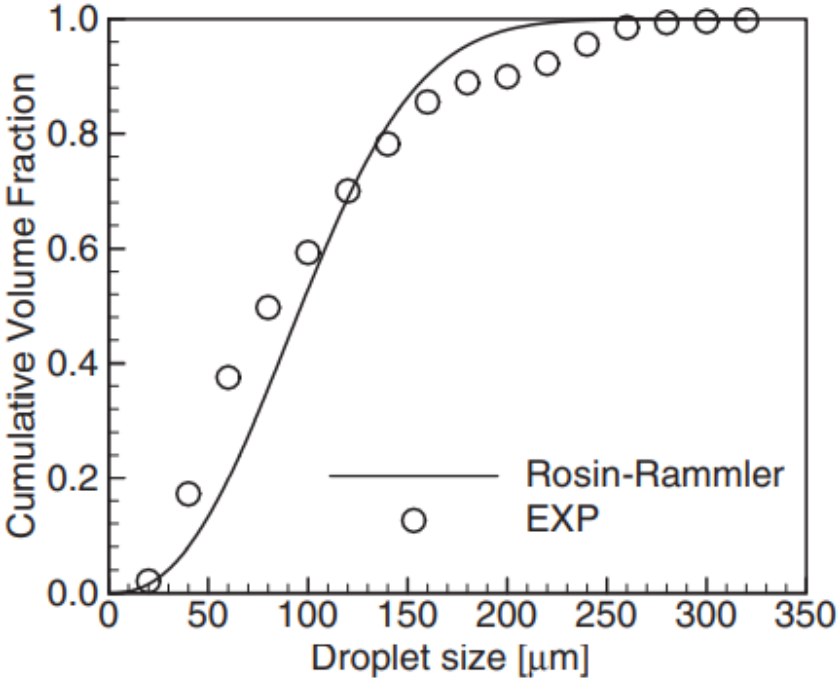

Figure 2.7 Cumulative volume fraction of the droplet size [9]

Husted [10] has used water mist for fire extinguishment in his experiment, the aim of his thesis was to verify the effectiveness of the spray system. The objective of his thesis was to facilitate the CFD, FDS code by giving necessary inputs. Measurement of droplets velocities, diameters and water flux distribution had been carried out from his thesis. A strong analysis of mist flow formation had been analysed using FDS 4.07 version. This method explains that in droplet and air moving downward at high velocities were expected. Due to limited transfer of momentum, the simulation lacks on sufficient mixing. The researcher has modelled the scenario using FDS as shown in the Figure 2.8

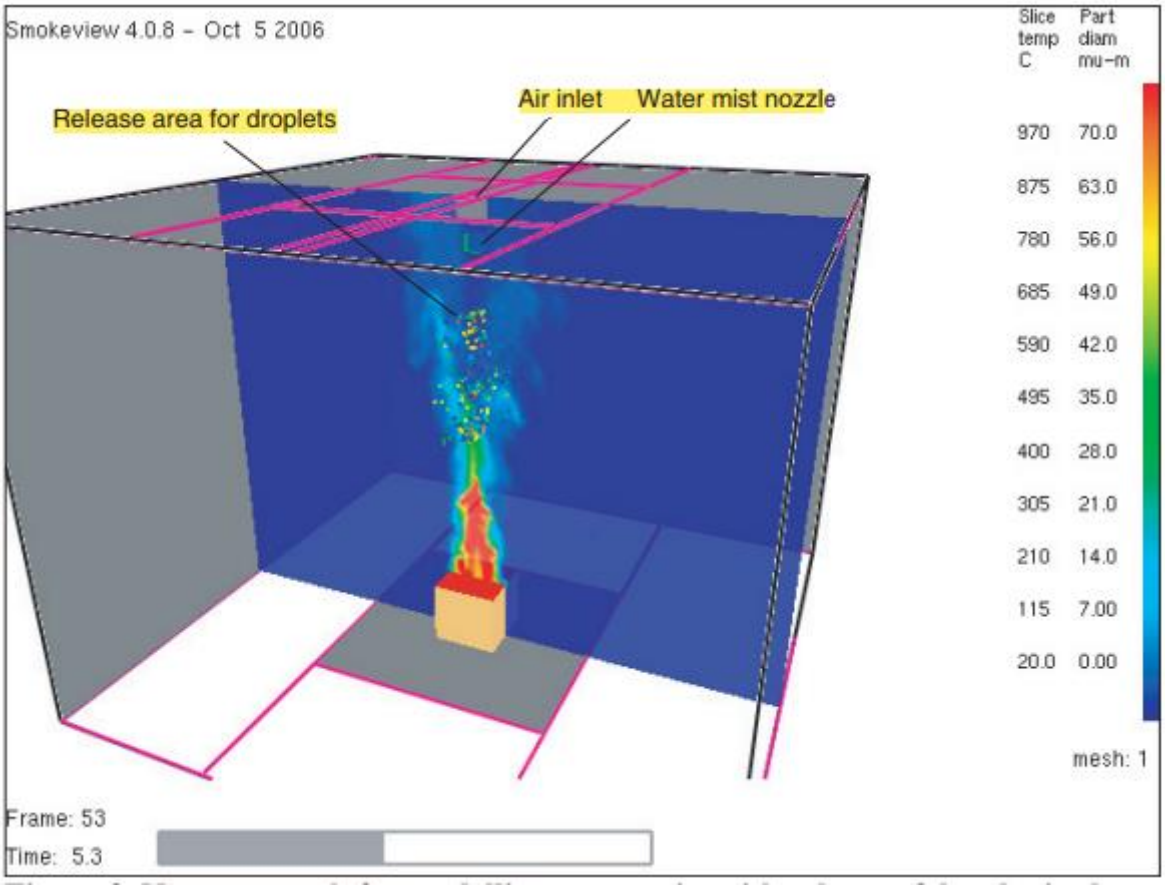

Figure 2.8 Releasing the droplet in the turbulent zone and introduction of an air jet (new approach)[10]

The output data regarding droplet size distribution at 300 mm below the nozzle as well as the fitted distribution. The input to the FDS is chosen of the scan of the entire spray, where the parameters used for $\sigma = 0.43107$, $\gamma = 3.96$ & $d_m = 46\ \mu m$ in the Eqn (2.1). The result from the scan shows the distribution at 30mm and 60mm from the center but at the center it tends to be overestimated. The mass flux is distributed evenly over the spray 300 mm above the PDA. The droplet size distribution has been adopted by McGrattan et al. [11] in FDS technical guide which is based on mass and the volume mean diameter is d_m .

$$F(d) = \begin{cases} 2\frac{1}{\sqrt{2\times\pi}}\int_0^d \frac{1}{\sigma\times d'} \times e^{-\frac{\left[\ln\left(\frac{d'}{d_m}\right)\right]^2}{2\times\sigma^2}} d\mathrm{D} & (d \le d_m) \\ 1 - e^{-0.693\left(\frac{d}{d_m}\right)^{\lambda}} & (d_m < d) \end{cases} \qquad (2.1)$$

Similarly, Lefebvre has described an overview of other distributions and a better review was given by Verheijen, but Tak-Sang Chan investigated and identified that, droplets from sprinkler could be both lognormal and Rosin-Rammler distribution. Thus, McGrattan et al had applied this formula for combined cumulative distribution based on volume [10]. Apart from droplet size distribution, velocity with fire and without fire has also been reported in his work with a chosen input of distance 300 mm below the nozzle. The first position after the collapse of the

spray at 150 mm, where the measurement is taken from PDPA or PDA. At this position the drop velocity is influenced by fire. The behavior of the velocity 550mm and 700mm below the nozzle as depicted in the Figure 2.9. And the droplet size distribution is showed in the Figure 2.10

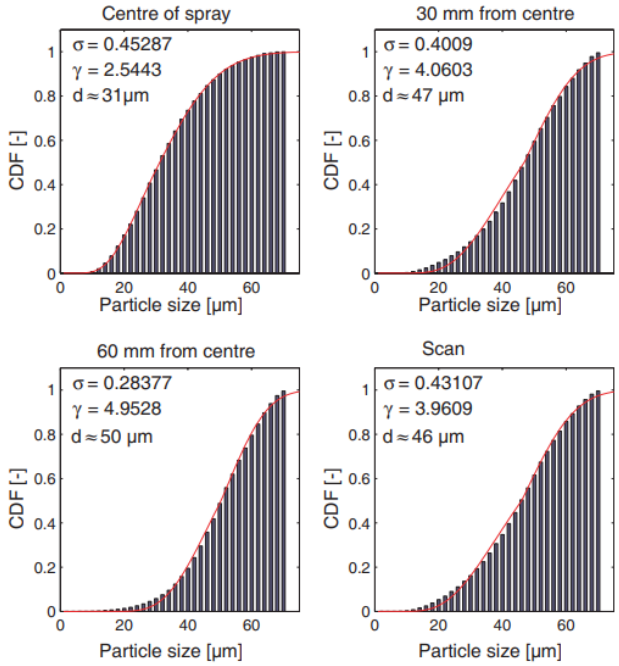

Figure 2.9 Drop size distribution at 300 mm below the nozzle, based on mass. The curves show the fitted distribution using Equation (1). PDA – measurement [10]

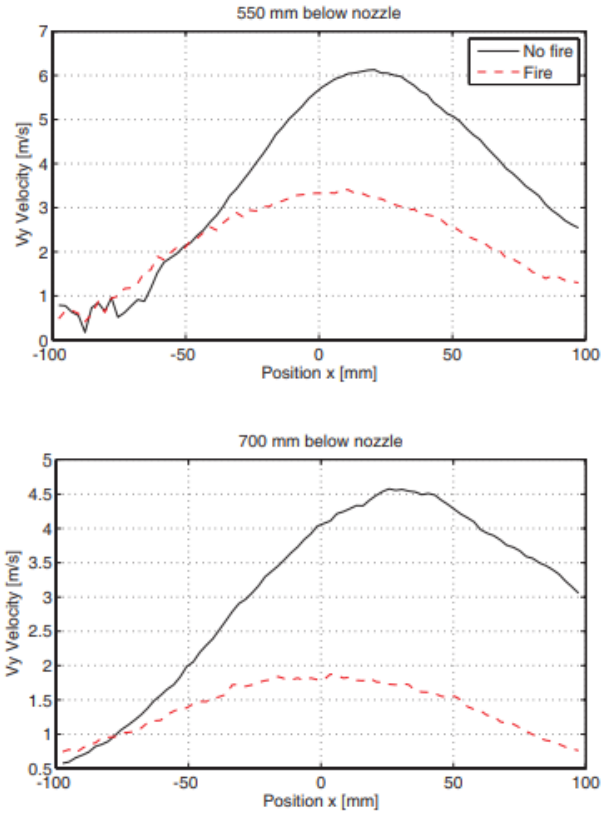

Figure 2.10 Velocity distribution at 550 and 700 mm below the nozzle with and without fire [10]

Mahmud [12] using FDS tried to research on efficacy of Water Mist Fire Suppression System (WMFSS) which was always considered as a suitable candidate for fire suppression. The efficacy of WMFSS has been investigated through, empirical and numerical analysis. The combinational study of an experiment, semi empirical equation-based model and CFD based fire model. The author has done extensive research on simulating behavior of (1) evaporation of water droplets at high temperatures induced by fire (2) flux distribution of water mist nozzle sprays (3) Polymethyl methacrylate (PMMA) fires with and without water-mist sprays. The key findings from this paper were the small diameter droplet suspended in air for a longer period have a higher rate of evaporation of droplets. Also, it's obvious that large diameter has higher capability of penetrating the smoke layer. The secondary aim was to validate FDS in terms of single droplet evaporation against semi empirical model. The model predicts a terminal velocity of 4% of the experimental data, and a saturation temperature of 5% of adiabatic saturation. The fire suppression effectiveness is influenced by distribution pattern on a horizontal surface. Thus, it is very essential that CFD based model, will be able to predict the distribution of flux densities of a spray. The result prediction gives a good agreement with the experimental data. Additionally, the FDS has predicted burning rate is within 23% the experimental data. From this thesis its concluded that FDS accurately predicts the evaporation of droplets, spray distribution, & burning and suppression of sprays and result exhibits better performance in fire suppression.

Effectiveness of water mist, interacting pool fire suppression was performed by Dasgotra et al [12]. The scenario of pool fire has been simulated in this paper, as Single Pool Fire (SPFs) will

multiply into Multiple Pool Fire (MPFs) after interaction which may cause a serious damage in warehouse. FDS had been used for this research, using Pyrosim and Smoke-View for postprocessing. The key findings were defining the effectiveness of the suppression system is the function of water flow rate and height of ceiling and particle size in the water nozzle. Thenceforth an overall safety review had been given in this current paper by assessing the ratio of distance between the pools and diameter of the pool i.e., S/D ratio which was the deciding factor. The behaviour of HRR at fire dynamic at S/D= 0.1, 0.2, 0.4 and 0.8 shown in the Figure 2.14 [13].But in this paper droplet size distribution, water flux distribution and velocity distribution parameters were not discussed.

Another important factor that profoundly influence the efficacy of the fire extinguishment is median droplet diameter in any suppression system. Using FDS it is easy to determine the median droplet size. Mahmud et al. [14] described the determination methodology of median droplet size by conducting two experiments to determine the mass flux distribution generated by nozzle with two operating pressure. FDS program was used in this paper for estimating the median diameter of the water spray under this condition. The ultimate objective for this paper was to give a Standard Operating Procedure (SOP) in determining the diameter of droplets even though unavailability of direct measurement data of droplet diameter.

The major numerical model used here was Equation (2.1) which is droplet size distribution by log-normal and Rosin-Rammler distribution. The second approach was Lagrangian model. The droplet velocity and position are computed using Equation (2.2) and drag coefficient C_d, that depends on Reynolds number (Re) based on droplet – air relative velocity in Equation (2.4)

$$\frac{d}{dt}\left(mv_p\right) = mg - \frac{1}{4}\rho C_d \pi D_p^2 \left(v_p - v_a\right)\left|v_p - v_a\right| \tag{2.2}$$

$$\frac{dx_p}{dt} = v_p \tag{2.3}$$

$$C_d = \begin{cases} \frac{24}{Re} & Re < 1 \\ \frac{24\left(0.85+0.15Re^{0.687}\right)}{Re\ 1} & < \mathrm{Re} < 1000 \\ 0.44 & Re > 1000 \end{cases} \tag{2.4}$$

Here The Re , Reynolds number for the droplets is defined by Equation (2.5)

$$Re = \frac{\rho|v_d - v_a|D_p}{\mu(T)} \tag{2.5}$$

where $\mu(T)$ is the dynamic viscosity of air at temperature T. The model is present in FDS technical guide. And distribution of flux validation is well proven in FDS [14]. For finding the water flux distribution, the approach in FDS, AMPUA method was employed as shown in the Figure 2.11(a) but an experimental depiction is shown in the Figure 2.11(b) for having a clear idea of working.

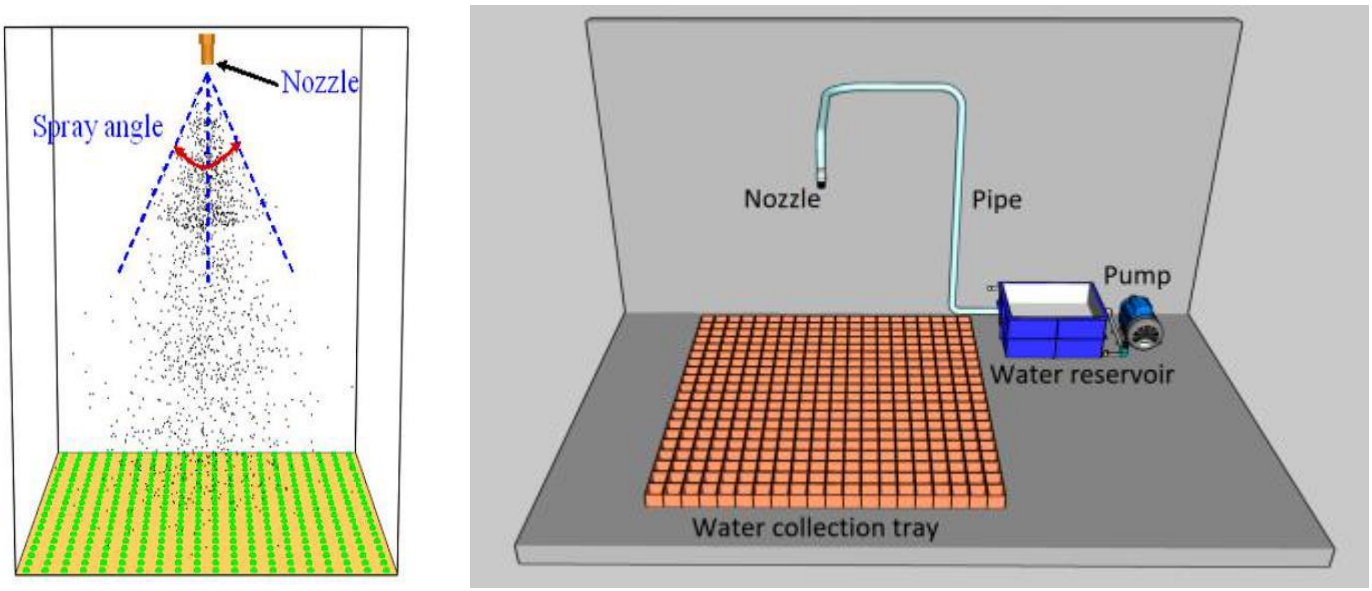

Figure 2.11 (a) &(b) FDS depiction vs experimental schematic setup [12]

A flow chart for this methodology is described using a flow chart which is mentioned in the Figure 2.12 for easy understanding.

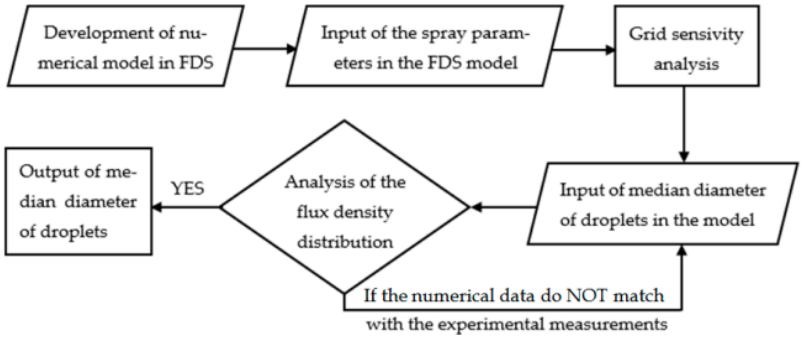

Figure 2.12 Schematic flow chart of numerical [12]

As a result, from simulation, and following the flow chart as a procedure the author achieved the value of simulation and experiment and validated which is showed in the Figure 2.13 for droplet size 275 μm.

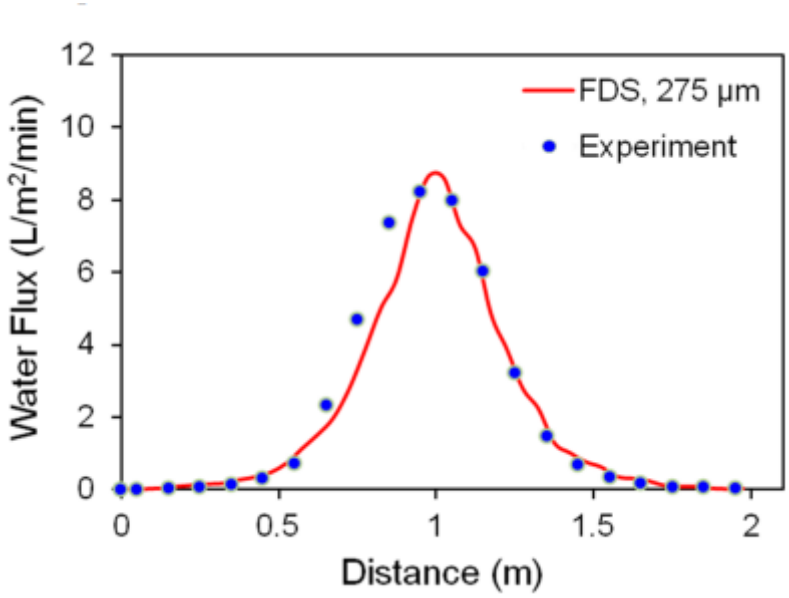

Figure 2.13 Validation of the calculated median droplet size [12]

The findings from this paper were FDS were capable to predict the mass flux distribution of water droplets generated by spray nozzle. The result shows that the median droplet size was 275 µm at 75.8 bar [14]. But, in this present thesis, PDPA analysis were used to measure the water flux distribution at various pressure and droplet diameter [16].

A different work was conducted by Khoat et al., performing a numerical analysis of the fire characteristics after the sprinkler is activated in the compartment. This paper gives reader an idea on fire safety design using FDS using 6.7.0 by throwing a light on gas phase interaction under influence of sprinkler spray. Factors like temperatures, velocity, and mass flow rate in the gas phase. Extinguishing coefficient 3.0 was shown as an optimised value for fire suppression model. An experimental setup has been visually showed in the Figure 2.15 [15].

In the numerical model, computational domain with 3.5m (W) × 11.4m (L) × 4.4m (H) were created in FDS as per the experiment. The wood and polyether foam were considered in the simulation. A burner was modelled, for HRRPUA in KW/m^2. Sprinkler and thermocouples were kept in the domain to measure the temperature at different heights. A typical FDS model is described in the Figure 2.16. Growth of HRR has been halted at 165 KW at 70th second and stopped at 10KW at 400th second when extinguishing coefficient of 3.0 was opted [16].

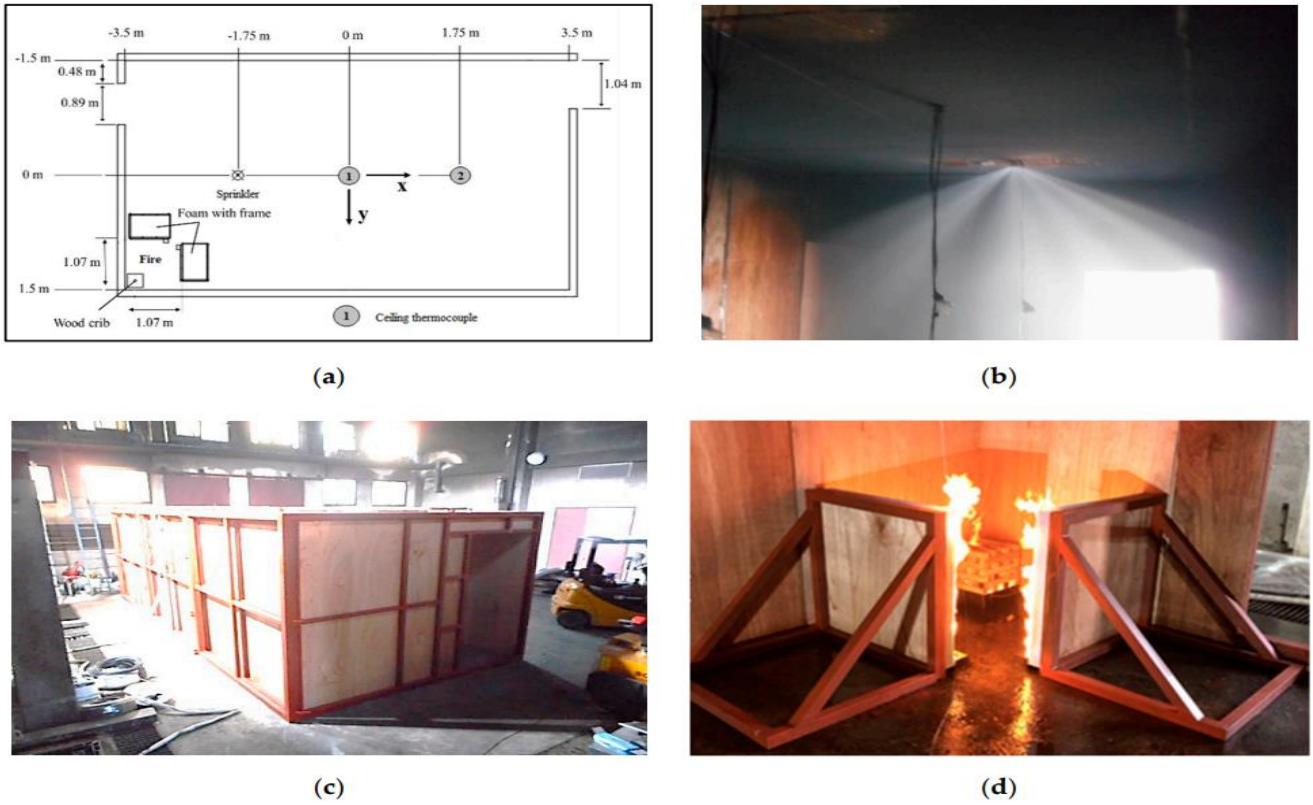

Figure 2.15 Detailed drawings of the experiment (a) compartment drawing (b) Sprinkler spray (c) test compartment (d) fire source [15]

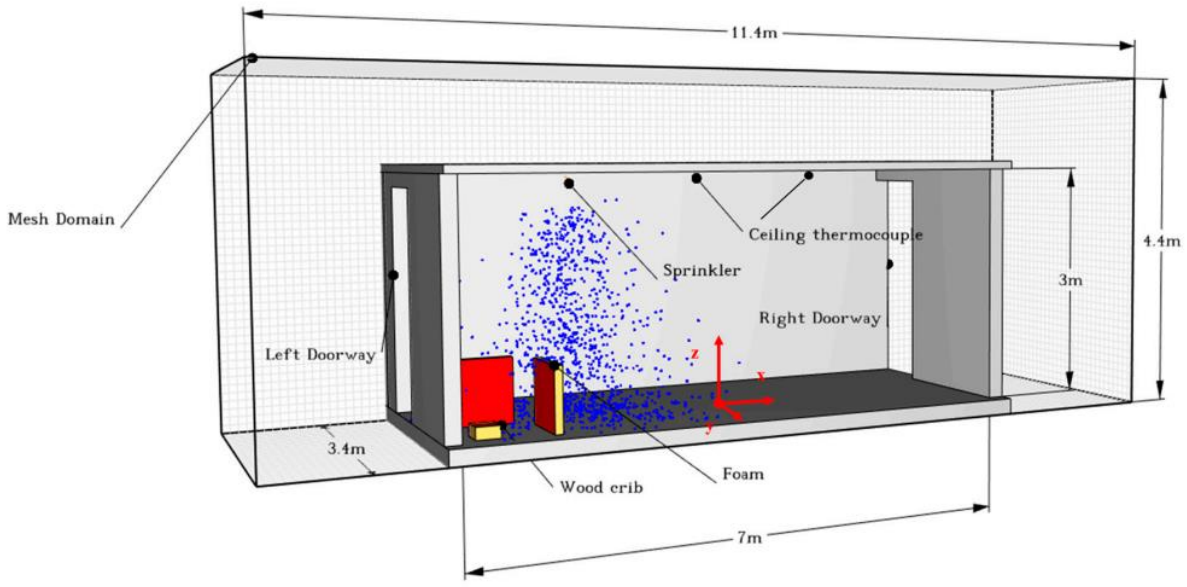

Figure 2.16 FDS 3 – D schematic view of the compartment model [15]

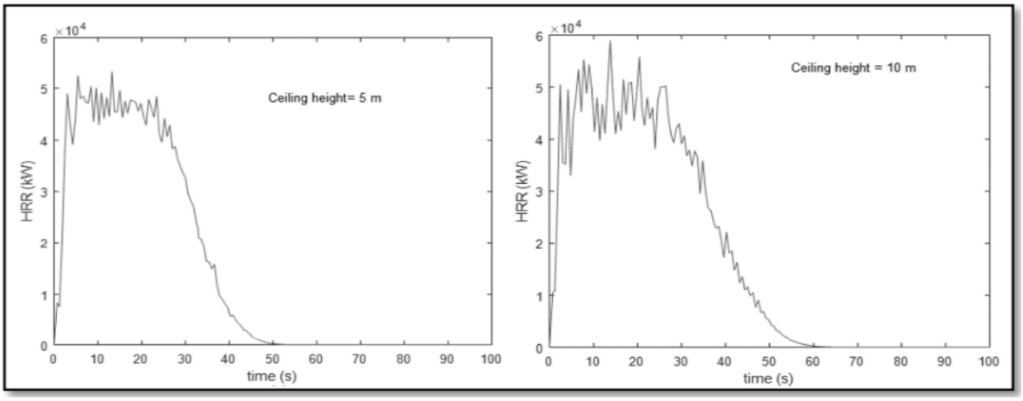

(c) Fire suppression dynamics at S/D = 0.4

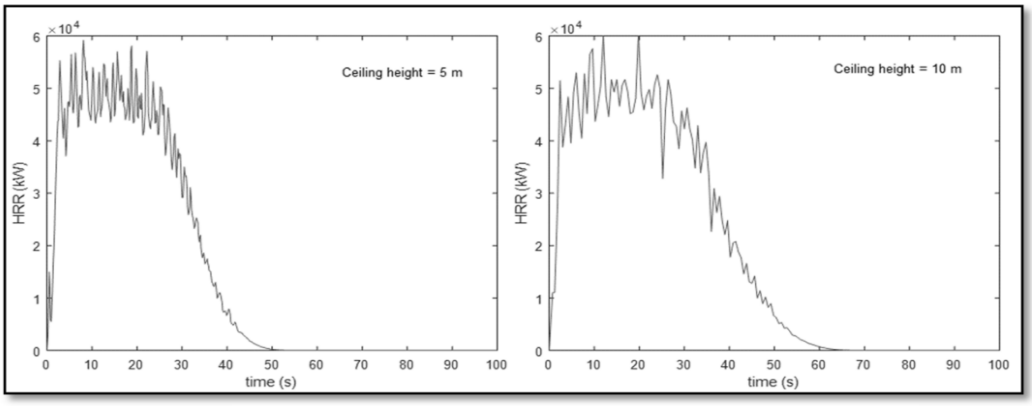

(b) Fire suppression dynamics at S/D = 0.2

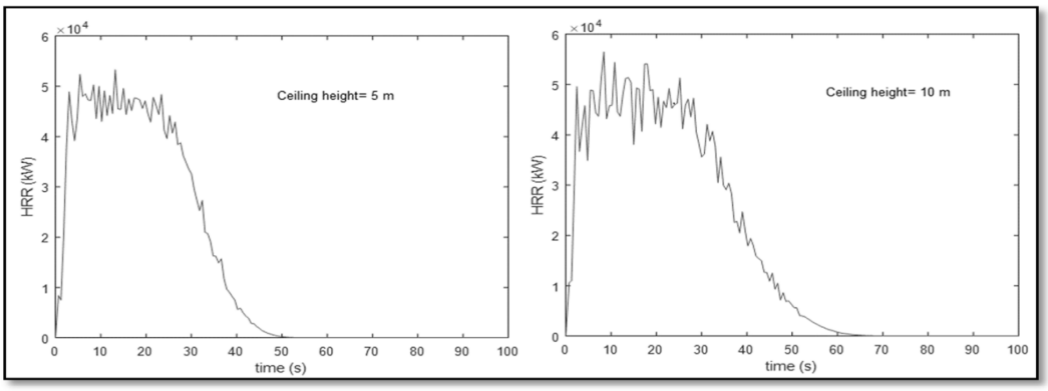

(a) Fire suppression dynamics at S/D = 0.1

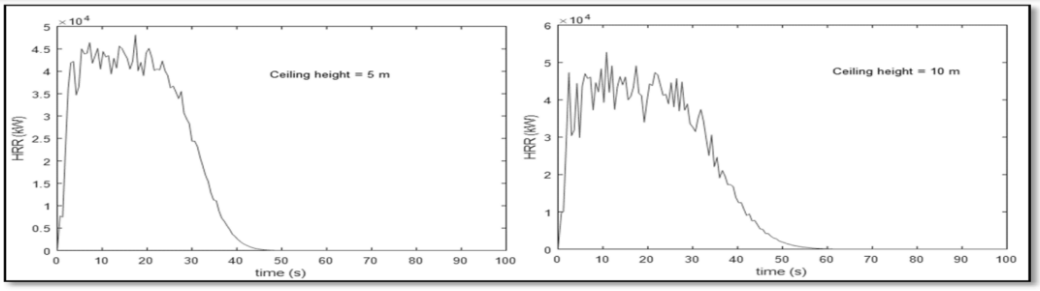

(d) Fire suppression dynamics at S/D = 0.8

Figure 1.14 Fire suppression dynamics at S/D = 0.1,0.2,0.4 & 0.8 [11]

The optimization of water mist droplet size using CFD for fire suppression was validated by Wang [16] simulating in FDS software. The simulation resulted towards the optimal droplet size range to have an effective fire suppression. The droplet size is often an important parameter for the suppression parameter. The Figure 2.15 shows the suppression time with respect to the flow rate is considered as the optimal droplet size [16].

Flow Rate (L/min)	Size (μm)								
	100	200	300	400	500	600	700	800	900
5	22.3	41.2	94.1	–	–	–	–	–	–
10	15.5	35.5	33.9	39.0	52.4	74.8	–	–	–
15	13.5	13.8	16.9	10.2	33.0	14.0	21.6	17.8	71

Figure 2.15 Extinguishment time vs droplet size at different flow rates [16]

2.3 Outcome of literature review

An intensive literature review was performed on relative research works published in prior works by various researchers. From these literatures it was evident that, several researchers worked on several factors like median diameter, water flux distribution, fire suppression time, velocity distribution both empirical analysis and computational analysis.

Fu et.al used PDPA analyzer to map the velocity and droplet histories in a polydisperse spray when the droplets approach on a heated surface made by a copper plate. The effect of buoyancy on the trajectory of single droplet, effect of evaporation of the single droplet, decrease in surface temperature due to drop impingement, spreading and evaporation on surface combustion. The experimental data were generated under these sub-models [3].

However, this study describes a scenario of explaining the sub-models with PDPA, no factors of spray suppression parameters were explained in depth. But still velocity history and Sauter Mean Diameter (SMD) were explained which is relatable to the present thesis.

Experiment conducted by Sijs et al., [5] to study the droplet size measurement using different measuring instrument like PDPA, laser diffraction, stroboscopic imaging and Image analysis visiSizer were compared. The result until now were homogenous water spray but the effect of inhomogeneities were expected to affect the PDPA method. It important that, PDPA will work perfectly under homogenous droplet, transparent and spherical. However other factors were not discussed other than droplet size distribution, in this present thesis PDPA is being used to measure the droplet size distribution, velocity distribution and flux distribution are being discussed.

While considering Gupta et al.,[7] experimental research on evaluating the fire suppression characteristics of twin fluid water mist system, fire suppression index was developed as an indicative measure using n-heptane fuel in the process. A clean sense of information on thermocouple reading is being experimentally measured, but in this present thesis the thermocouple is being simulated and temperature was measured.

While reviewing the research of Sæbø and Wighus [6] based on empirical model for extinguishing the fire using water mist, the major findings was studying about PDA technique on small droplets. Finding VMD for both medium and high velocity nozzle and comparing between was a major focus of study. Additionally, a study was conducted comparing the PDPA method and oxford photographic method for both the type of nozzle were the major findings. Especially for the HVK44 nozzle, a decent number of droplets greater than 1200 μm were found with the imaging technique. These droplets were not detected by the PDPA technique, meaning that this method gives lower VMDs for the HVK44 nozzle. When the MVK41 nozzle was used, none of the methods detected larger droplets than about 1600 μm. Thus, PDA technique thus captured most of the largest droplets, and the VMDs achieved using the two techniques are because of that more similar.

A numerical simulation was performed by Desjardin et al., [9] as mentioned in the previous Chapter 2.2, using sub-grid model in VULCAN, KAMELON software which was based on $k-\varepsilon$ turbulence model and other allied models and schemes. From this study, three important points were discussed as mentioned previously. Though the findings were related to model the effects of water spray suppression on large pool fires, the numerical model applied in this research in this paper are totally related to the present thesis especially flame extinguishment model. In 2007 [17] Santangelo et al., performed a laser diffraction based test to characterise the spray released by water mist injector at high pressure. Drop size and initial velocity over a prescribed range of operative pressure. A classic predictive formula for SMD was validated through physical analysis on inviscid-fluid assumption. Velocity distribution was studied using PIV technique. Additionally, evaluation of spray cone angle was realized because of the PIV tests. Figure 2.15 and 2.16 shows the behaviour of average mass flux distribution at different pressure range and droplet size vs CVF distribution at 80 bar pressure.

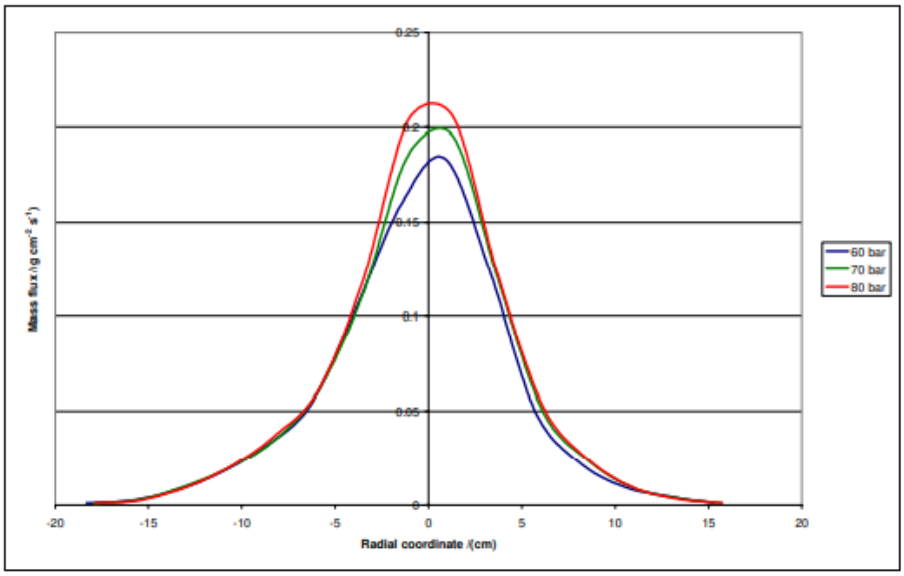

Figure 2.15 Average mass - flux distribution at 60,70 & 80 bar pressure [17]

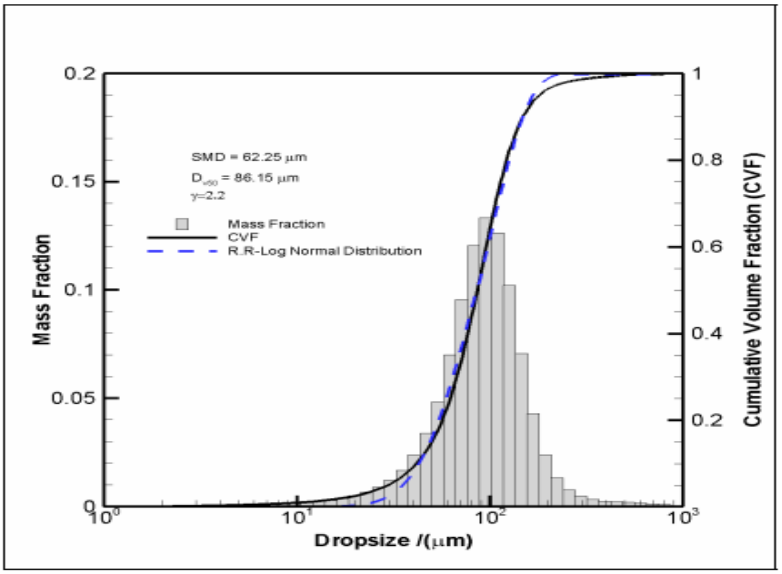

Figure 3 Droplet size vs CVF distribution at 80 bar [16]

From the literature of Muhammad et al., [14] for formulating SOP to identify the median diameter of droplets in the water mist spray, through simulating the accumulated mass per unit area in FDS gives a clear picture on bucket test for measuring mass flux distribution. But still a straightforward simulation method can be implemented PDPA through the simulation which is implemented in this present thesis.

So, finally in this present thesis is constructed through methodology by introducing PDPA in the simulation for measuring the history trace data of velocity distribution, mass flux distribution, droplet size distribution and number of droplets for mist and sprinkler fire suppression system with and without fire scenario. All the simulations are compared with different pressure, at monodisperse and polydisperse condition which is an innovative study presented in this thesis. Thus, this present thesis is an entire package for fire safety engineers to understand the comparison with two different scenarios.

The reason for comparing monodisperse and polydisperse is, monodisperse spray is quite unreal, and it represents the characterization of example 10,000 droplets in an entire volume of spray. Thus, monodisperse spray can be made as a comparison study against polydisperse spray which is interesting.

3 Numerical model

As some insights have been given from the previous chapters about numerical model. A detailed numerical model with some literature review has been mentioned in this present chapter.

However, FDS is using LES model as a basis, there are other governing Equation used by FDS version 6.7.7 to compute the suppression factors of sprinkler and water mist system.

3.1 Governing Equations for FDS

The domain that was created computationally, is discretized into multiple cells or control volumes and the value of unknown variable ϕ is calculated at center of the cell. While considering these computational domains, they are much smaller to capture turbulent eddies, turbulence models are solved along the flow Equation. It is usual that, governing mass, momentum, and energy Equations are discretized at each node to generate direct algebraic Equations and numerically solved to obtain the values of all the required variable ϕ at all the centers. The governing Equations have been presented below that are used in FDS.

3.1.1 Modelling of mass, species, and energy transport

FDS numerically solves the Navier-Stokes equation appropriate for low thermally driven flow, Mach number < 0.3 which emphasize on smoke and heat transport from fires for hydrodynamic model.

The conservation equation for mass and momentum for a Newtonian fluid are presented as a set of partial differential equations and solved by FDS. The airflow, including the thermal distribution is simulated by solving one set of the coupled state conservation of mass, momentum, and energy [11].

(1) Conservation of mass

The mass transport equation is solved using the basic predictor-corrector scheme. Conservation of mass equation can be described as mass flows flow into control volume must flow out. Conservation of mass states rate of mass storage due to change in density in the control volume which is balanced by net rate of inflow of mass by convection [18].

$$\frac{\partial \rho}{\partial t}(\rho Z_\alpha) + \nabla.(\rho Z_\alpha u) = \nabla.(\rho D_\alpha \nabla Z_\alpha) + \dot{m}'''_\alpha + \dot{m}'''_{b,\alpha} \quad (3.1)$$

In the right-hand side addition of mass from evaporating droplets or other sub-grid scale particles. This represents the sprinkler and fuel spray, vegetation, and unresolvable object. These objects are assumed to occupy no volume. They are seen as governing equations as point for mass, momentum, and energy.

$$\frac{\partial \rho}{\partial t} + \nabla \cdot (\rho \boldsymbol{u}) = 0 \quad (3.2)$$

$\frac{\partial \rho}{\partial t}$	$\nabla \cdot (\rho \mathbf{u})$	**u**
Change in density with respect to time	Mass convection	Vector describing velocity in u, v & w directions

(2) Momentum transport equation

$$\rho \frac{\partial u}{\partial t} + \rho(u.\nabla)u + \nabla\rho = f + \rho g + \nabla.\tau_{turb} \quad (3.3)$$

$\rho \frac{\partial u}{\partial t}$	$\rho(u.\nabla)u$	$\nabla\rho$	f	ρg	$\nabla.\tau_{turb}$
Momentum forces	Inertia forces $u -$ filtered velocity	Change in pressure	External force vector $\tau_{ij} = \mu(2S_{ij} - \frac{2}{3}(\nabla.\bar{U})\delta_{ij})$	Pressure &gravity	Filtered turbulence, sub-grid scale Reynolds stress

Where, $viscous\ stress$ is given by product of viscosity and measure of velocities that the fluid volume is subjected. A deformation tensor is used to account for the velocity term. For LES the sub grid analysis was developed by Smagorinsky to model the viscosity. This model uses the deformation factor to reach a value for the local turbulent viscosity based on the density of fluid.

But momentum conservation Equation can also be written in non-conservative form where the model is linked with Lagrangian particles. Introduction of mass from sub-grid particles (evaporation of water droplets) by using the continuity Equation.

$$\bar{\rho}\frac{Du}{Dt} = -\frac{\partial \bar{p}}{\partial x_i} - \frac{\partial \tau_{ij}^{dev}}{\partial x_j} + \bar{\rho} g_i + \bar{f}_{d,i} + \bar{m}_b{}'''(\widetilde{u_{b,\iota}} - \tilde{u}_\iota) \quad (3.4)$$

Where, $\bar{f}_{d,i} + \bar{m}_b{}'''(\widetilde{u_{b,\iota}} - \tilde{u}_\iota)$ is absorbed into the bulk sub grid force term, $\bar{f}_{b,i}$ is responsible for the drag on Lagrangian particle, which will be discussed in upcoming chapter.

FDS uses LES method to model turbulence in which LES, dissipative process that occur at length scales smaller than those are explicitly resolved on the numerical grid. FDS models turbulence using four different models.

1) Smagorinky model
2) Dynamic Smagorinky model
3) Deardorff model
4) Vreman's model

(3) Conservation of energy

The energy equation evaluates for the energy accumulation due to internal heat and kinetic energy and energy fluxes associated with convection, conduction, radiation, the inter diffusion of species and the work done on the gases by viscous stresses and body forces [18].

$$\frac{\partial}{\partial t}(\rho h) + \nabla.\rho h u - \frac{\partial \rho}{\partial t} + u.\nabla\rho = q''' - \nabla.q_r + \nabla.k\nabla T + \nabla.\sum_1 h_1(\rho D)_1 \nabla Y_1 \qquad (3.5)$$

Left Hand Side (L.H.S)	**Right Hand Side (R.H.S)**
$\frac{\partial}{\partial t}(\rho h) + \nabla.\rho h u - \frac{\partial \rho}{\partial t} + u.\nabla\rho$	$q''' - \nabla.q_r + \nabla.k\nabla T + \nabla.\sum_1 h_1(\rho D)_1 \nabla Y_1$
Net rate of accumulation	Energy gain or loss term to this accumulation at left hand side

$\bar{p} -$ background pressure

$R -$ molar gas constant $= 8.3145$ KJ/(kmol. K),

$M -$ molecular weight

(4) Conservation of species

Smoke transport simulation is possible in FDS. This software tracks six gas species like $Fuel, O_2, CO_2, H_2O, CO, N_2$ plus soot particulate [11]. The following species equation is solved for each species represented by Y_i where $i = 1,2,3 \ldots etc.$

$$\frac{\partial(\rho Y_i)}{\partial t} + \frac{\partial}{\partial x}(\rho u Y_i) + \frac{\partial}{\partial x}(\rho v Y_i) + \frac{\partial}{\partial x}(\rho w Y_i) = \nabla.\rho D_i \nabla Y_i + \dot{w}''' \qquad (3.6)$$

$\dot{w}''' -$ production rate of i^{th} species during combustion

$D_i -$ Diffusion coefficient of i^{th} species.

$\frac{\partial(\rho Y_i)}{\partial t} + \frac{\partial}{\partial x}(\rho u Y_i) + \frac{\partial}{\partial x}(\rho v Y_i) + \frac{\partial}{\partial x}(\rho w Y_i)$	$\nabla.\rho D_i \nabla Y_i + \dot{w}'''$
Accumulation of species due to change in density and 2nd term is inflow and outflow of species.	Inflow or outflow of species from control volume due to diffusion & production rate.

3.1.2 Radiation transport

The FDS provides a mathematical model to model the model the radiation. But, in this present thesis, radiation has been neglected to simplify the model. Still, just for discussion, water droplets are capable to absorb and scatter the thermal radiation. It is vital that involving water-

mist suppression systems and sprinkler cases. The absorption and scattering coefficients are based on Mie theory [12].

3.1.3 Combustion modelling

For LES model, FDS uses mixture fraction model. LES assumes turbulent mixing of combustion gases with surrounding atmosphere. It is considered that, mixing controls combustion and species that is of interest should be represented by a variable term known as mixture fraction (Z). The mixture fraction model, is based on large-scale convective and radiative transport phenomenon can be simulated easily, but processes occurring at small time scales must be shown in an approximate manner [18].

The mixture fraction is a conserved quality showing the factor of material at a given point.

$$Z = \frac{sY_f - (Y_0 - Y_0^{\infty})}{sY_f^1 + Y_0^{inf}} \; ; s = \frac{v_0}{v_f} \times \frac{M_0}{M_f} \tag{3.7}$$

Z varies from 1 in the region containing only fuel, to zero where the oxygen where the oxygen mass fraction equals its ambient value, Y_0^{inf}.

Combustion model approximates the combustion process in space and time so that the fire can be simulated efficiently. This model also considers the large-scale convection and radiation transport. Since combustion processes is on a shorter span of time scale when comparing to convection process an infinite reaction rate is considered. Fuel-Oxygen can be never exist to gather [18].

At one point, both species vanishes and their mass fraction dropping to zero. This leads to simplification of Equation (3.12) to obtain the flame mixture fraction Z_f. Z_f is the flame in computational domain. This is referred to flame sheet.

$$Z_f = \frac{Y_0^{inf}}{sY_f^{li} + Y_0^{inf}} \tag{3.8}$$

The assumption that fuel and oxidizer can't co-exist leads to the 'state relation' between oxygen mass fraction Y_0 and Z [18].

$$Y_0(Z) = Y_0^{inf}\{1 - \frac{Z}{Z_f}\} \qquad <Z_f \tag{3.9}$$

$$0 \qquad Z>Z_f$$

The mass fraction of all other species of interest is based on individual state relation based on mixture fraction. The local oxygen mass fraction can be applied to determine the oxygen rate of consumption. To calculate local HRR, the product of HRR per unit mass of oxygen (ΔH_0) [18].

1) Heat release rate

The heat release per unit volume, defined as summing the species mass production rate times the respective heat of formations:

$$\dot{q}'''_F \equiv \sum_\alpha \dot{m}_\alpha''' \Delta h^0_{f,\alpha} \quad (3.10)$$

3.1.4 Water mist modelling

1) Heat and Evaporation of liquid droplet

In FDS, droplets are represented through Lagrangian particles which is discrete spheres travelling via air. In course of time, the grid cell evaporates as a function of the liquid equilibrium vapour mass fraction of particle, $Y_{\alpha,l}$, the local air phase vapour mass fraction $Y_{\alpha,g}$, the droplet temperature T_p and local gas temperature T_g, 'g' is the average of quantity in the cell occupied by droplet $A_{p,s}$ is the area of liquid droplet. c_w is the specific heat of solid and m_w is the mass of the first node of the solid.

$$\frac{dm_p}{dt} = -A_{p,s} h_m \rho_f (Y_{\alpha,l} - Y_{\alpha,g}) \quad (3.11)$$

$$\frac{dT_w}{dt} = -\frac{A_{p,s} h_w}{m_w c_w} (T_w - T_p) \quad (3.12)$$

2) Droplet transport model

FDS uses Lagrangian approach for droplet transport model. The velocity and position of a droplet is obtained from conservation of momentum. The trajectory and position of each droplet satisfies the following equations:

$$\frac{d}{dt}(mv) = mg - \frac{1}{2}\rho C_d \pi r^2 v^2 \quad (3.13)$$

$$\frac{dx}{dt} = v \quad (3.14)$$

The drag coefficient C_d, is the function of Reynolds number based on the droplet terminal velocity, that is represented by:

$$C_\mathrm{d} = \begin{cases} 24/\mathrm{Re} & \mathrm{Re} < 1 \\ 24(0.85 + 0.15\mathrm{Re}^{0.687})/\mathrm{Re} & 1 < \mathrm{Re} < 1000 \\ 0.44 & \mathrm{Re} > 1000 \end{cases} \quad (3.15)$$

Reynolds number of droplet is represented by

$$Re = \frac{\rho v D}{\mu} \quad (3.16)$$

3) Droplet size distribution model

FDS takes one spherical droplet as a sample to calculate the distribution pattern. The droplet size distribution is expressed in terms of its cumulative volume fraction (CVF). This is represented by a combination of lognormal and Rosin-Rammler distribution [11].

$$F(d) = \begin{cases} \frac{1}{\sqrt{2\times\pi}} \int_0^d \frac{1}{\sigma \times d'} \times e^{-\frac{\left[\ln\left(\frac{d'}{d_m}\right)\right]^2}{2\times\sigma^2}} d\mathrm{D} & \left(d \le d_{v,0.5}\right) \\ 1 - e^{-0.693\left(\frac{d}{d_m}\right)^{\lambda}} & \left(d_m < d_{v,0.5}\right) \end{cases} \quad (3.17)$$

Where, d is the generic droplet diameter and d_m is the median droplet diameter. Where, γ and σ are empirical constants for curve fitting of distribution patterns.

The median droplet diameter is a function of both sprinkler and nozzle orifice diameter, operating pressure, and geometry.

A research results from Factory Mutual yielded correlation for median droplet diameter.

$$\frac{D_{v,0.5}}{d} \propto We^{-1/3} \quad (3.18)$$

$$We = \frac{\rho_{p.} u_p^2 d}{\sigma} \quad (3.19)$$

3.1.5 Sprinkler modelling

Heskestad and Bill has estimated the temperature for sensing element of automatic fire sprinkler. The term to account for cooling of link by water droplets in gas stream phase from activated sprinklers [11].

$$\frac{\mathrm{d}T_l}{\mathrm{d}t} = \frac{\sqrt{|\mathbf{u}|}}{\mathrm{RTI}}\left(T_g - T_l\right) - \frac{C}{\mathrm{RTI}}\left(T_l - T_m\right) - \frac{C_2}{\mathrm{RTI}}\beta|\mathbf{u}| \quad (3.20)$$

$\mathrm{u} -$ gas velocity

$\mathrm{RTI} -$ response time index

$\mathrm{T_l} -$ link temperature

$\mathrm{T_g} -$ gas temperature

$\mathrm{T_m} -$ sprinkler mount temperature

$\mathrm{C} -$ Factor are determined experimentally

The sensitivity of sprinkler is characterized by RTI and C2 is an experimental value derived by DiMarzio and the value is to be $6 \times 106\ K/(m/s)^{1/2}$.

3.1.6 PDPA model in FDS

A detailed suppression parameters are taken from spray parameters using Phase Doppler Particle Analysis to provide droplet size distribution, number concentration, velocity, and water flux distribution. FDS provides the output quantity that is available for PDPA. It's said that PDPA computes the measurement using `PROP` line [19].

PDPA device output at time t is computed as a time integral

$$F(t) = \frac{1}{\min(t,t_e)-t_s}\int_{t_s}^{\min(t,t_e)} f(t)\,dt \tag{3.21}$$

$$F(t) = f(t) \tag{3.22}$$

The function $f(t)$ has two forms:

$$f_1(t) = \left(\frac{\sum_i n_i D_i^m \phi}{\sum_i n_i D_i^n}\right)^{\frac{1}{m-n}} \quad ; \quad f_2(t) = \frac{\sum_i n_i \phi}{V} \tag{3.23}$$

QUANTITY	ϕ	f	Unit
'DIAMETER' (default)	1	f_1	μm
'ENTHALPY'	$(4/3)\rho_i r_i^3 (c_{p,i}(T_i)T_i - c_{p,i}(T_m)T_m)$	f_2	kJ/m^3
'PARTICLE FLUX X'	$(4/3)\rho_i r_i^3 u_i$	f_2	kg/m^{2}s
'PARTICLE FLUX Y'	$(4/3)\rho_i r_i^3 v_i$	f_2	kg/(m$^2\cdot$s)
'PARTICLE FLUX Z'	$(4/3)\rho_i r_i^3 w_i$	f_2	kg/(m$^2\cdot$s)
'U-VELOCITY'	u_i	f_1	m/s
'V-VELOCITY'	v_i	f_1	m/s
'W-VELOCITY'	w_i	f_1	m/s
'VELOCITY'	$(u_i^2 + v_i^2 + w_i^2)^{\frac{1}{2}}$	f_1	m/s
'TEMPERATURE'	T_i	f_1	°C
'MASS CONCENTRATION'	$(4/3)\rho r_i^3$	f_2	kg/m^3
'NUMBER CONCENTRATION'	1	f_2	

Figure 3.1 Output quantities available for PDPA [19]

`PDPA_M`, M, exponent m of diameter.

`PDPA_N`, N, exponent n of diameter.

`PDPA_RADIUS`, defines the concentration based on the sampling volume V.

4 Simulation in FDS

For simulating the model in FDS it was obvious to choose optimal grid should be selected, vent creation, burner installation, PDPA should be attached to measure the parameters with respect to radial distance -1.5m to 1.5m.

4.1.1 Grid selection

To achieve high accurate result or accuracy in convergence of result, the mesh size should be spaced, eventually by grid sensitivity study. For simulating the buoyant plumes, the mesh size selection is given by Equation 4.1 which is a non-dimensional expression $D^*/\delta x$ where D^* is the characteristics fire diameter. $\dot{Q}$ is the total heat release rate of the fire.

$$D = \left[\frac{\dot{Q}}{\rho_\infty c_\infty T_\infty \sqrt{g}}\right]^{2/5} \quad (4.1)$$

To optimize the grid size, the simulation model should be identified multiple times. But according to validation guide of FDS the grid cell size δ_{x10} is referred to the case where $D^*/\delta x = 10$ [20]. So, the initially the grid was chosen accordingly as per the Figure 4.1. As HRR was considered as 500 KW the grid size was selected approximately in between the range. 303 KW and 756 KW was considered and interpolated to achieve grid size of 0.070m

Q^*	$\dot{Q}$ (kW)	D^* (m)	δx_5 (m)	δx_{10}	δx_{20}
0.1	151	0.45	0.090	0.045	0.022
0.2	303	0.59	0.119	0.059	0.030
0.5	756	0.86	0.171	0.086	0.043
1	1513	1.13	0.226	0.113	0.057
2	3025	1.49	0.298	0.149	0.075
5	7564	2.15	0.430	0.215	0.108
10	15127	2.84	0.568	0.284	0.142
20	30255	3.75	0.749	0.375	0.187
50	75636	5.40	1.081	0.540	0.270
100	151273	7.13	1.426	0.713	0.356
200	302545	9.41	1.882	0.941	0.470
500	756363	13.6	2.715	1.357	0.679
1000	1512725	17.9	3.582	1.791	0.895
2000	3025450	23.6	4.726	2.363	1.182
5000	7563625	34.1	6.819	3.409	1.705
10000	15127250	45.0	8.997	4.499	2.249

Figure 4. 1 Grid cell size δ_{x10} referring to $D^*/\delta x = 10$ [20]

Three simulations are carried out for (-2,2), (-2,2), (-2,2) in x, y, z dimension of a room. Grid sizes were chosen to be $20 \times 20 \times 20$ cm, $5 \times 5 \times 5$ cm and simulated accordingly. And the distance from the nozzle to fire is 1.5m with 4000 KW/m^2 as HRRPUA.

4.1.2 Input file specification

As FDS is CFD software which is well known that it uses LES turbulence model to simulate the case model input file should be given in .FDS file which the file can be written in text editor like notepad or notepad++. For easy method notepad++ has been used as convenient text editor.

A sample FDS file, is considered for a detailed explanation. The input file can be categorized into

1) General configuration
2) Computational domain
3) Properties
4) Solid geometry
5) Output

```
1.  !!! General configuration
2.  *creating the header and title
3.  &HEAD CHID= '100_bars_mono_fire_mist', TITLE= 'fire suppression'/
4.
```

The general configuration gives an idea on creating &HEAD line to mention character ID, CHID, the TITLE of the file.

```
1.  !!! Computational domain
2.  *computational domain from Joachim experiment
3.  &MESH  IJK= 20,20,20, XB=-2,2,-2,2,-2,2, / *number of meshes is 20 in all sides
```

The computational domain is invoked in &MESH XB and IJK 20 cells in the x, y & z direction. From the code it is understood that the grid size would be 10cm.

i, e., $2/0.1 = 20$, 2 m length when divided by 0.1m is 20 number of cells.

```
1.  *simulation end time
2.  &TIME T_END= 300. / *the total simulation times
```

&TIME is the simulation time, which is called T_END which is the computational time of the model.

```
1.
2.  *To invoke water vapor (liquid) properties define Species_ID
3.  &SPEC ID ='WATER VAPOR' /
```

The &SPEC line in which the water droplets are invoked as lagrangian particles.

```
1.   *Define device location, orientation, and activation delay
2.  &DEVC ID='Scale 3 nozzle'
3.    XYZ =0,0,0.9
4.    ORIENTATION=0,0,-1
5.    PROP_ID ='ln02'
6.    QUANTITY='TIME'
```

```
7.    SETPOINT =10 /
```

&DEVC is the line which FDS assigns the nozzle in the geometry with the position in the geometry with the position XYZ, ORIENTATION and SETPOINT written as 10 where the sprinkler or nozzle will start to flow the water out to suppress the fire.

```
1.  *Defining nozzle properties
2.  *https://components.semcomaritime.com/wp-content/uploads/SemSafe.pdf,
3.  *(offset, k_factor, operating pressure, and droplet velocity
4.  *From Lundberg experimental reference 2021)
5.  &PROP ID='ln02'
6.    PART_ID ='water drops'
7.    OFFSET =0.30
8.    K_FACTOR =1.2
9.    OPERATING_PRESSURE =100
10.   PARTICLE_VELOCITY=60
11.   SPRAY_ANGLE =0.,55.,
12.   PARTICLES_PER_SECOND =10000
13.   SPRAY_PATTERN_SHAPE='UNIFORM'
14.    /
```

&PROP is the nozzle in which the Lagrangian particles is allowed to flow at K_FACTOR =1.2 from experiment at an OPERATING_PRESSURE=100 with PARTICLE_VELOCITY=60 and SPRAY_ANGLE is assigned for the flow angle of water.

The PARTILCES_PER_SECOND was chosen as 10000 as 5000 was default for FDS. SPRAY_PATTERN_SHAPE is assigned to be UNIFORM which will give the user a uniform distribution of spray pattern.

```
1.  &PART ID='water drops'
2.    SPEC_ID = 'WATER VAPOR'
3.    DIAMETER=40.
4.    MONODISPERSE=.TRUE. /
```

The DIAMETER was assigned for 40 in the first simulation and other two simulation were 80 and 100 to see the behaviour of the pattern and QUANTITIES was 'PARTICLE' 'DIAMETER'.

```
1.   !!!activating fire block
2.  *Creating obstruction for the fire
3.  &OBST XB=-0.20,0.20,-0.20,0.20,-0.70,-1.00/
```

This block is invoked to activate the fire obstruction block through &OBST. The Figure 4.2 shows the model description in FDS and gives am understanding about the geometry.

```
1.   *Defining fuel, heat of combustion in KJ/kg, soot yield is fraction of fuel converted
    into soot.
2.  &REAC ID ='PROPANE'
3.    SOOT_YIELD =0.01
4.    CO_YIELD=0.02
```

```
5.    HEAT_OF_COMBUSTION =46460
6.    CRITICAL_FLAME_TEMPERATURE =1267/
```

```
1.  *Define fuel, heat of combustion in KJ/kg, soot yield is fraction of fuel converted into
    soot.
2.  &REAC ID ='PROPANE'
3.    SOOT_YIELD =0.01
4.    CO_YIELD=0.02
5.    HEAT_OF_COMBUSTION =46460
6.    CRITICAL_FLAME_TEMPERATURE =1267/
```

For the burning of fire, Propane fuel was used as fuel. `&REAC` line is the one where user can invoke fuel. `HEAT_OF_COMBUSTION` and `CRITICAL_FLAME_TEMPERATURE` was mentioned for propane.

```
1.  *fire activation through HRRPUA
2.  &SURF ID='fire', HRRPUA = 2000/*obst_Area=0.25m^2 and HRR=500kw
```

The fire in the FDS and its Heat Release Rate Per Unit Area `HRRPUA` is mentioned to create the quantity of heat in terms of KW. `&SURF` is the line where the user can mention the quantity.

```
1.   *placing a vent plane for fire
2.  &VENT XB=-0.20,0.20,-0.20,0.20,-0.70,-0.70, SURF_ID='fire',/
```

This piece of code is used to invoke the fire on the obstruction with the help of plane in FDS.

```
1.  !!!declaring geometry
2.  &VENT MB='XMIN', SURF_ID='OPEN'/*BC open for left
3.  &VENT MB='XMAX', SURF_ID='OPEN'/*BC open for right
4.  &VENT MB='YMIN', SURF_ID='OPEN'/*BC open for front
5.  &VENT MB='YMAX', SURF_ID='OPEN'/*BC open for back
```

As shown in Figure 4.2, an open boundary condition assumes that ambient conditions exist beyond that `VENT`. `OPEN` can only be defined at an exterior boundary of the computational domain.

This is the end of the script, and the input file is ready for simulation.

```
1.  &SLCF PBX=-0.1, QUANTITY='TEMPERATURE'/
2.  &SLCF PBY=-0.1, QUANTITY='TEMPERATURE'/
3.  &SLCF PBX=-0.1, QUANTITY='PARTICLE FLUX Z', PART_ID = 'water drops', VECTOR=.TRUE. /
4.  &SLCF PBX=-0.1, QUANTITY='W-VELOCITY' /
5.
6.  &SLCF PBY=0.0, QUANTITY='TEMPERATURE' /
7.  &SLCF PBY=0.0, QUANTITY='MASS FRACTION', SPEC_ID='WATER VAPOR' /
8.  &SLCF PBY=0.0, QUANTITY='MPUV', PART_ID='water drops' /
9.  &SLCF PBZ=0.1, QUANTITY='PARTICLE FLUX Z', PART_ID='water drops' /
10.
11. &BNDF QUANTITY='WALL TEMPERATURE'/*boundary file
12. &BNDF QUANTITY='NET HEAT FLUX'/*boundary file
```

The output file is given in the above piece of code where, TEMPERATURE, PARTICLE FLUX, W-VELOCITY, MASS FRACTION, MPUV and PARTICLE FLUX Z at the respective positions at X and Y plane.

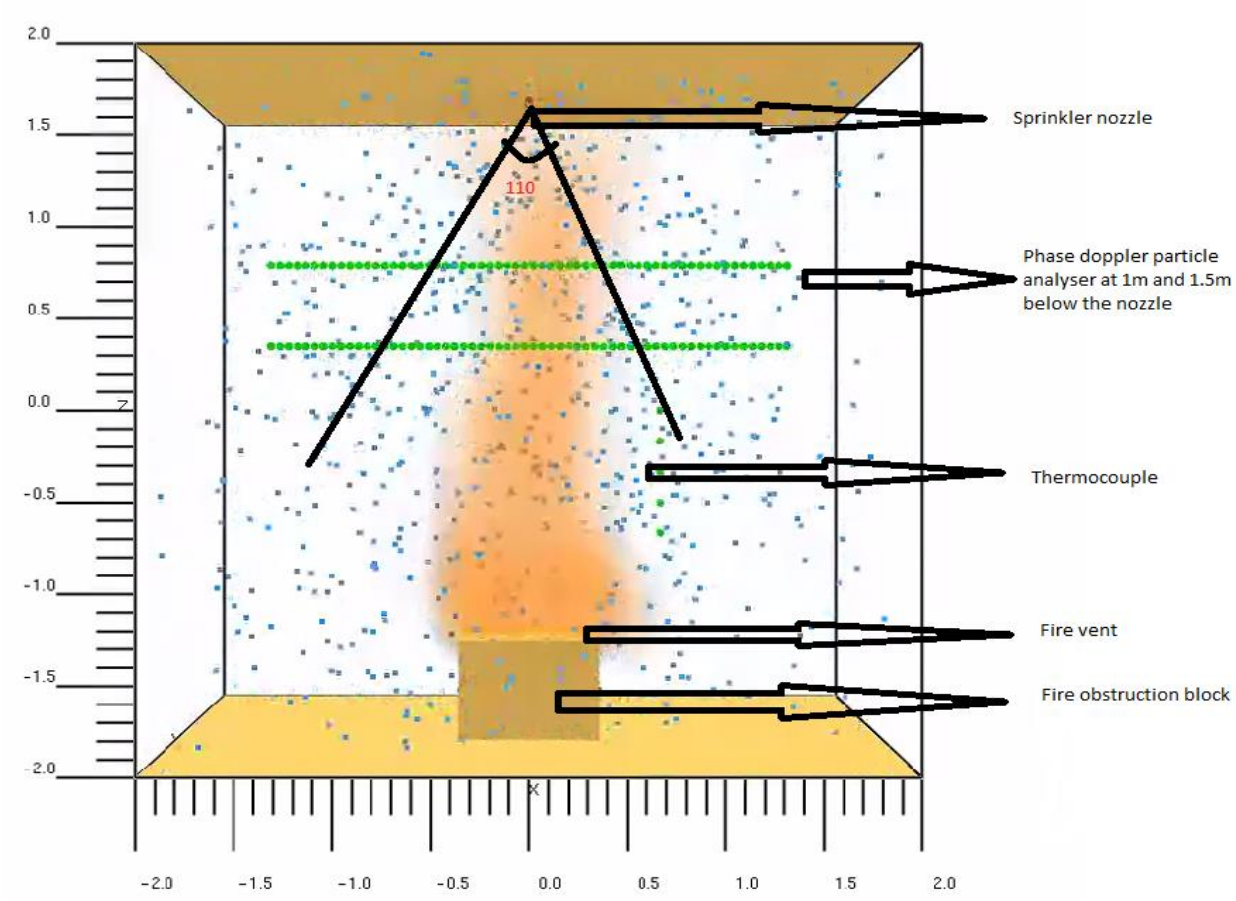

Figure 4.2 FDS simulation model describing parts and obstruction

```
!!! Activating the thermocouple block
*Adding device thermocouple for measuring the temperature at various points
&DEVC ID='TEMP1', XYZ=0.8,0.8,-0.8, QUANTITY='THERMOCOUPLE'/
&DEVC ID='TEMP2', XYZ=0.8,0.8,-0.6, QUANTITY='THERMOCOUPLE'/
&DEVC ID='TEMP3', XYZ=0.8,0.8,-0.4, QUANTITY='THERMOCOUPLE'/
&DEVC ID='TEMP4', XYZ=0.8,0.8,-0.2, QUANTITY='THERMOCOUPLE'/
&DEVC ID='TEMP5', XYZ=0.8,0.8,0.0, QUANTITY='THERMOCOUPLE'/
```

This above block of code specifies the thermocouple where it is placed in the side of the room at different height for to compare temperature at different levels. The &DEVC is the line where devices can be called in as in the Figure 4.2

```
&PROP ID='pdpa_w00'
      PART_ID='water drops'
      QUANTITY='W-VELOCITY'
      PDPA_RADIUS=0.012
```

```
5.        PDPA_START=11
6.        PDPA_END=250.0
7.        PDPA_M=0
8.        PDPA_N=0
9.       /
10.
11. &PROP ID='pdpa_w33'
12.       PART_ID='water drops'
13.       QUANTITY='W-VELOCITY'
14.       PDPA_RADIUS=0.012
15.       PDPA_START=11
16.       PDPA_END=250.0
17.       PDPA_M=3
18.       PDPA_N=3
19.      /
20.
21. &PROP ID='pdpa_n'
22.       PART_ID='water drops'
23.       QUANTITY='NUMBER CONCENTRATION'
24.       PDPA_RADIUS=0.012
25.       PDPA_START=11
26.       PDPA_END=250.0 /
27.
28. &PROP ID='pdpa_d10'
29.       PART_ID='water drops'
30.       QUANTITY='DIAMETER'
31.       PDPA_RADIUS=0.012
32.       PDPA_START=11
33.       PDPA_END=250.0
34.       PDPA_M=1
35.       PDPA_N=0
36.       /
37.
38. &PROP ID='pdpa_d32'
39.       PART_ID='water drops'
40.       QUANTITY='DIAMETER'
41.       PDPA_RADIUS=0.012
42.       PDPA_START=11
43.       PDPA_END=250.0
44.       PDPA_M=3
45.       PDPA_N=2
46.       /
47.
48.
49.
50. &PROP ID='pdpa_f'
51.       PART_ID='water drops'
52.       QUANTITY='PARTICLE FLUX Z'
53.       PDPA_RADIUS=0.012
54.       PDPA_START=11
55.       PDPA_END=250.0 /
56.
```

All PDPA measurement is recorded using the above piece of code where the PDPA is in introduced in `&PROP` line with a name list `ID` and give a `QUANTITY` with a `PDPA_RADIUS` denoting the size of the PDPA which is a green color ball lined horizontally as shown in the Figure 4.2. `PDPA_START` and `PDPA_END` is the line of code where PDPA starts to record the entire measurement of all parameters with respect to radial distance.

```
1.  *end FDS script
```

```
2. &TAIL/
```

This above FDS code is the end of the input file.

4.1.3 Modelling of sprinkler and mist in FDS

Both sprinkler and water mist system are modelled in FDS in a similar manner. The location of `DEVC` line along with properties of water mist and sprinkler which are specified in `PROP` line.

Volume median diameter (VMD)

The size distribution of sprays is characterized by the VMD that has been specified using `DIAMETER` in micrometers. This diameter represents the point in distribution where 50% of water volume is made of droplets having smaller diameters than higher values.

Droplet size distribution

In FDS, the default setting in droplet size distribution is `ROSSIN-RAMMLER-LOGNORMAL` that is combination of log-normal and Rossin-Rammler probability density functions. This option can be changed between the two functions as a single function. The possibility of simulating a mono-disperse spray by adding `MONODISPERSE=.TRUE.` in the `PART` line. And if the polydisperse needed to simulate then only `GAMMA_D`, $\gamma = 2.4$ value needed to be in the input.

4.1.4 Modelling of sprinkler and mist in FDS

The spray parameters setup is discussed below.

Placement of Droplets

When water stream comes out of the nozzle, it travels in the gas phase and gets a creation of separate water droplets once it has reached to a certain distance has been travelled by water particles depending on nozzle configuration. This is also referred to as 'break-up' or 'atomization' of water droplets from the literature [21]. In FDS, to show this stream of spray, the droplets away from the nozzle head location. `OFFSET` when set in `PROP` line specifies the FDS to maintain the distance. `OFFSET= 0.3` Using too small offset gave unrealistic results so the offset was raised to 0.3m since the computational domain was coarse. This parameter is set based on computational domain and offset in this case is large as to distribute the incoming droplets among large enough number of computational cells. This effect is related to the transfer of momentum from disperse phase to gas phase [22].

Spray Cone Shape

Market provides a user with varied specification of nozzles for different applications. A conical spray angle $'\theta'$ is being defined by FDS using `SPRAY_ANGLE` input, in which for most 0,55 and 0,56 for mist and sprinkler has been used respectively. Where inner angle is defined as 0 here.

Orifice Diameter

Orifice diameter is used in FDS via `ORFICE_DIAMETER` in the FDS code via `PROP` line. 0.0096m has been used in the sprinkler.

K-factor

The sprinkler and mist nozzle has different "K-factors" specifications. For water mist nozzle the K-factor is 1.19 and for Sprinkler is 58.8 which is mentioned in FDS through the input line `K_FACTOR` in PROP line. If K-factor is mentioned, it is not required to mention the flow rate as the FDS, self will calculate the same.

$$K = Q/\sqrt{p} \tag{4.2}$$

Where Q is the flow rate of the water and p is the water pressure measured at the spray head. The unit of K-factor is $\mathrm{L}/(\mathrm{min.\,bar}^{1/2})$

PARTICLES_PER_SECOND:

The water spray is represented in FDS through `PARTICLES_PER_SECOND`. The number is 5000 as default in FDS and can also increase to produce the spray distributed among a higher number of computational droplets.

5 Results from FDS

There were several numbers of simulation conducted for this thesis to study the comparisons with different scenarios. The study was conducted for mist and sprinkler fire suppression systems. The flow chart is constructed as in the Figure 5.1

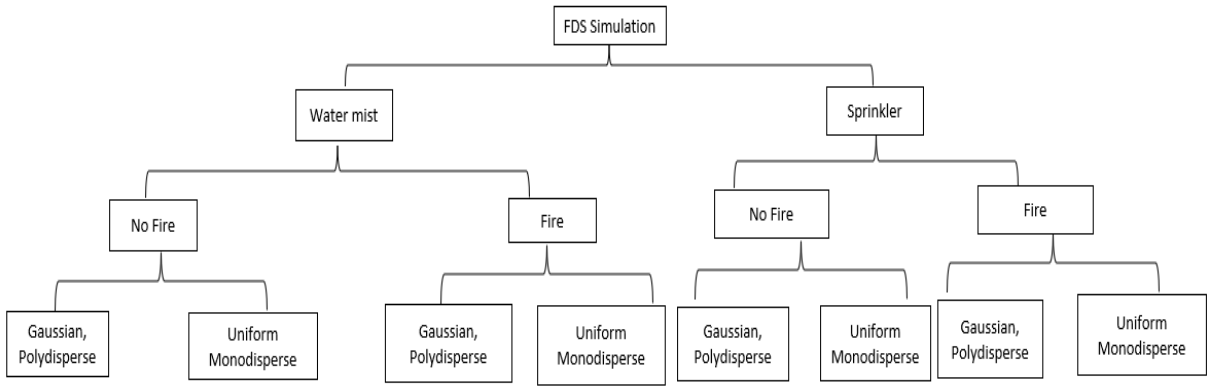

Figure 5.1 Flow chart of FDS simulation for this thesis

The simulation was taken into 50 and 100 bar operating pressure with 112 spray angles respectively. The sprinkler was simulated at 2 bar, 5 bar and 8 bar at $D_{v,50}$, 419, 315 and 304 microns respectively.

The comparison shall be made between the fire and non-fire scenario so see the behavior of the droplets with respect to the parameters. The simulation was run for 300 seconds with same parameter keeping constant for sprinkler and water mist.

5.1.1 Scenario overview

Comparison of 2 bar monodisperse vs poly disperse measured at 1m and 1.5m below the sprinkler nozzle with and without fire.

Scenario 1: Non-fire vs fire for 2 bar at diameter 419 microns for at 1m below and 1.5m below the sprinkler to analyse the suppression parameters,

1) Number of droplets
2) Droplet size distribution, Sauter mean diameter, d_{32}
3) Velocity distribution

Scenario 2: Non-fire vs fire for 5 bar at diameter 315 microns for at 1m below and 1.5m below the sprinkler to analyse the suppression parameters,

1) Number of droplets
2) Droplet size distribution, Sauter mean diameter, d_{32}
3) Velocity distribution

Scenario 3: Non-fire vs fire for 8 bar at diameter 304 microns for at 1m below and 1.5m below the sprinkler to analyse the suppression parameters,

1) Number of droplets

2) Droplet size distribution, Sauter mean diameter, d_{32}
3) Velocity distribution

Scenario 4: Non-fire vs fire for 100 bar at diameter 40 microns for at 1m below and 1.5m below the nozzle to analyse the suppression parameters,

1) Number of droplets
2) Droplet size distribution, Sauter mean diameter, d_{32}
3) Velocity distribution

Scenario 5: Grid sensitivity analysis

5.1.2 Scenario 1: Droplet Number Concentration – 2 bar 419 µm

The droplet number concentration was compared between monodisperse and polydisperse spray simulation with absence and presence of the fire of 4000 KW/m^2. The Figure 5.1 (a) and (b) are the representing the measurement taken from the below 1m and 1.5m below the nozzle. A firm comparison has been made, from the plot, the number of concentrations seems promising for polydisperse spray as there is varied value of approximately 2.5E7 droplets have been measured at 1m and 1.5 m. But with fire scenario, (c) and (d) the droplets get evaporated and due to fire the larger droplet only penetrates through the fire plume, which shows a reduction in number of droplets at 0 m radial distance. The monodisperse spray represented in orange colour shows a disagreement as major of computational domain has not resolved properly by FDS which seems like a shortcoming in grid selection.

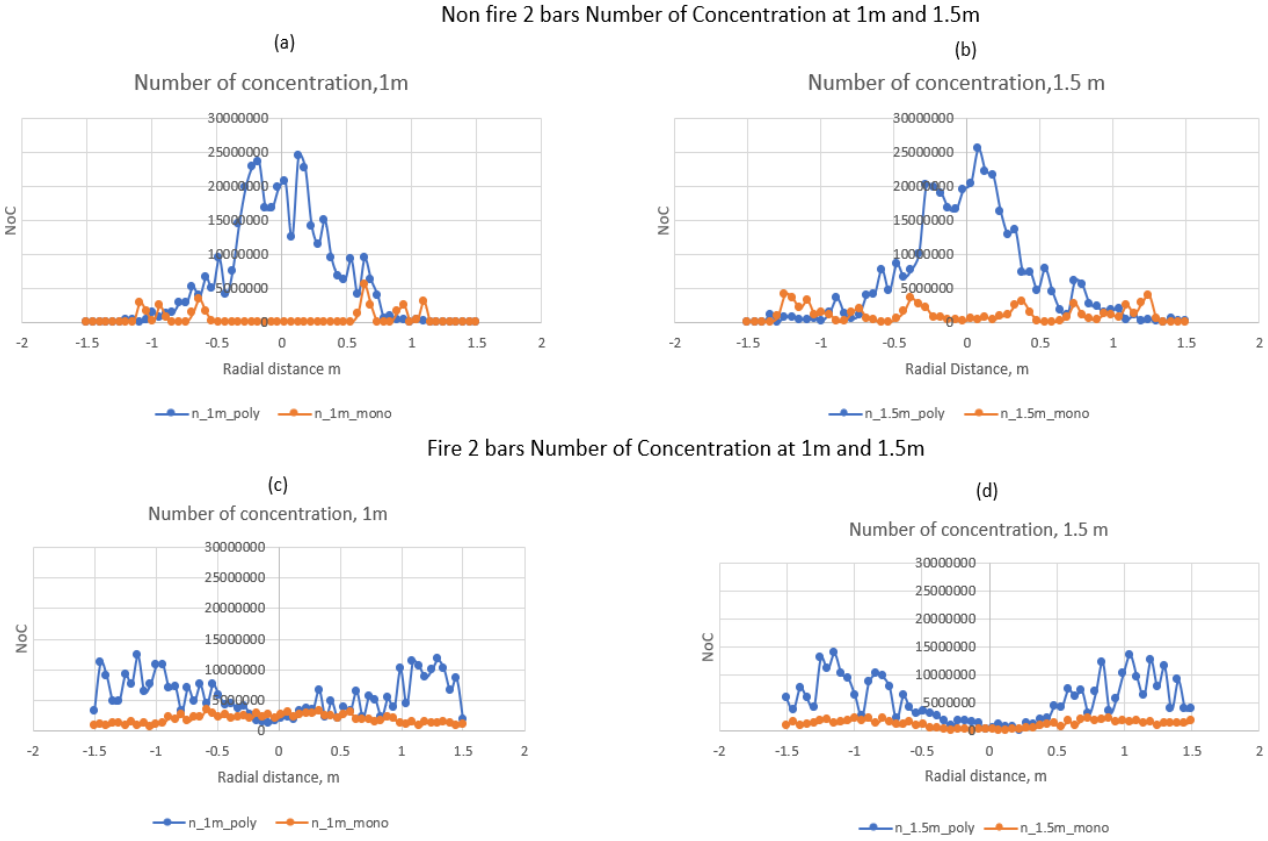

Figure 5.1 Droplet concentration at 1m and 1.5m with non-fire vs fire scenario

5.1.3 Scenario 1: Droplet Size Distribution, SMD, d_{32}2 bar 419 µm

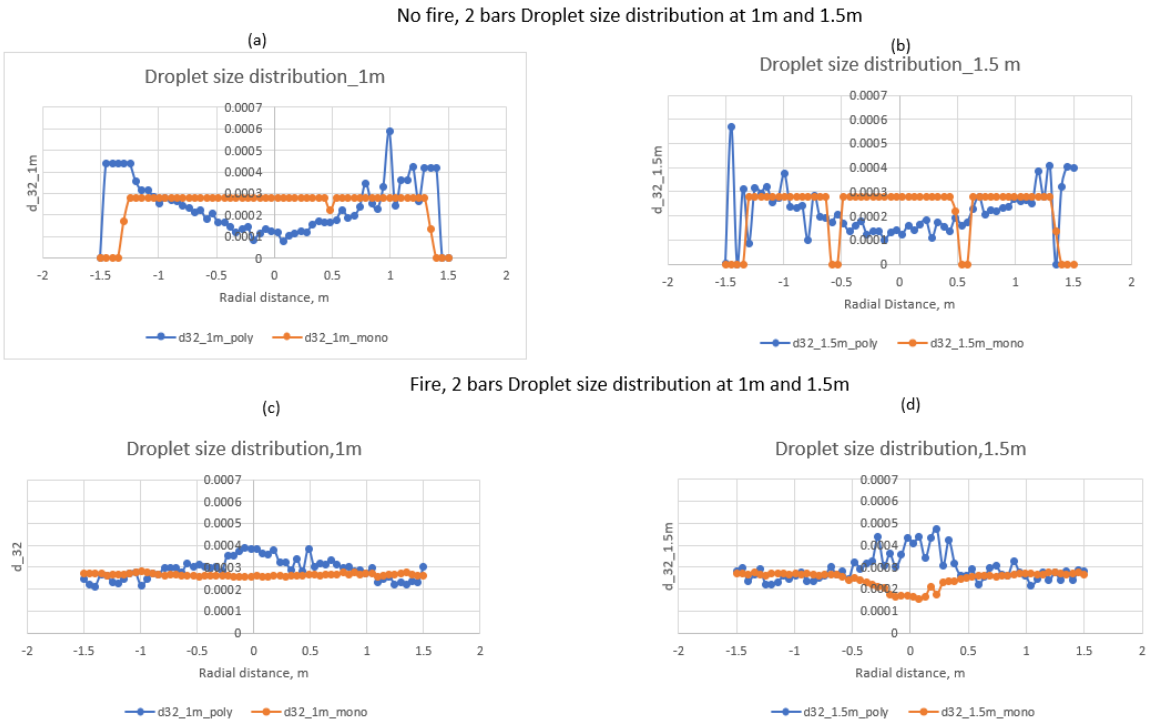

Figure 5.2 Droplet size distribution at 1m and 1.5m with non-fire vs fire scenario

The droplet size distribution in which Sauter Mean Diameter (SMD) is calculated as a standard representative diameter in FDS through PDPA. In Droplet size distribution, there is an incorrectness can be spotted in Figure 5.2 (a),(b),(c)&(d) as the FDS results 300 μm in monodisperse spray. This is because the PDPA device averages the PDPA calculation over time. The fact is that at every time step there is a droplet located in 1.2 cm of radius of PDPA volume that have been chosen in the thesis for 5000 droplets per second at the nozzle. The fact is monodisperse of 419 microns distribution having PDPA return of approximately 300 microns indicates that the simulation has a drop present in the PDPA radius has 63% of time. Likelihood it can be considered as lesser particles per second.

5.1.4 Scenario 1: Velocity distribution, 2 bars 419 µm

Since the droplet is falling in 'W'-direction the velocity axis is in negative values. The Figure 5.3 (a), (b) represents non fire scenario. The monodisperse spray and poly disperse spray at 1m down the nozzle. The time when the droplets spray out of the nozzle promising as PDPA has measured 6 m/s at 1m below the nozzle and at 1.5 m below the nozzle. With the presence of fire, the plot interprets showing positive values as the fire of 4000 KW/m^2 blows the sprays and suppresses the velocity of droplets. The plot shows that some droplets can penetrate down the fire plume to suppress the fire.

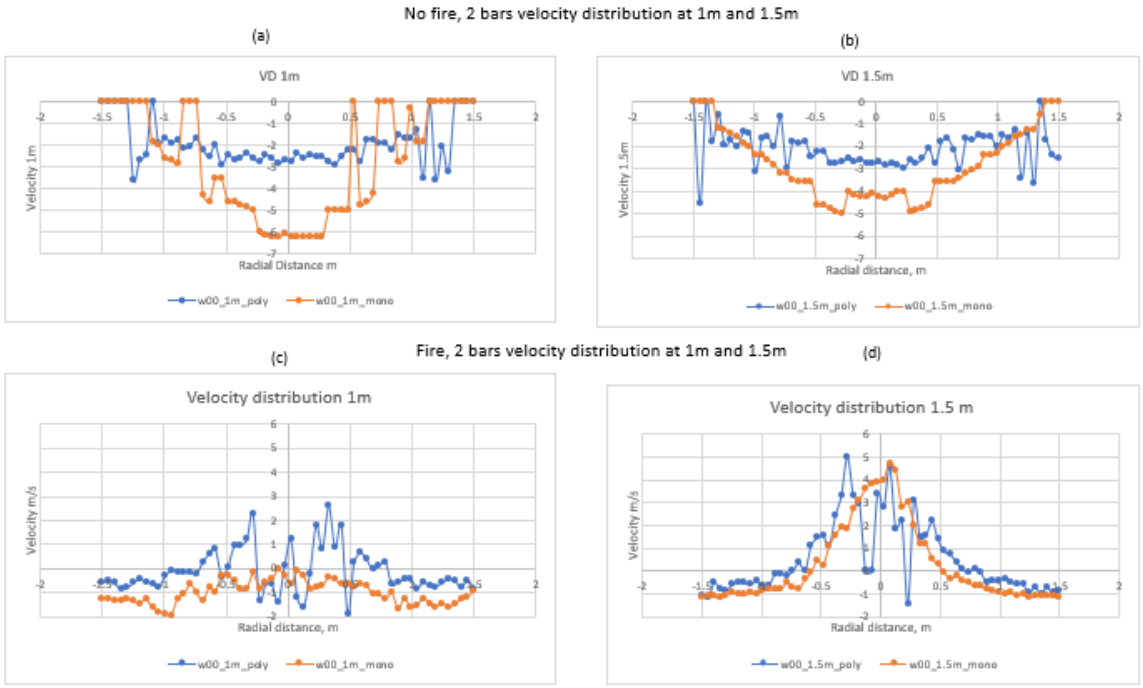

Figure 5.3 Velocity distribution at 1m and 1.5m with non-fire vs fire scenario

5.1.5 Scenario 2: Droplet Number Concentration, 5 bar & 315 µm

This scenario represents only the change of pressure and median droplet diameter Dv_{50}.The pressure here is 5 bars and median diameter is 315 microns. The droplet concentration without fire seems less in the center while comparing the sides. The peak of the +0.3 to -0.3 radial distance for polydisperse case. But monodisperse case seems resolved incorrectly due to reduced grid resolution. But still there is a distribution above zero.

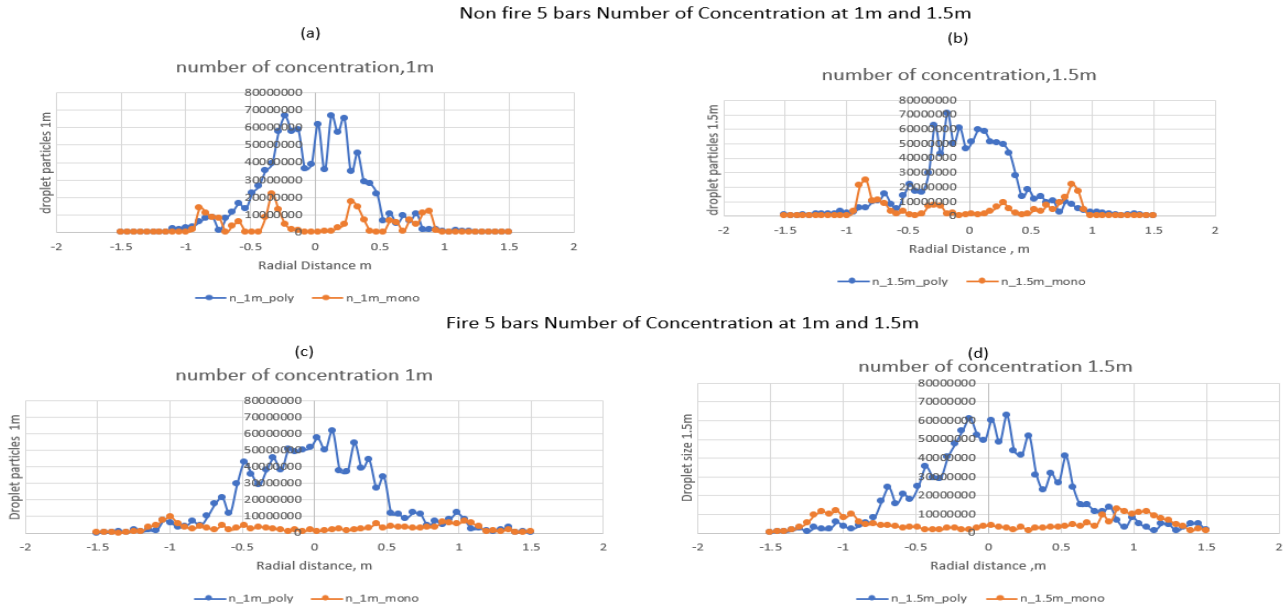

Figure 5.4 Droplet concentration at 1m and 1.5m with non-fire vs fire scenario

5.1.6 Scenario 2: Droplet size distribution 5 bars & 315 µm

The Figure 5.5 shows the droplet size distribution at 1m (a) and (b) with absence of fire and 5.5 (c) and (d) with presence of fire. The droplet size distribution, for 5 bar at 315 microns, seems 200 microns for monodisperse plot because of the reduced volume of PDPA and 5000 droplets per second as denoted in the previous case. This is due to time average that, the drops present in PDPA is approximately 63% of the time as per previous case. 315 microns multiplied by 0.63 gives 200 microns.

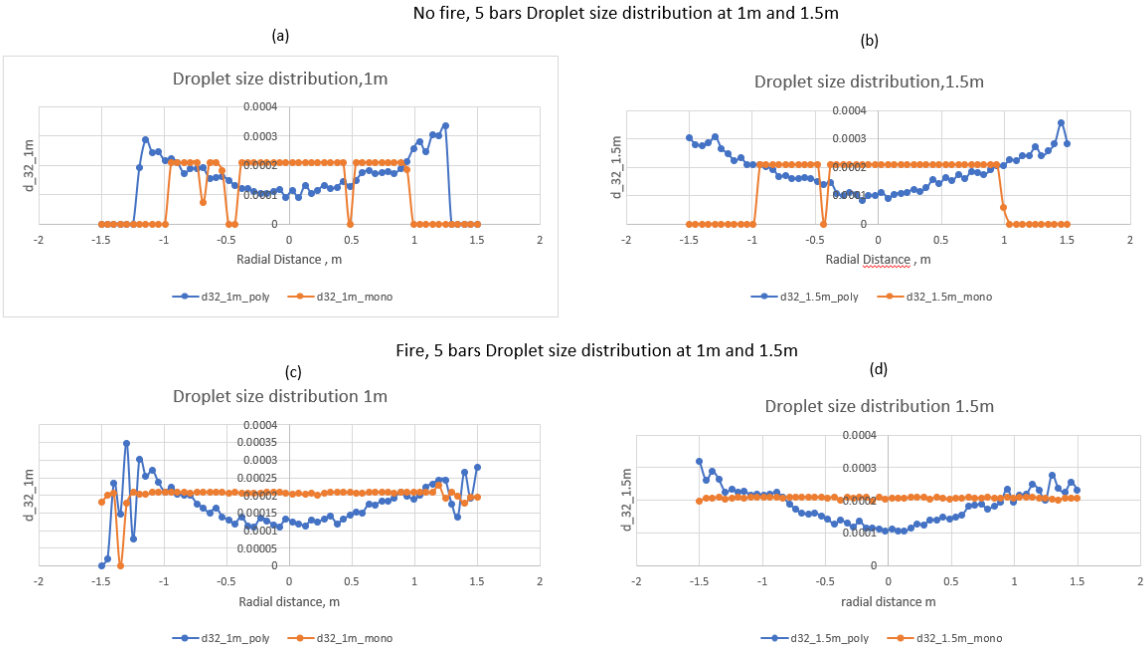

Figure 5.5 Droplet size distribution at 1m and 1.5m with non-fire vs fire scenario

5.1.7 Scenario 2: Velocity distribution 5 bars & 315 µm

Since the pressure is higher than the previous case as the velocity is increased and trying to penetrate towards the fire plume. Here Figure 5.6 (a) and (b) shows velocity distribution at 1m below the nozzle shows slight difference approximately at 5 m/s in both sprays but polydisperse and monodisperse 1.5m down the sprinkler agrees each other at 4 m/s.

The Figure 5.6 (c) and (d) with fire scenario, the droplets of 315 μm at 5 bars tries to penetrate down the fire plume. Here monodisperse spray performs well than polydisperse spray. There is a slight change in polydisperse spray when compared to 1m and 1.5m down the sprinkler.

Figure 5.6 Velocity distribution at 1m and 1.5m with non-fire vs fire scenario

5.1.8 Scenario 3: Droplet number concentration 8 bars 304 µm

Figure 5.7 (a) and (b) shows the difference between the number of droplets with monodisperse and polydisperse spray droplet number concentration. The polydisperse spray gives a good value at 1m and 1.5m down the nozzle. But with fire from Figure 5.7(c) and (d) shows there is no concentration in monodisperse spray since it is unresolved. May be increasing the grid resolution yields better result.

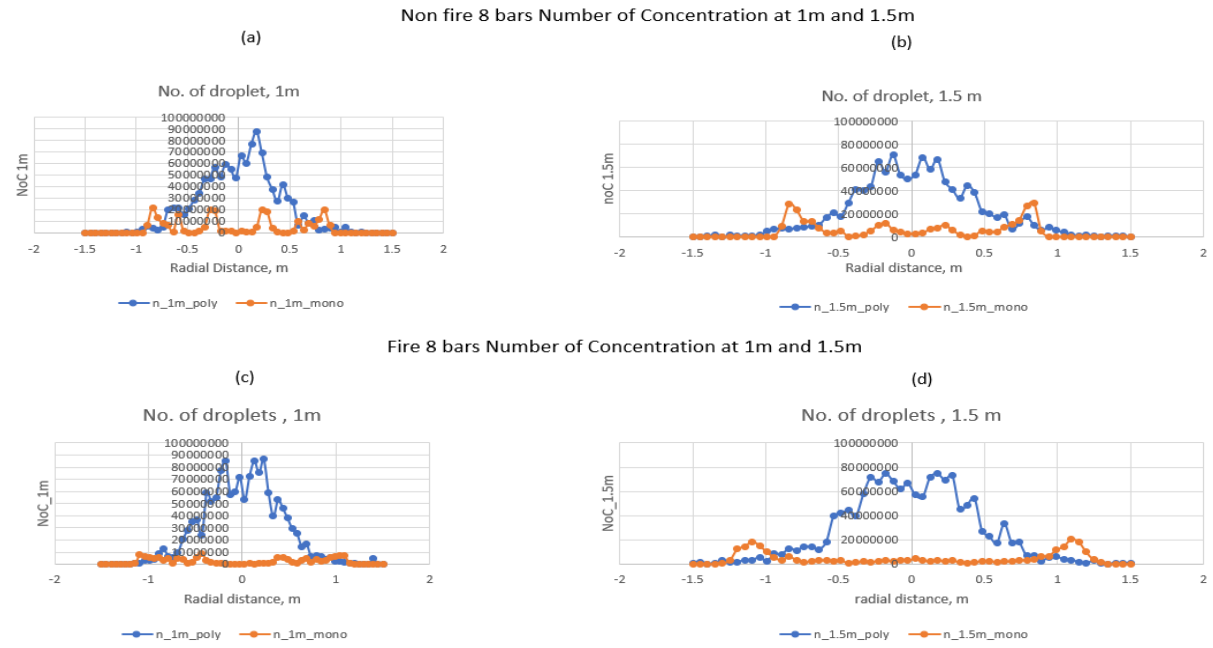

Figure 5.7 Droplet concentration at 1m and 1.5m with non-fire vs fire scenario

5.1.9 Scenario 3: Droplet size distribution 8 bars 304 µm

The droplet size distribution in this scenario is described in Figure 5.8 (a), (b),(c)&(d) at 1m and 1.5m with absence and presence of fire. Due to the PDPA small PDPA volume the diameter tends to be 63% less than the input value as seen in the previous cases. But when polydisperse spray is observed, the droplets tend to break down as it is flowing downwards. Thus, there is a varied flow of diameter in this case. Likewise, the with fire FDS was not able to predict the actual distribution due to coarse cells spacing in both the levels.

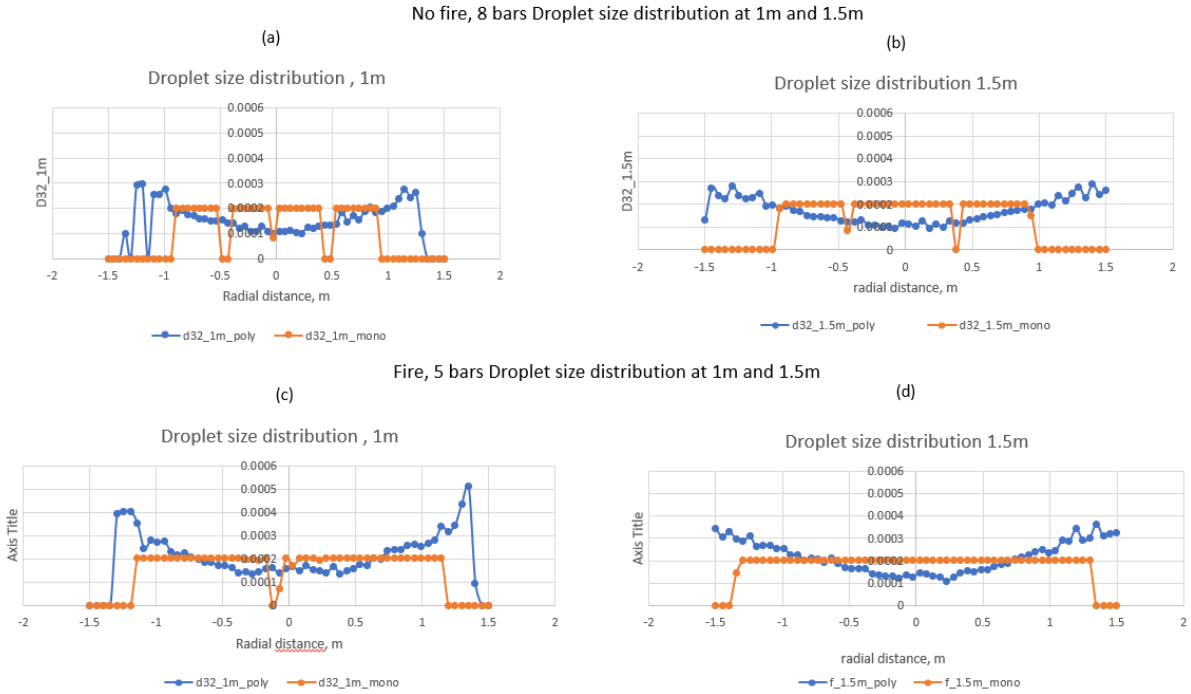

Figure 5.8 Droplet size distribution at 1m and 1.5m with non-fire vs fire scenario

5.1.10 Scenario 3: Velocity distribution 8 bars 304 µm

The velocity distribution as per the Figure 5.9 (a) and (b) shows the velocity is reached at 6 m/s approximately and here monodisperse and polydisperse spray shows an agreement in droplet velocity. With fire scenario 5.9 (c) and (d) the polydisperse spray has lesser value when comparing to the monodisperse spray. Since the diameter of monodisperse spray is same, it has a sound terminal velocity when compared to polydisperse spray.

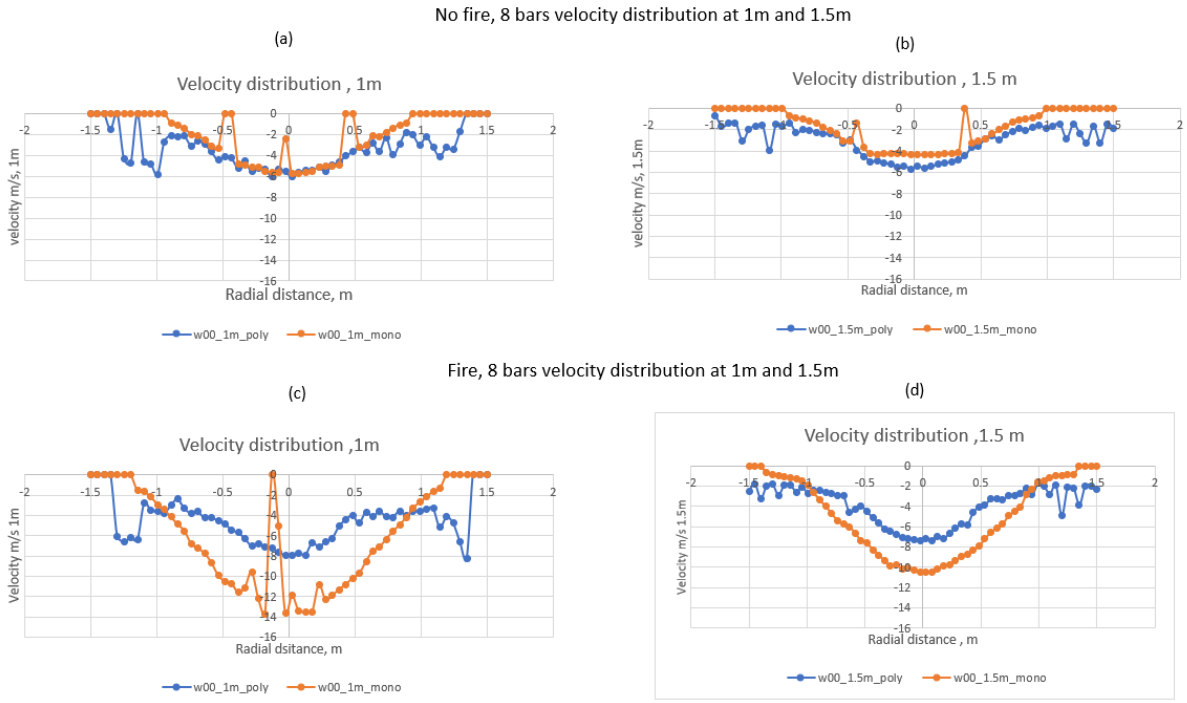

Figure 5.9 Velocity distribution at 1m and 1.5m with non-fire vs fire scenario

5.1.11 Scenario 4: Droplet Number Concentration 100 bar 40 µm

The water mist spray differentiates from normal deluge spray by diameter size and high pressure. Thus, small diameter size of 40 microns with 100 bars pressure have been accounted in simulation. Thus, the monodisperse assumption vs polydisperse spray distribution have been simulated. From the Figure 5.10 (a) and (b) shows no fire situation at 1m and 1.5m down the nozzle. Since the pressure in water mist is 100 bars, the monodisperse spray shows less number concentration when compared to polydisperse spray. The center of the nozzle shows less droplet concentration for monodisperse spray. The same behavior is present at 1.5m down the nozzle. The Figure (c) and (d) shows a slight agreement in with both the type of sprays.

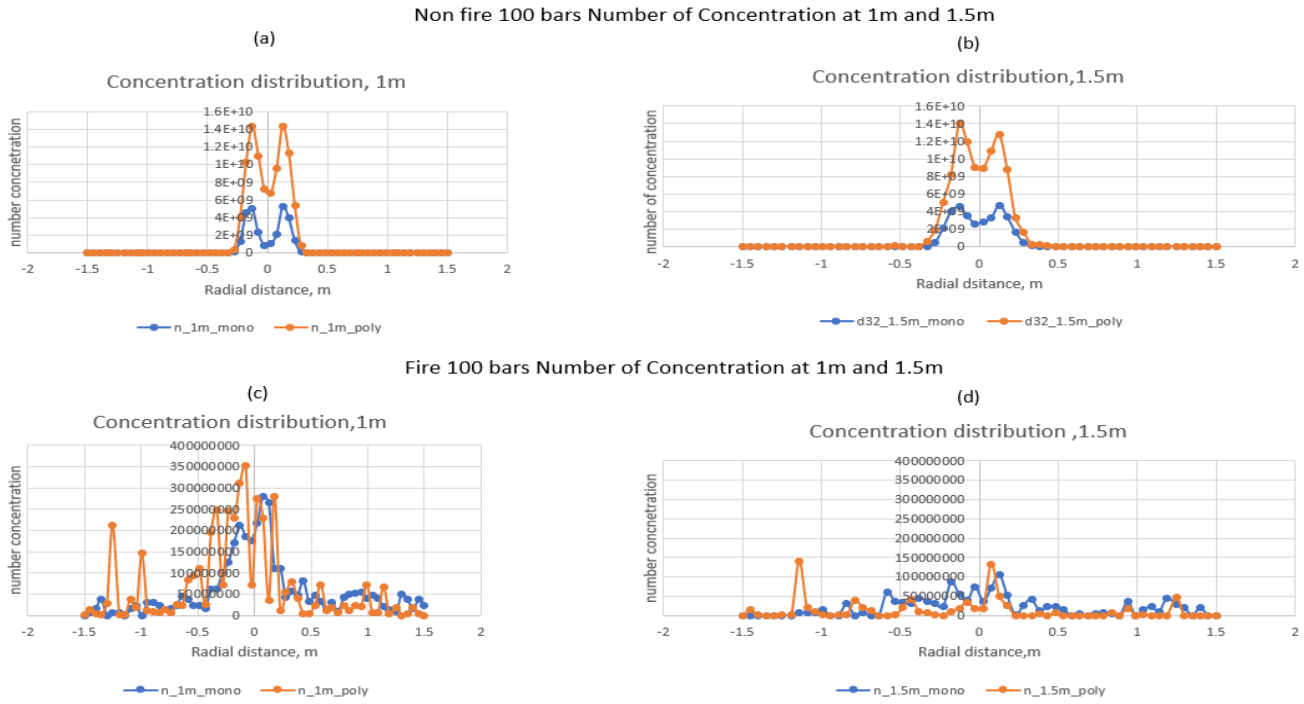

Figure 5.10 droplet size distribution at 1m and 1.5m with non-fire vs fire scenario

5.1.12 Scenario 4: Droplet Size Distribution, 100 bar 40 µm

The Figure 5.11 (a) and (b) shows the droplet size distribution at 1m and 1.5m below the nozzle where the as mentioned previously the FDS is calculating only the 63% of the monodisperse spray due to the lesser volume of PDPA and 5000 droplets per second [23]. The Figure 5.11 (c) and (d) with fire scenario shows the varied droplet size distribution in both 1m and 1.5m down the nozzle.

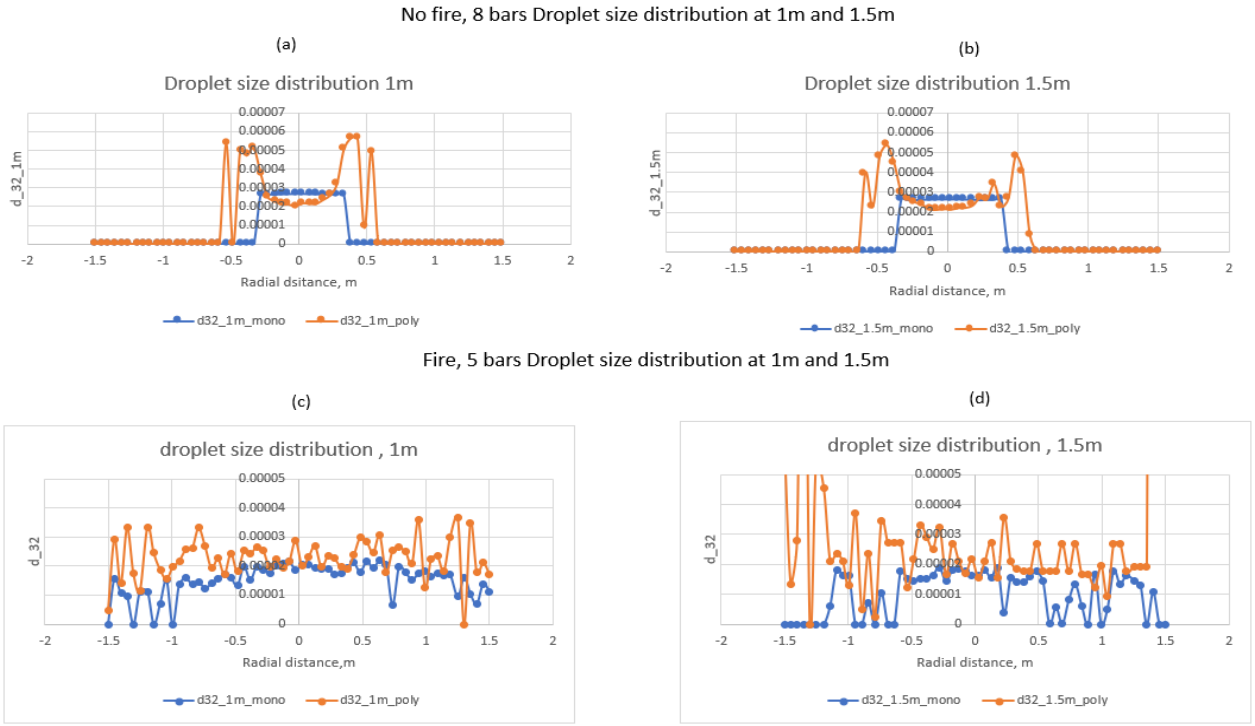

Figure 5.11 Droplet size distribution at 1m and 1.5m with non-fire and fire scenario

5.1.13 Scenario 4: Velocity Distribution, 100 bars 40 µm

The velocity is distributed at non fire scenario as shown in the Figure 5.12 (a) and (b), and the maximum droplet velocity is achieved approximately 3.8 m/s at 1m and 1.5m. This is due to 100 bars pressure and small 40 microns. There is a fluctuation in velocity in the droplet with

fire which tend to show the agreement in both monodisperse and polydisperse spray as shown in Figure (c) and (d).

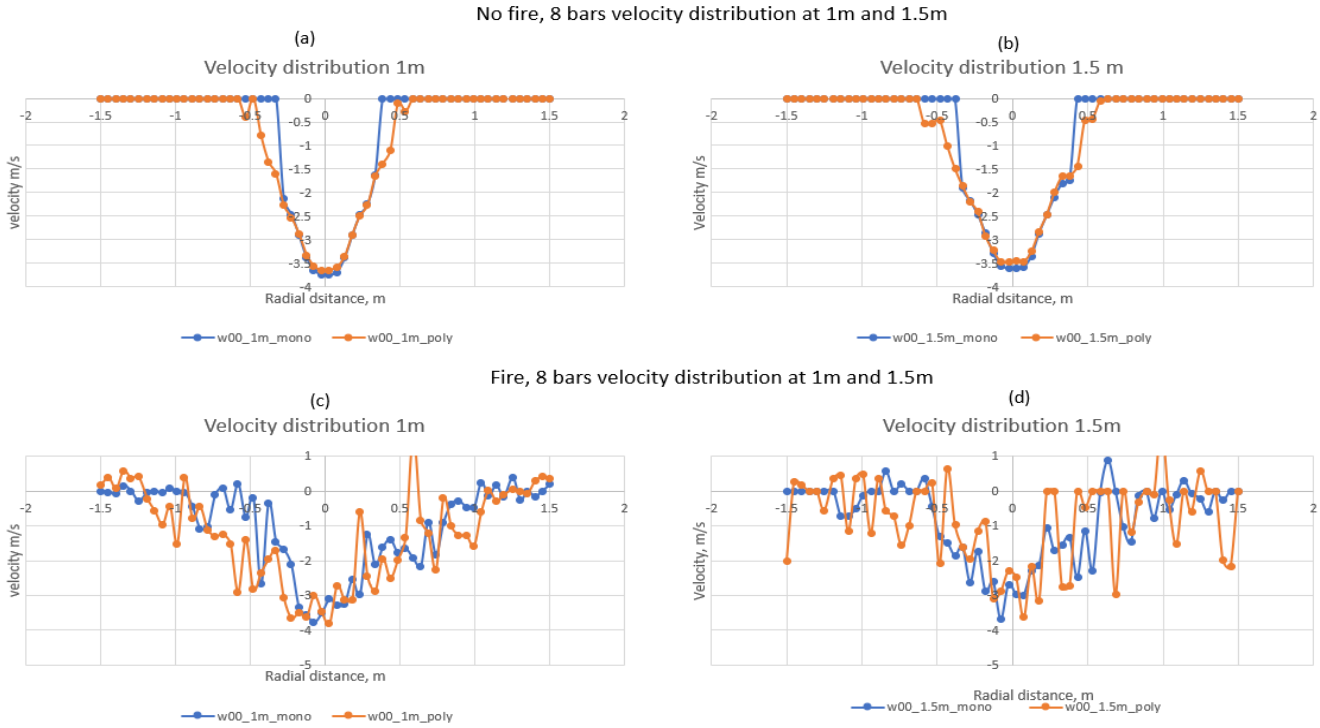

Figure 5.12 Velocity distribution at 1m and 1.5m with non-fire and fire scenario

6 Grid Sensitivity Analysis

The quality of simulation can be improved by performing the grid resolution. In this case, the geometry has been modified by changing from `&MESH IJK= 20,20,20,` from to `IJK=80,80,80,` for `XB=-2,2,-2,2,-2,2 .` Here `XB` is the dimension of geometry.

Reducing the mesh size increase of grid size resolution for providing better results. Mostly the calculations may be resolved and provides better result than coarse mesh. Sprinkler simulation for 5 bars 315μm, results show a varied change when 20 cm grid is when compared to 5cm on same condition for monodisperse spray under absence of fire condition.

The Figure 6.1 shows the difference in mesh size. In previous cases the grid size was coarse and was chosen as 20cm. Here, 5cm fine mesh size is being chosen and results from FDS is depicted in the Figure 6.2 and 6.3. Figure 6.4 depicts the 10cm grid size which is considered in the simulation.

The number droplet concentration and droplet size distribution, the cells are being resolved in the fine mesh when compared to 20 cm grid size. The velocity distribution, when compared between both the cells there is a sound distribution in fine mesh when compared to coarse mesh.

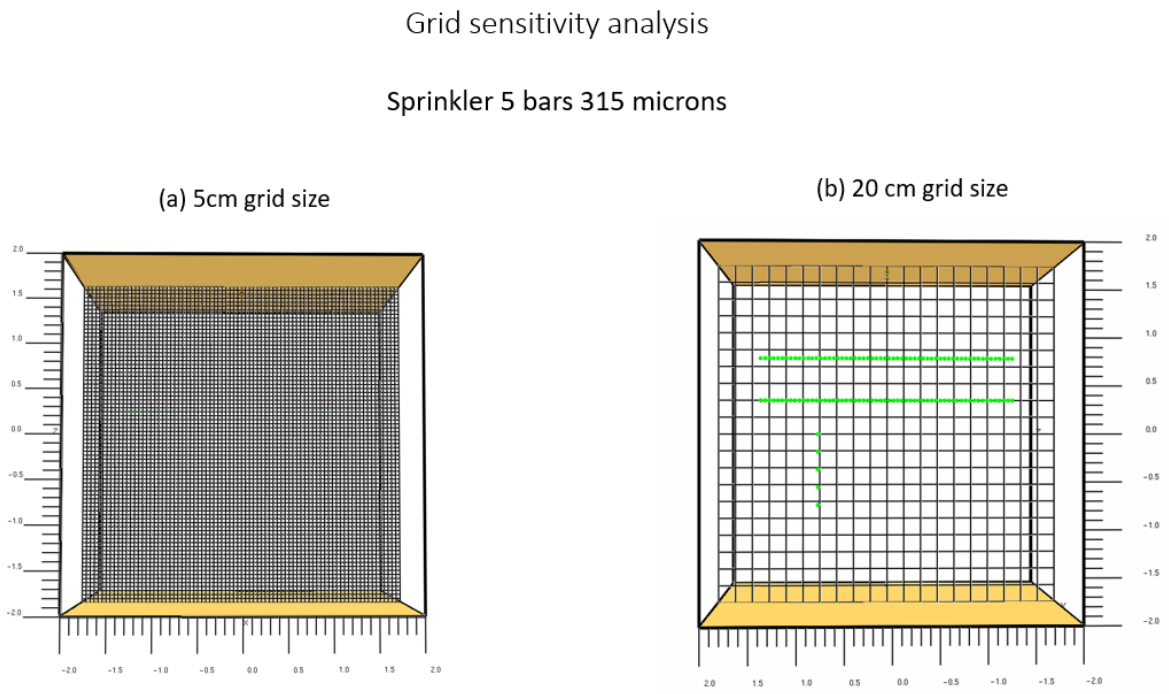

Figure 6.1 Grid sensitivity analysis for 5 cm and 20 cm grid size

6.1.1 Scenario 5: Droplet concentration, Droplet Size Distribution & Velocity Distribution for 5bar, 5cm vs 20cm

The Figure 6.2 and 6.3 shows the Droplet concentration, DSD, and Velocity distribution respectively under absence of fire. The number of droplets plot for 20cm shows irregularities in high change in value. But, fine mesh, 5cm the shows high resolving capacity and give better

results comparatively as shown in Figure 6.2. Figure 6.2 (Right) shows the uniform distribution of diameter for 5 cm when compared to coarse mesh. While seeing Figure 6.3 the 5cm shows a better outcome than 20cm.Thus, 5cm is considered as highly fine mesh and 20cm is coarse mesh. The intermediate is 10cm is chosen to reduce the spend less time and give a competitively good result. The Figure 6.4 is the 10cm grid size for the computational domain.

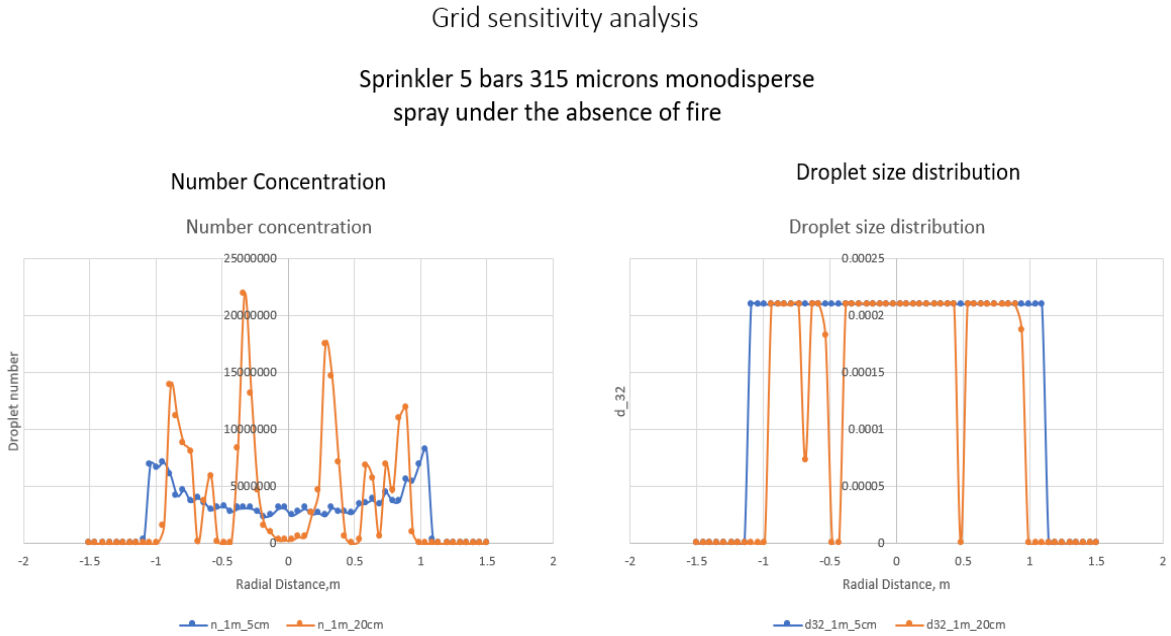

Figure 6.2 Number concentration (Left) and droplet size distribution (Right) for Sprinkler 5 bar 315μm diameter for monodisperse spray under absence of fire.

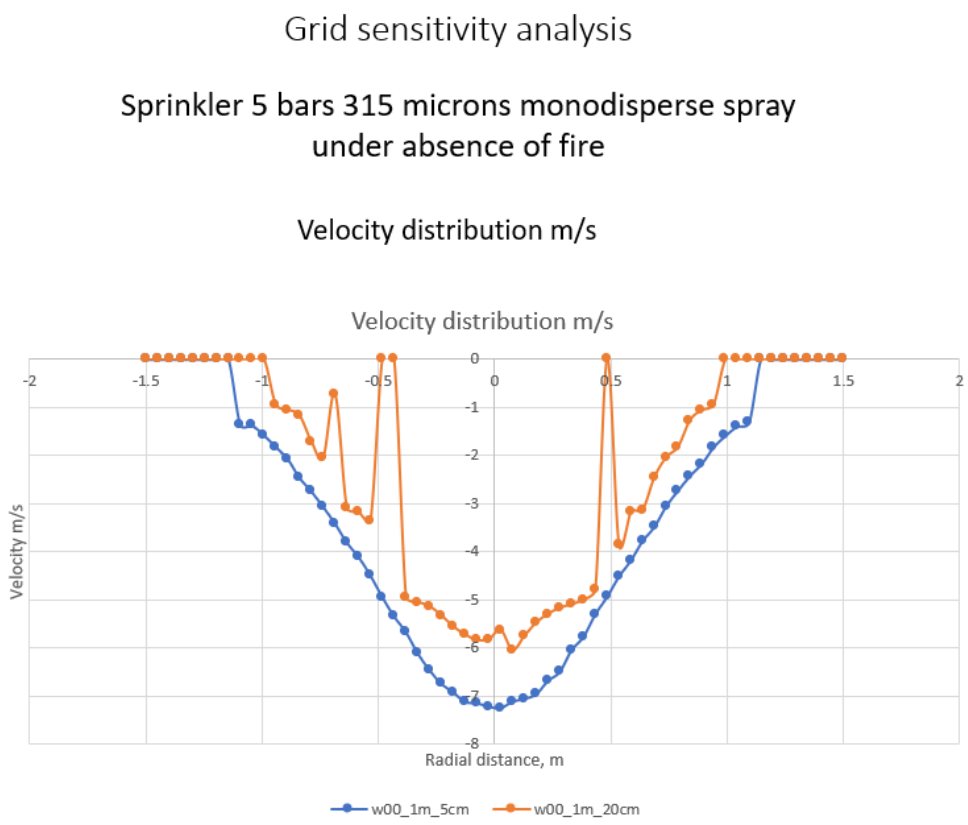

Figure 6.3 Velocity distribution for Sprinkler 5 bar 315μm diameter for monodisperse spray under absence of fire.

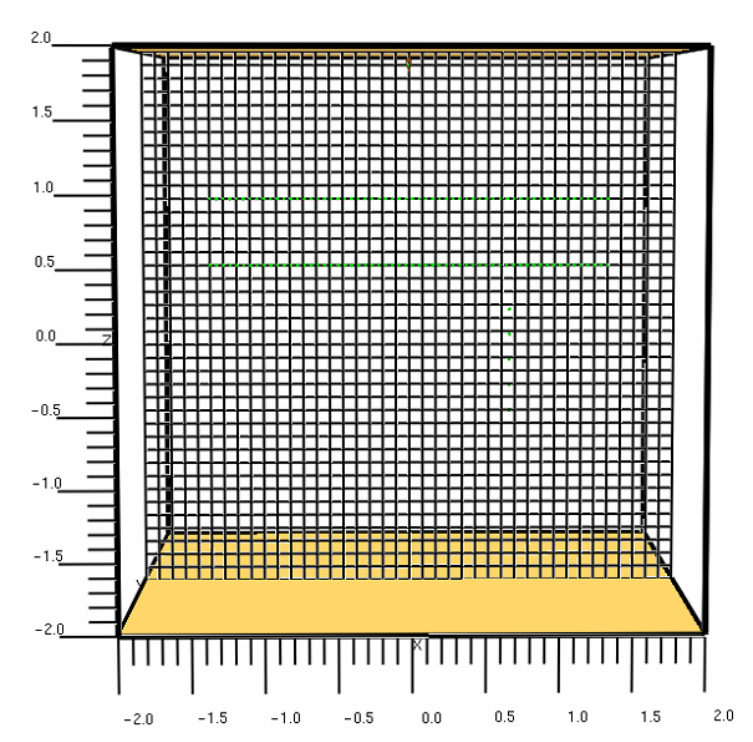

Figure 6.4 Grid sensitivity analysis for 10cm grid size

6.1.2 Scenario 5: Droplet concentration water mist 100 bar, mono vs poly under fire

The results of 100 bar, 10cm grid size have been presented in this sub-chapter. In the previous chapter 20cm grid size, coarse mesh was chosen. While investigating the scenario under the condition of 10cm cells have been resolved. The peak monodisperse is $4E+09$ while for polydisperse is $9E+09$, In general polydisperse spray is always approximately $3-4$ times greater than the monodisperse spray [24]. The radial coverage is less here as the pressure is very high.

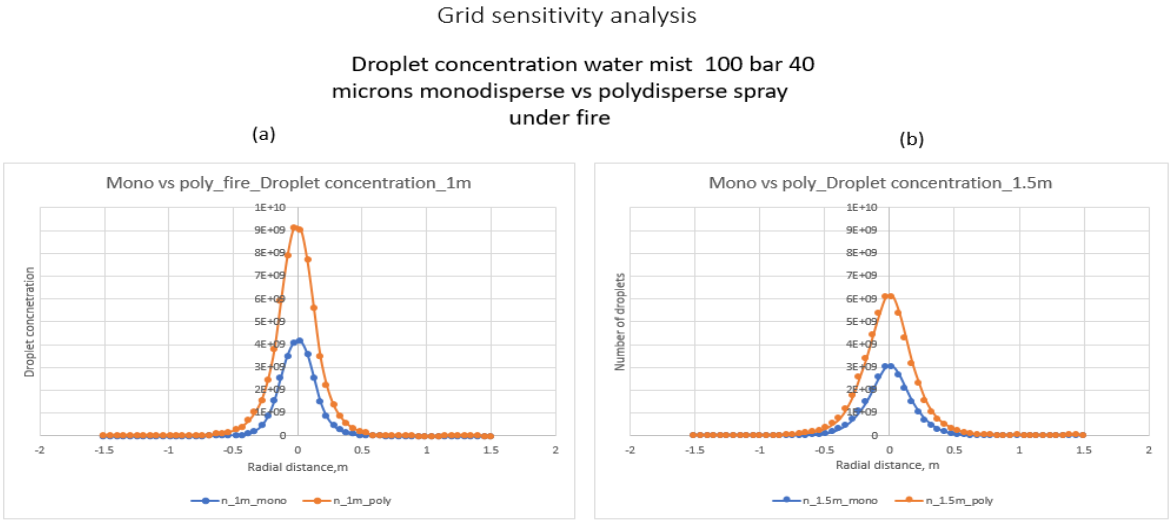

Figure 6.5 Grid sensitivity for monodisperse vs polydisperse at 100 bar 40 microns under fire for droplet concentration

6.1.3 Scenario 5: Droplet size distribution water mist 100 bar, mono vs poly under fire

Droplet size distribution for SMD here the peak is for monodisperse spray is 23 micrometers and for polydisperse spray is 20 micrometers. As the PDPA radius is less which 0.1m was used, and default droplet per second was 5000, 63% of time been recorded on PDPA. Both Figure 6.6 (a) and (b) have been have same type of distribution.

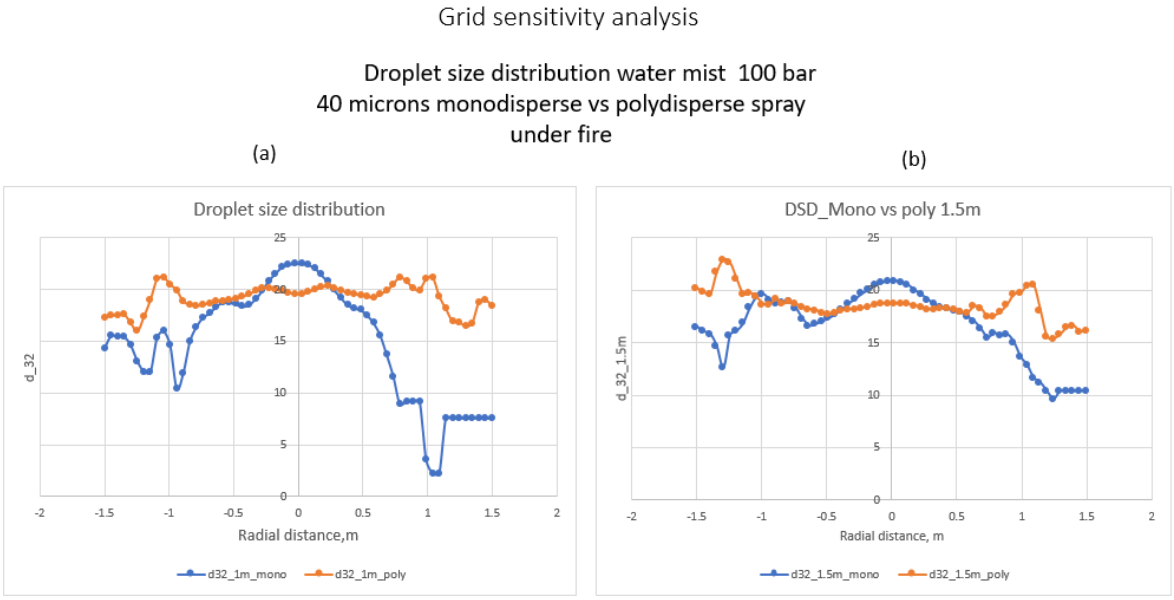

Figure 6.6 Grid sensitivity for monodisperse vs polydisperse at 100 bar 40 microns under fire for droplet size distribution

6.1.4 Scenario 5: Velocity distribution water mist 100 bar, mono vs poly under fire

Upon 100 bars with 40 microns, the peak of velocity is 8 m/s for monodisperse and 7 m/s for polydisperse. Under the presence of fire, the droplet due to high pressure was able to achieve the peak for monodisperse at 1m down the nozzle. Parallelly polydisperse spray, the small droplet tends to lose diameter and gets evaporated with reduction in velocity comparatively, since there is no chance of having 40 microns as a uniformity as per Figure 6.7 (a).

Likewise applying the same concept, the velocity is further reduced while reaching 1.5m down the nozzle as per shown in the Figure 6.7 (b).

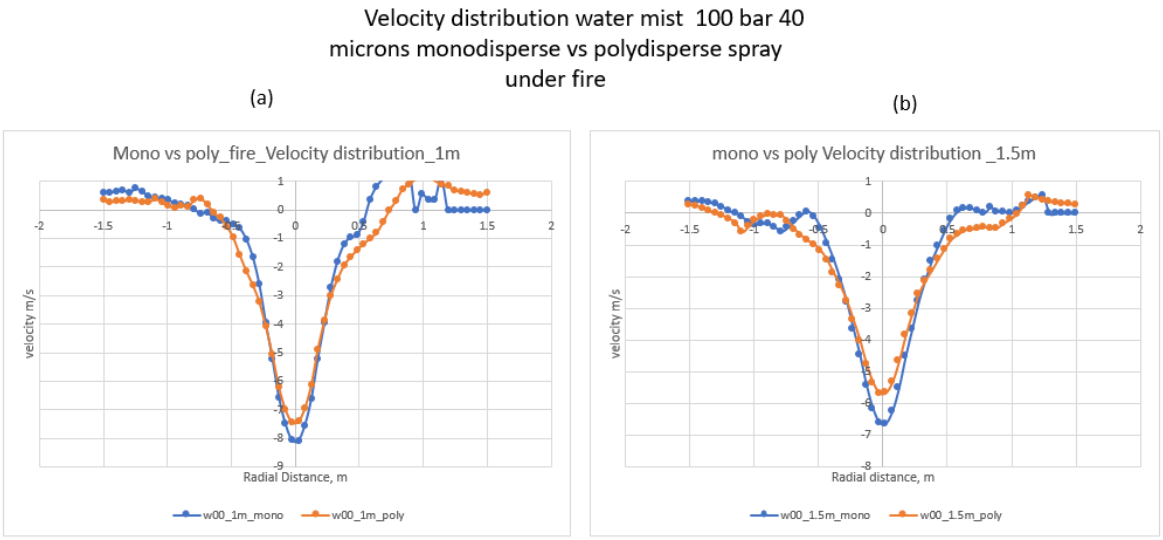

Figure 6.7 Grid sensitivity for monodisperse vs polydisperse at 100 bar 40 microns under fire for velocity distribution

7 Modification in geometry & simulation

Thanks to the FDS forum members, as these results were the output from the advice FDS developers and experienced users. As per the suggestion, the geometry was modified to `&MESH IJK= 60,60,40, XB=-3,3,-3,3,-2,2,` and simulation time were reduced to 100s. `PARTICLES_PER_SECOND =40000` was increased as previous was 5000. Only 2bar pressure was able to run as there weren't enough time to perform 5 and 8 bar.

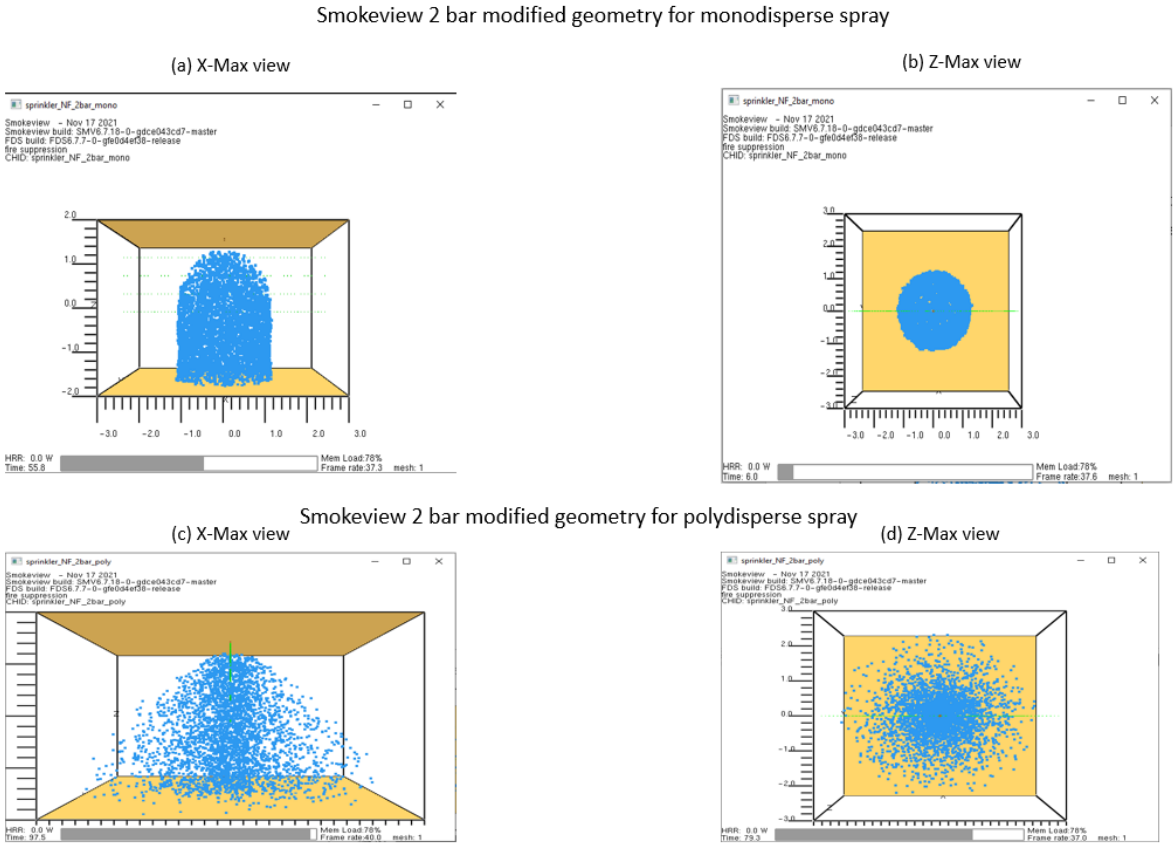

Figure 7.1 Smokeview for monodisperse vs polydisperse spray for 2 bar

Figure 8.1 describes a sample where, it visualizes the user, about the spray pattern for monodisperse and polydisperse spray at θ=55 deg spray angle

7.1.1 Scenario 6: Droplet Number Concentration – 2 bar 419 µm

The droplet number concentration is plotted radially as shown in the Figure 8.2. The size distribution is recorded under without and with fire scenario for monodisperse and polydisperse spray. Under absence of fire scenario, the peak is at -0.5m and +0.5m where it reaches at 2.5E7 and gradually decreases radially at -1m and +1m for polydisperse spray. But in case of monodisperse, the peak is 5E6. Parallelly the same behavior is found at 1.5m down the nozzle. But comparing to monodisperse spray at 1m down the sprinkler, the number concentration seems to be less at 1.5m down the nozzle. `PDPA_RADIUS=0.012` is used here and the PDPA run time is taken as 250 seconds. The radial coverage is comparatively high here as the pressure is 2 bar .

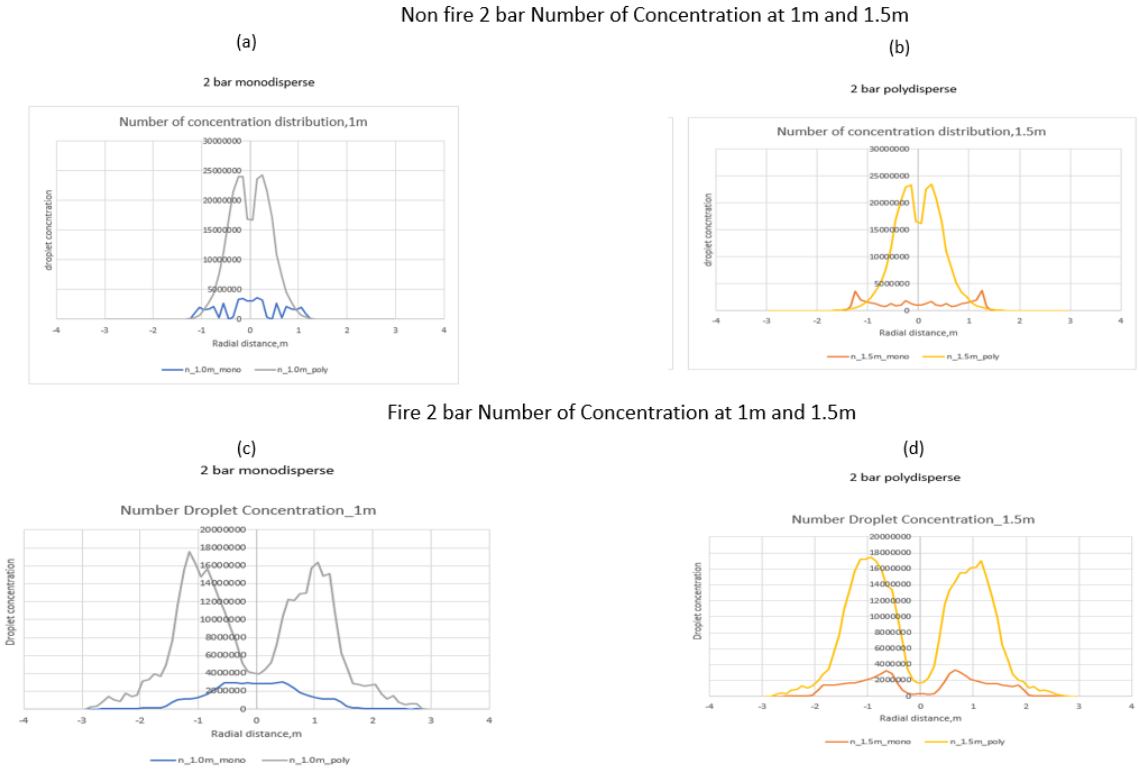

Figure 8.2 Droplet concentration 1m and 1.5m below the nozzle with and without fire

7.1.2 Scenario 6: Droplet Number Concentration – 2 bar 419 µm

The droplet size distribution is represented using SMD in the Figure 8.3 (a), where the measurement is taken 1m and 1.5m down the nozzle for presence and absence of fire. PDPA radius is 12 cm and now it has capacity to record the diameter upon entire volume. The $d_{32} =$ 419 µm is being recorded as constant from -1m to +1m radially for monodisperse spray. And there is a wide distribution in polydisperse spray were the 600 µm is recorded at -1.5m and +1.5m. Parallelly Figure 8.3 (b) records the same for monodisperse spray and the largest diameter is 800 µm at 1.5m down the sprinkler nozzle.

In the fire scenario, the droplets start to agitate against the fire plume in the gas phase and tend to evaporate. The droplet is non-uniform and the there is no constant value for diameter. There is a varying value for monodisperse spray at 1m down the nozzle. And for polydisperse spray, the maximum value is 350 µm at the center and decreases gradually while reaching -2.5 m to +2.5 m radial distance as per show in the Figure 8.3 (c). As shown in the Figure 8.4 (d) at 1.5m down the nozzle, there is slight changes and disturbance in value when comparing to 1m.

7.1.3 Scenario 6: Velocity distribution – 2 bar 419 µm

With non-fire scenario the monodisperse spray has the maximum velocity of 12m/s and 6m/s for monodisperse and polydisperse. The zero value in the plot seems that the cell has not resolved properly or there is no droplet travelling at that point as shown in the Figure 8.4 (a). Parallelly while droplet reaches at 1.5m down the nozzle, and the maximum velocity of the monodisperse is 9 m/s and polydisperse is 5 m/s. Under fire scenario, the velocity is highly reduced, and droplet is traveling upwards. Figure 8.4 (c) shows this behavior and depicts that

monodisperse spray is better than polydisperse spray since it has higher velocity. At 1.5m down the nozzle when recorded, polydisperse seems better than monodisperse as the velocity is higher as shown in the Figure 8.4 (d).

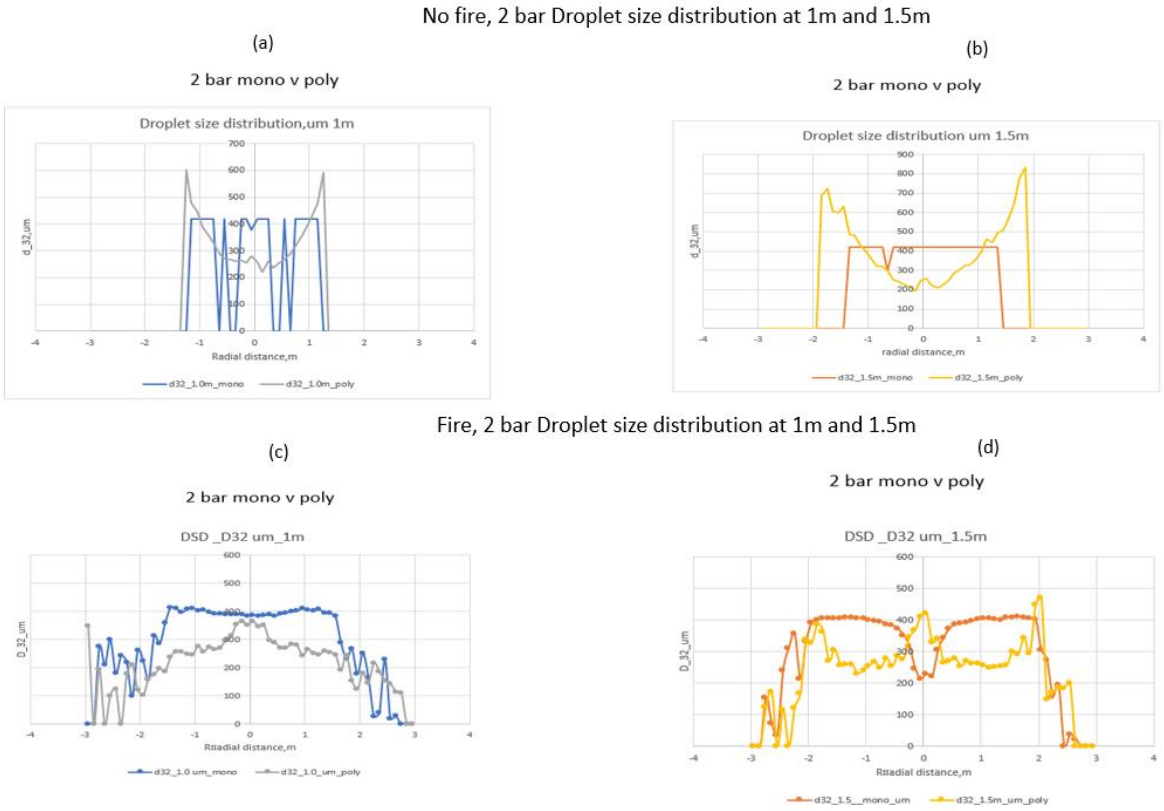

Figure 8.3 Droplet Size Distribution for 1m and 1.5m below the nozzle with and with and without fire

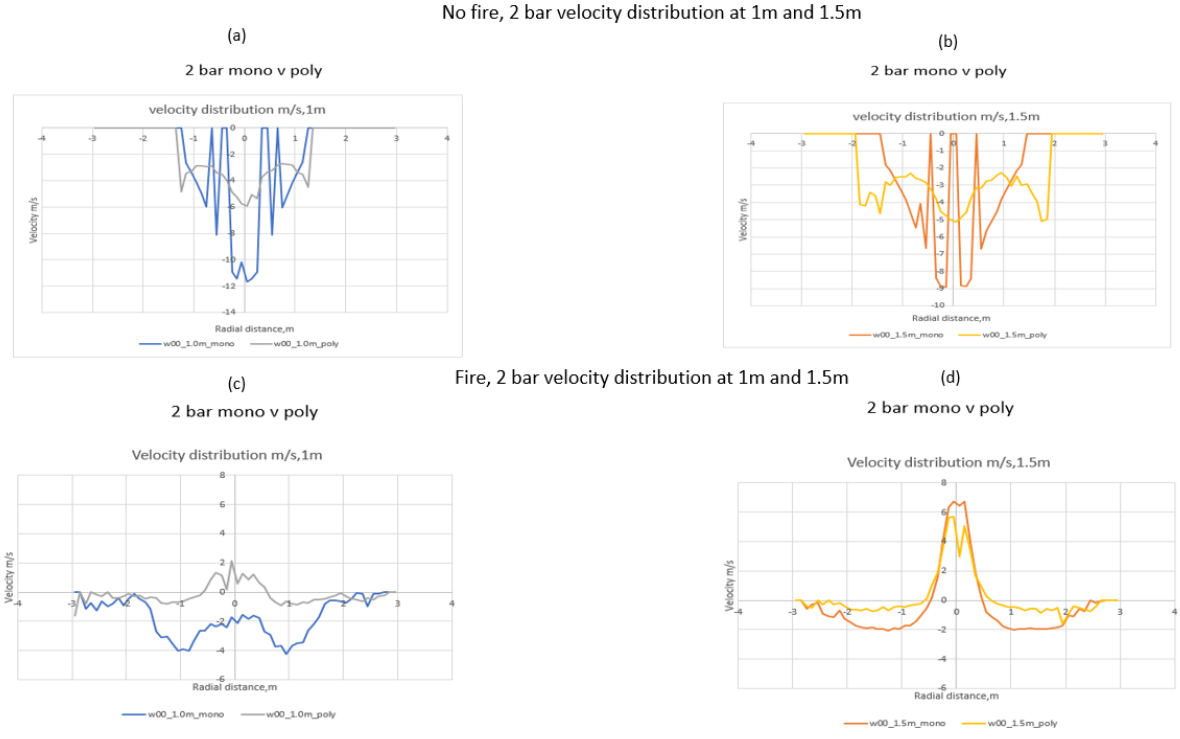

Figure 8.4 Velocity Distribution for 1m and 1.5m below the nozzle with and with and without fire

7.1.4 Cumulative Distribution Function

The CDF can be plotted under the `CHECK_DISTRIBUTION=.TRUE.` in the FDS code for default `GAMMA_D` value 2.4. The Cumulative Number Fraction (CNF) at 0.5 shows the half of the diameter as 210 µm. But Cumulative Volume Fraction (CVF) is 419 µm. Thus Dv,50 is 419 µm as the `DIAMETER` is mentioned in the FDS code. By default, this is Rosin Rammler Lognormal distribution function taken by FDS.

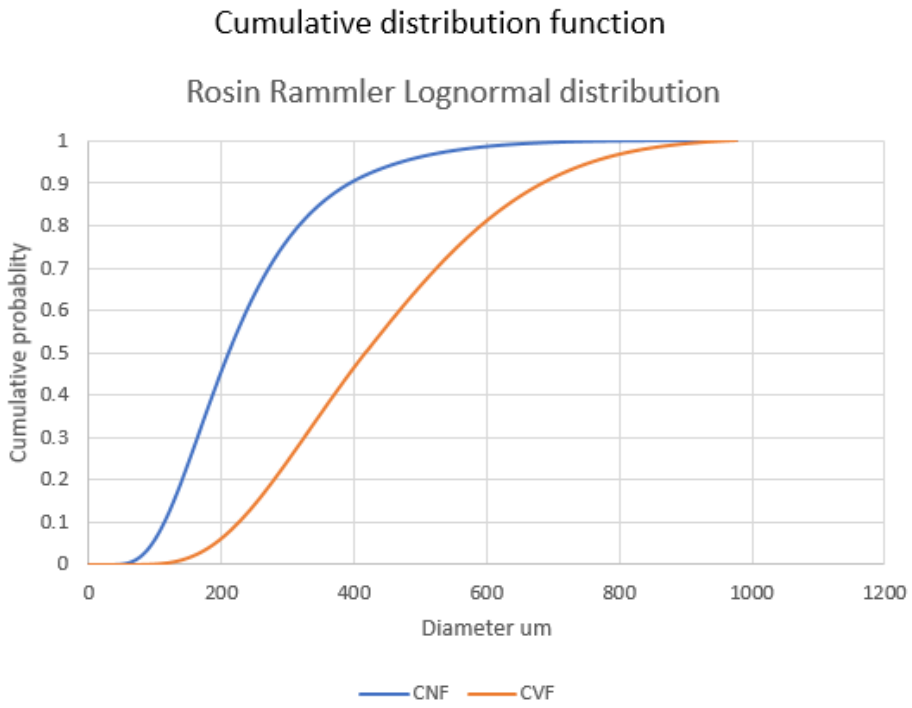

Figure 8.5 Cumulative Distribution Function for default FDS gamma value.

7.1.5 HRR vs Time, MFR & Temperature profile

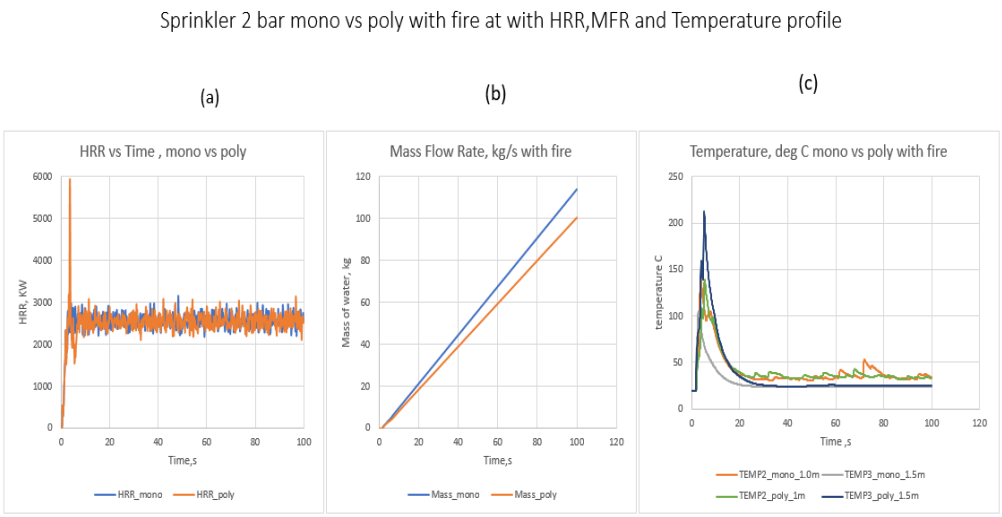

Figure 8.6 (a) Heat release rate vs time (b) Mass Flow Rate of Water (c) Temperature profile at 1m and 1.5m down the nozzle

As per the Figure 8.6 (a) the HRR vs Time is being depicted and here at 5th second, when the fire is ignited, the HRR seems to touch the peak at 6000 KW and gradually comes to the steady variation at the range of 2500 KW - 2900 KW. The Figure 8.6 (b) shows the mass flow rate of the water for polydisperse spray is 116 kg and for monodisperse is 100 kg. Here polydisperse consumes less water than monodisperse under fire scenario. Figure 8.6 (c) shows the temperature profile, where the temperature starts at ambient temperature at 20°C and touches at peak 215°C at 5s for polydisperse spray and drops drastically at 6th second. But monodisperse spray simulation the temperature peaks till 100°C and drops down drastically. Thus, this can conclude that monodisperse spray may suppress the polydisperse spray efficiently.

7.1.6 Scenario 7: 100 bar mist under fire vs fire Number of Concentration distribution

The mist nozzle sprays out the water at 100 bar. Two simulations were run and number of concentrations for 100 bar was recorded under fire and absence of fire scenario. The monodisperse spray at both the heights 1m and 1.5m recorded as same number. But the polydisperse spray simulation has 6E+10 at 1.5m down the nozzle. The number of concentrations, at fire scenario, has less distribution comparatively because the small diameter of 40 microns will evaporate and goes as vapor in the gas phase shown in Figure 8.7. Thus, the concentration of droplets is 2E+10 approximately on both heights.

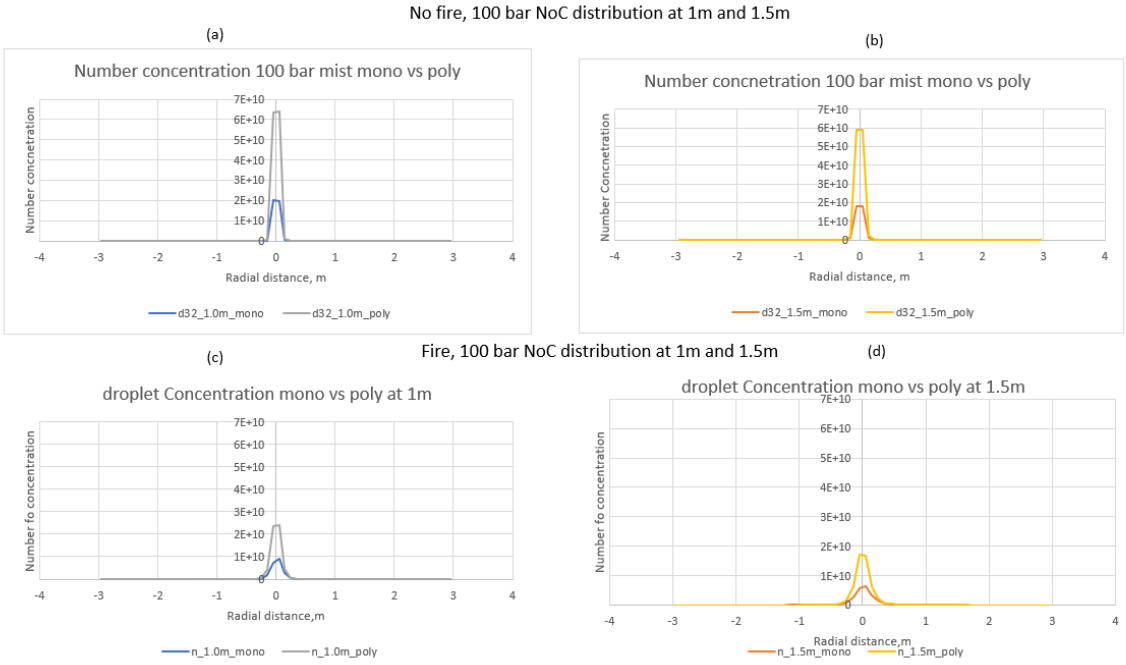

Figure 8.7 Number concentration distribution under at 100 bar with and without fire.

7.1.7 Scenario 7: 100 bar mist under fire vs fire velocity distribution

Figure 8.8 shows the velocity distribution, at 100 bar for fire and non-fire approach. Due to the high pressure, the velocity of the spray is not reduced where it is recorded as approximately as the same at non-fire approach on both the heights. For fire scenario the velocity is increased,

and droplet tend to move upward which opposite to the fire plume which is practically possible. Under this condition FDS predicts monodisperse and polydisperse behaves identical. The velocity distribution for the scenario under fire seems different where, the velocity reaches maximum at 10m/s approx. for both 1m and 1.5m below the nozzle. Since the pressure is high the velocity is not reduced and can penetrate the fire plume.

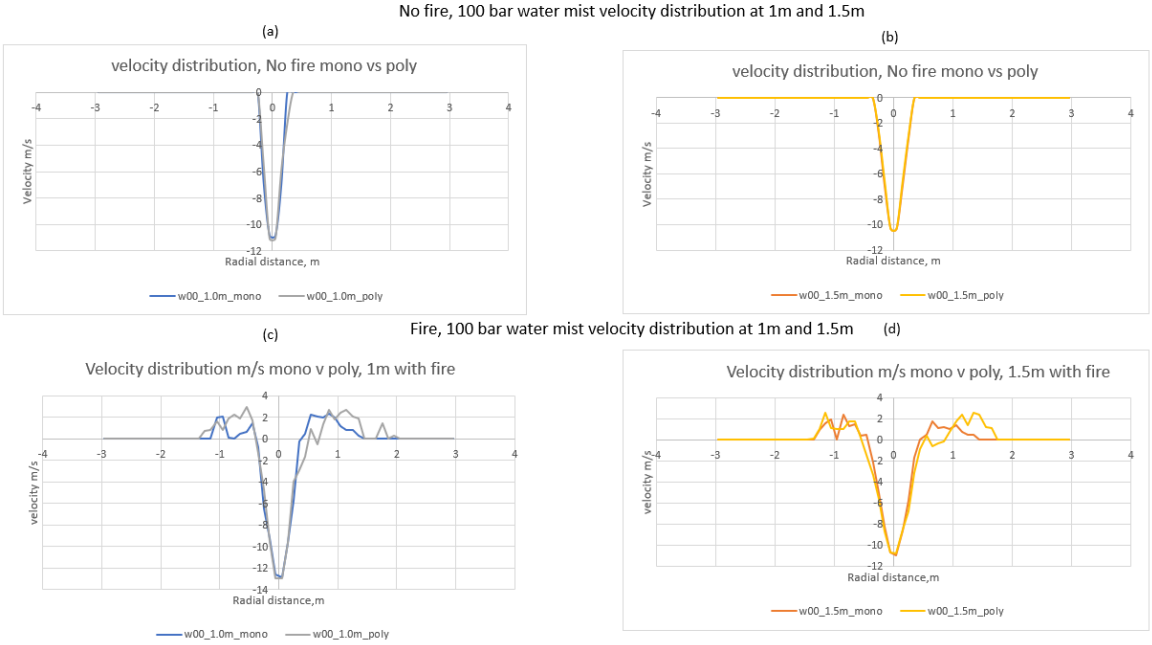

Figure 8.8 Velocity distribution under at 100 bar for water mist with and without fire.

7.1.8 Scenario 7: Droplet size distribution for 100 bar mist under fire vs non-fire

The uniform distribution of droplets size is represented in the Figure 8.9 for fire and non-fire scenario. For monodisperse spray the diameter is 40 microns but polydisperse is 55 microns. The data is identical for the nozzle at 1.5m below the nozzle. For fire scenario, both monodisperse and polydisperse at 1m down the nozzle gives different output as droplet distribution. The droplet shows different sizes as it evaporates due to the fire plume. The maximum diameter is recorded 55 and 45 microns for monodisperse at 1m and 1.5m down the nozzle. For polydisperse spray the droplet size is 35 microns in both the scenario. Hence monodisperse seems to be more effective than polydisperse spray for fire suppression.

The CFD, for the 100 bar, 40 microns with `GAMMA_D = 2.4`. At 0.5 probability distribution, gives 40 microns which proves to be right under this scenario. Figure 8.10 describes the CDF for the mist spray.

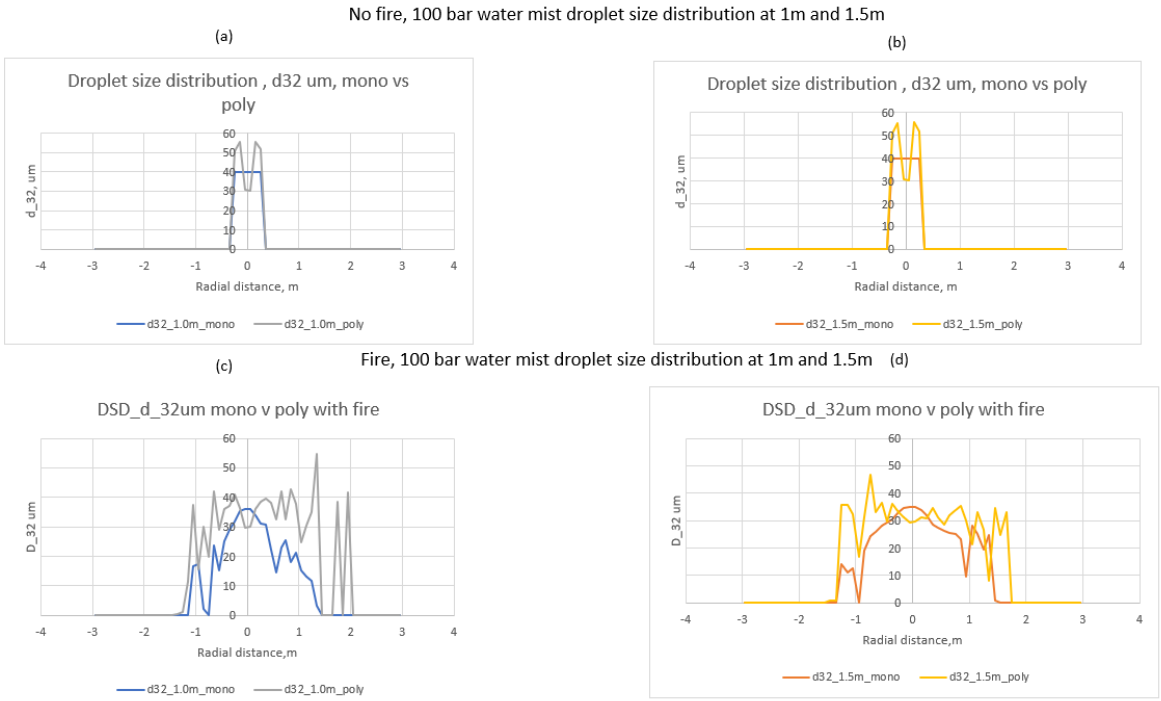

Figure 8.9 Droplet size distribution under at 100 bar for water mist with and without fire.

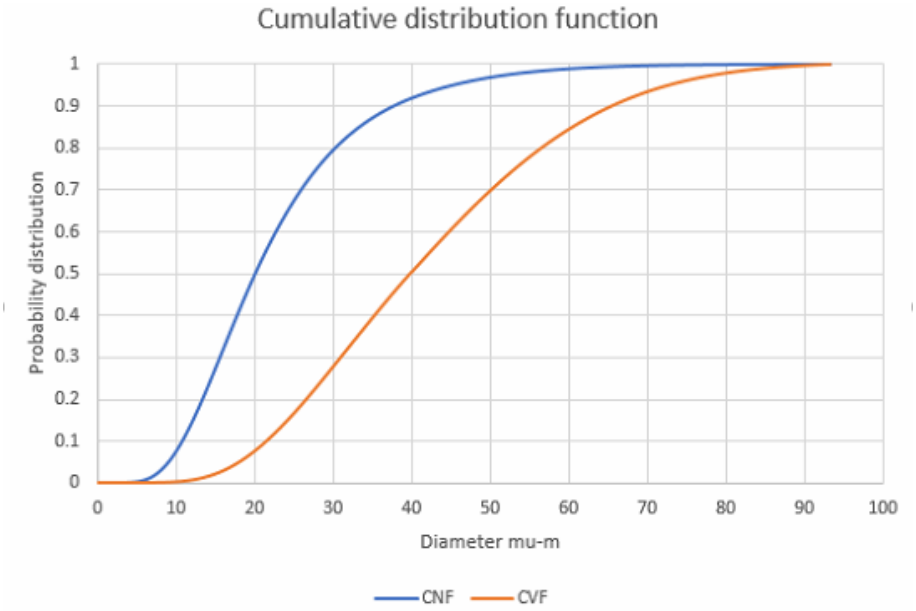

Figure 8.8 Cumulative distribution function for water mist nozzle

Figure 8.11 shows the effect of mist spray over temperature with reference to time. When compared to sprinkler Figure 8.6 (c), the temperature in the water mist domain seems lesser over time when compared to sprinkler. This may be because the high velocity spray may penetrate to the fire plume and suppresses the fire effectively than sprinkler.

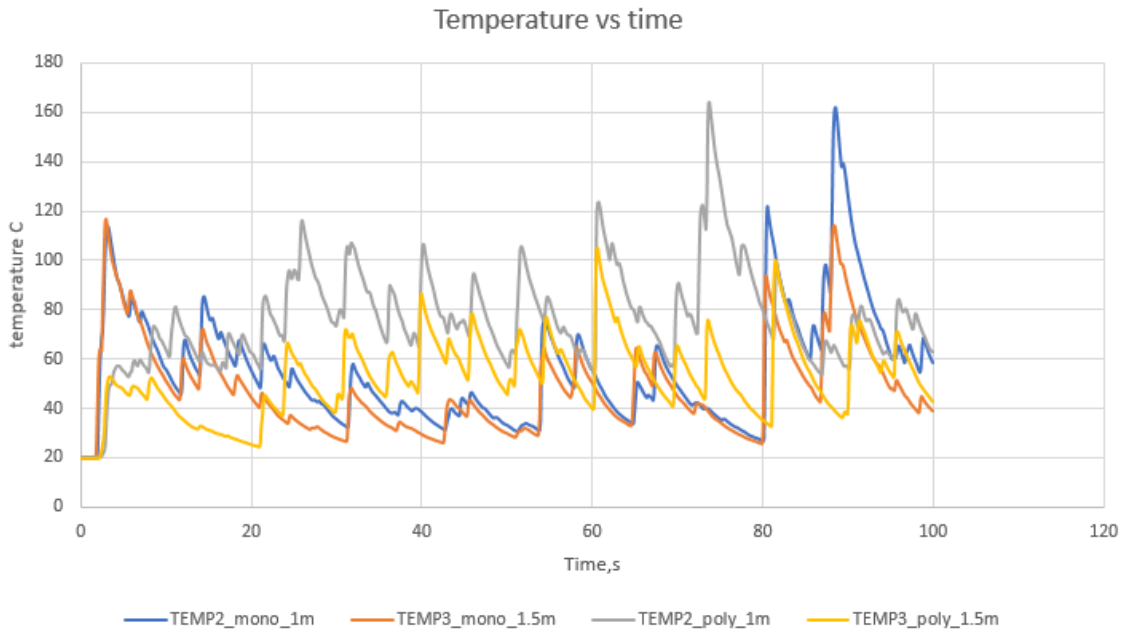

Figure 8.11 Temperature profile for water mist system

8 Conclusion

The motivation of this thesis was to understand the behavior of deluge sprinkler spray and water mist spray under fire and non-fire scenario. Inputs were taken from Lundberg [] [2]for water mist and sprinkler system.

Using the inputs, simulation model files were setup through FDS. The FDS model has PDPA and thermocouple for measuring the suppression parameters. Simulation was run for 300 seconds, and modified geometry was run for 100 seconds. Grid sensitivity analysis was performed. Monodisperse and polydisperse type of behavior was discussed in the results and compared respectively. The measurements were taken at 1m and 1.5m down the nozzle and sprinkler to view the behavior.

Results under different water pressure shows the following effects under fire scenario:

In the chapter, 5.1.2 to 5.1.10 the sprinkler results were discussed under presence and absence of fire for monodisperse and polydisperse spray. The number of droplets, SMD and velocity distribution were discussed for 2 bar, 5 bar and 8 bar respectively. 5.1.11 to 5.1.13 discusses the results from the water mist spray system.

Under 2 bar pressure 419 μm was used to see the behavior, and plots denoted that due to default particles per second and coarse mesh, there were some irregularities in the results. There were convergence and cell resolving issues. The number of concentrations shows less droplets which is 2.5E7 without fire and 0.5E7 at the center with fire. The SMD were identical for monodisperse spray at 1m and 1.5m down the nozzle. But the polydisperse spray has shown its multiple diameters under the range of 300-500 microns approximately. With fire scenario, the droplet diameter shows lesser value due to fire. For velocity profile, the monodisperse spray seems to be travelling in a high velocity without fire and has a negative velocity under fire scenario.

Thus, the same type of behavior seems to be in other two pressures 5 and 8 bar, the radial convergence seems decreased. And velocity of droplets seems increasing at increasing in pressure. But in this thesis diameter of droplet is different for 2,5,8 bar pressure, which can't be compared accurately.

The mist spray has 100 bar which confirms that there is lesser area coverage and high velocity when compared to sprinkler model. Chapter 6 discusses the grid sensitivity analysis which gives a better convergence.

For the modified geometry in Chapter 7, the droplets per seconds were increased and simulation were run for 2 bar, under same conditions, surprisingly the shortcomings were removed upon all the parameters. The droplet size distribution, number of droplets and velocity profiles has good improvement when results were plotted. When seeing the droplet size distribution, its proved that PDPA has captured the 100% of the droplets upon time for both mist and sprinkler scenario.

Thus, for higher coverage, the sprinkler can be used and for higher velocity mist system can be used. It can be said that mist is better than sprinkler or vice-versa but based on application both systems play its vital role.

9 Summary and Future Scope

It is suggested that FDS results can be validated in OpenFoam using fireFoam solver. Grid sensitivity can be performed in all the scenarios to check the accuracy in convergence. Further simulations can be performed in the modified geometry for better results. Only 100 bar and 2 bar mist and sprinkler simulations were performed under fire and non-fire scenario with modified geometry, but other pressure can be considered for simulation. Turbulence phenomena can be analyzed and explained as an expanded work for this thesis. Multiple micronozzles can be considered as a further study as single micro nozzle is being modelled here. Validation with real time experiment can be done as a future scope to compare the simulation and experimental data. Slice files for temperature, W-velocity & MPUV properties can be investigated and explained as a future scope

References

[1] J. Lundberg, “Image-based sizing techniques for fire water droplets,” 2015.

[2] J. Lundberg, “Characterization of a medium velocity deluge nozzle for offshore installations,” *Journal of Loss Prevention in the Process Industries*, vol. 71, p. 104510, Jul. 2021, doi: 10.1016/j.jlp.2021.104510.

[3] C. Fu, P. E. Sojka, and Y. R. Sivathanu, “On The Interaction Between Evaporating Sprays and Heated Surfaces,” p. 6.

[4] T. Wijesekere, “Numerical Modelling of Water Spray Impingement Cooling,” Ghent University, Belgium, 2021.

[5] R. Sijs, S. Kooij, H. J. Holterman, J. van de Zande, and D. Bonn, “Drop size measurement techniques for sprays: Comparison of image analysis, phase Doppler particle analysis, and laser diffraction,” *AIP Advances*, vol. 11, no. 1, p. 015315, Jan. 2021, doi: 10.1063/5.0018667.

[6] A. Opstad Sæbø and R. Wighus, *Droplet sizes from deluge nozzles*. 2009. Accessed: Apr. 01, 2022. [Online]. Available: http://urn.kb.se/resolve?urn=urn:nbn:se:ri:diva-44732

[7] M. Gupta, R. Rajora, S. Sahai, R. Shankar, A. Ray, and S. R. Kale, “Experimental evaluation of fire suppression characteristics of twin fluid water mist system,” *Fire Safety Journal*, vol. 54, pp. 130–142, Nov. 2012, doi: 10.1016/j.firesaf.2012.08.007.

[8] P. E. DesJardin, LA. Gritzo, and S. R. Tieszen, “MODELING THE EFFECT OF WATER SPRAY SUPPRESSION ON LARGE-SCALE POOL FIRES,” *Halon Options Technical Working Conference*, May 2000.

[9] S. C. Kim and H. S. Ryou, “An experimental and numerical study on fire suppression using a water mist in an enclosure,” *Building and Environment*, vol. 38, no. 11, pp. 1309–1316, Nov. 2003, doi: 10.1016/S0360-1323(03)00134-3.

[10] B. P. Husted, “Experimental measurements of water mist systems and implications for modelling i CFD,” Department of Fire Safety Engineering, Lund University, Lund, 2007.

[11] K. B. McGrattan, “Fire dynamics simulator (version 4) :: technical reference guide,” National Institute of Standards and Technology, Gaithersburg, MD, NIST SP 1018, 2006. doi: 10.6028/NIST.SP.1018.

[12] HM Iqbal Mahmud, “Simulation of suppression of fires using water mists,” Thesis (PhD thesis), Victoria University, 2016.

[13] A. Dasgotra, G. Rangarajan, and S. M. Tauseef, “CFD-based study and analysis on the effectiveness of water mist in interacting pool fire suppression,” *Process Safety and Environmental Protection*, vol. 152, pp. 614–629, Aug. 2021, doi: 10.1016/j.psep.2021.06.033.

[14] H. M. I. Mahmud, G. Thorpe, and K. A. M. Moinuddin, “An Approach to Determine the Median Diameter of Droplets in a Water-Mist Spray,” *Applied Sciences*, vol. 12, no. 3, p. 1073, Jan. 2022, doi: 10.3390/app12031073.

[15] H. T. Khoat, J. T. Kim, T. D. Quoc, J. H. Kwark, and H. S. Ryou, “A Numerical Analysis of the Fire Characteristics after Sprinkler Activation in the Compartment Fire,” *Energies*, vol. 13, no. 12, p. 3099, Jun. 2020, doi: 10.3390/en13123099.

[16] Z. Wang, “Optimization of water mist droplet size by using CFD modeling for fire suppressions,” *Journal of Loss Prevention in the Process Industries*, p. 7, 2016.

[17] P. E. Santangelo, N. Ren, P. Tartarini, and A. W. Marshall, “SPRAY CHARACTERIZATION OF HIGH PRESSURE WATER MIST INJECTORS: EXPERIMENTAL AND THEORETICAL ANALYSIS,” p. 8.

[18] Adam Bittern, “Analysis of FDS Predicted Sprinkler Activation Times with Experiments,” Department of Civil Engineering University of Canterbury, Christchurch, New Zealand, Fire Engineering Research Report 04/8, Apr. 2004.

[19] K. McGrattan, S. Hostikka, R. McDermott, J. Floyd, C. Weinschenk, and K. Overholt, “Fire Dynamics Simulator User’s Guide,” *NIST Special Publication*, p. 288.

[20] K. McGrattan, S. Hostikka, R. McDermott, J. Floyd, C. Weinschenk, and K. Overholt, “Fire Dynamics Simulator Technical Reference Guide Volume 3: Validation,” *NIST Special Publication*, vol. 3, p. 746.

[21] B. P. Husted, G. Holmstedt, and T. Hertzberg, “The physics behind water mist systems,” p. 16, 2004.

[22] T. Sikanen, J. Vaari, S. Hostikka, and A. Paajanen, “Modeling and Simulation of High Pressure Water Mist Systems,” *Fire Technol*, vol. 50, no. 3, pp. 483–504, May 2014, doi: 10.1007/s10694-013-0335-8.

[23] Dr.JFloyd, “diameter distribution in monodisperse spray,” May 08, 2022. [Online]. Available: https://groups.google.com/g/fds-smv/c/FS21u7KxqSU

[24] Dr.JFloyd, “number concentration with and without fire at 1m and 1,5m below the nozzle,” May 10, 2022. [Online]. Available: https://groups.google.com/g/fds-smv/c/lwnvO_36MIE

[25] Lundberg J. and , Sikka R., Vaagsaether K. Bjerketvedt D., “Water Mist Characteristics for Explosion Mitigation”.

Appendices

Appendix A: Sprinkler 2 bar with fire monodisperse spray

```
!!! General configuration
*creating the header and title
&HEAD CHID= 'sprinkler_Fire_2bar_mono_fire', TITLE= 'fire suppression'/

!!! Computational domain
*computational domain from Joachim experiment
&MESH  IJK= 60,60,40, XB=-3,3,-3,3,-2,2, / *number of meshes is 20 in all sides

*simulation end time
&TIME  T_END= 100. / *the total simulation time
&RADI RADIATION=F/
&MISC HUMIDITY=100/
*to invoke water vapor (liquid) properties define Species_ID
&SPEC ID ='WATER VAPOR' /

*define device location, orientation and activation delay
&DEVC ID='Spr_1',
  XYZ =0,0,1.9,
  ORIENTATION=0,0,-1,
  PROP_ID ='K-11',
  QUANTITY='TIME',
  SETPOINT =0 /

*defining nozzle properties
*https://components.semcomaritime.com/wp-content/uploads/SemSafe.pdf,
*(offset, k_factor, operating_pressure and droplet_velocity
*from Joachim's experimental reference 2021)
&PROP ID='K-11',
  QUANTITY='SPRINKLER LINK TEMPERATURE',
  PART_ID ='water drops',
  OFFSET =0.30,
  K_FACTOR=58.8,
  OPERATING_PRESSURE =2,
  ORIFICE_DIAMETER=0.0096
  SPRAY_ANGLE =0.,55.,
  PARTICLES_PER_SECOND =40000,
  SPRAY_PATTERN_SHAPE='UNIFORM',
   /*flow rate in L/min

&PART ID='water drops'
  SPEC_ID = 'WATER VAPOR',
  DIAMETER=419,
  MONODISPERSE=.TRUE.,
  CHECK_DISTRIBUTION=.TRUE./

!!!activating fire block
*creating obstruction for the fire
&OBST XB=-0.40,0.40,-0.40,0.40,-1.5,-2.0/

*define fuel, heat of combustion in KJ/kg, soot yield is fraction of fuel converted into
soot.
&REAC ID ='PROPANE',
  SOOT_YIELD =0.01,
  CO_YIELD=0.02,
  HEAT_OF_COMBUSTION =46460,
  CRITICAL_FLAME_TEMPERATURE =1267/

*fire activation through HRRPUA
&SURF ID='fire', HRRPUA = 4000/

```

```
*placing a vent plane for fire
&VENT XB=-0.40,0.40,-0.40,0.40,-1.5,-1.5, SURF_ID='fire',/


!!!declaring geometery
*mesh boundary MB

&VENT MB='XMIN', SURF_ID='OPEN'/*BC open for left
&VENT MB='XMAX', SURF_ID='OPEN'/*BC open for right
&VENT MB='YMIN', SURF_ID='OPEN'/*BC open for front
&VENT MB='YMAX', SURF_ID='OPEN'/*BC open for back

&SLCF PBY=-0.01, QUANTITY='U-VELOCITY',CELL_CENTERED=T/
&SLCF PBY=-0.01, QUANTITY='W-VELOCITY',CELL_CENTERED=T/
&SLCF PBY=-0.01, QUANTITY='PARTICLE FLUX Z', PART_ID = 'water drops',CELL_CENTERED=T /
&SLCF PBY=-0.01,QUANTITY='MASS FRACTION',SPEC_ID='WATER VAPOR',CELL_CENTERED=T /
&SLCF PBY=-0.01,QUANTITY='MPUV', PART_ID='water drops',CELL_CENTERED=T /

&BNDF QUANTITY='AMPUA',PART_ID='water drops'/

&PROP ID='pdpa_n',
      PART_ID='water drops',
      QUANTITY='NUMBER CONCENTRATION',
      PDPA_RADIUS=0.05,
      PDPA_START=5,
      PDPA_END=250.0 /

&PROP ID='pdpa_d32',
      PART_ID='water drops',
      QUANTITY='DIAMETER',
      PDPA_RADIUS=0.012,
      PDPA_START=5,
      PDPA_END=250.0,
      PDPA_M=3,
      PDPA_N=2
      /

&PROP ID='pdpa_w00',
      PART_ID='water drops',
      QUANTITY='W-VELOCITY',
        PDPA_RADIUS=0.012,
        PDPA_START=5,
        PDPA_END=250.0,
        PDPA_M=0,
        PDPA_N=0
       /


 &PROP ID='pdpa_f',
       PART_ID='water drops',
       QUANTITY='PARTICLE FLUX Z',
       PDPA_RADIUS=0.012,
       PDPA_START=5,
       PDPA_END=250.0 /

 !!! activating the thermocouple block
 *adding device thermocouple for measuring the temperature at various points
 &DEVC ID='TEMP1', XYZ=0.8,0.8,1.4, QUANTITY='THERMOCOUPLE' /
 &DEVC ID='TEMP2', XYZ=0.8,0.8,0.9, QUANTITY='THERMOCOUPLE' /
 &DEVC ID='TEMP3', XYZ=0.8,0.8,0.4, QUANTITY='THERMOCOUPLE' /
 &DEVC ID='TEMP4', XYZ=0.8,0.8,-0.1, QUANTITY='THERMOCOUPLE' /


 &DEVC ID='Mass',  XB=-3.0,3.0,-3.0,3.0,-2.0,-2.0, IOR=3, QUANTITY='AMPUA',
PART_ID='water drops', STATISTICS='SURFACE INTEGRAL'  /

 &DEVC XB= -2.95,2.95,0,0, 1.4, 1.4, QUANTITY='PDPA',PROP_ID='pdpa_n'
,POINTS=60,ID='n_0.5m'/
```

```
126.  &DEVC XB= -2.95,2.95,0,0, 0.9, 0.9, QUANTITY='PDPA',PROP_ID='pdpa_n'
    ,POINTS=60,ID='n_1.0m'/
127.  &DEVC XB= -2.95,2.95,0,0, 0.4, 0.4, QUANTITY='PDPA',PROP_ID='pdpa_n'
    ,POINTS=60,ID='n_1.5m'/
128.  &DEVC XB= -2.95,2.95,0,0,-0.1,-0.1, QUANTITY='PDPA',PROP_ID='pdpa_n'
    ,POINTS=60,ID='n_2.0m'/
129.
130.  &DEVC XB= -2.95,2.95,0,0, 1.4, 1.4, QUANTITY='PDPA',PROP_ID='pdpa_d32'
    ,POINTS=60,ID='d32_0.5m'/
131.  &DEVC XB= -2.95,2.95,0,0, 0.9, 0.9, QUANTITY='PDPA',PROP_ID='pdpa_d32'
    ,POINTS=60,ID='d32_1.0m'/
132.  &DEVC XB= -2.95,2.95,0,0, 0.4, 0.4, QUANTITY='PDPA',PROP_ID='pdpa_d32'
    ,POINTS=60,ID='d32_1.5m'/
133.  &DEVC XB= -2.95,2.95,0,0,-0.1,-0.1, QUANTITY='PDPA',PROP_ID='pdpa_d32'
    ,POINTS=60,ID='d32_2.0m'/
134.
135.
136.
137.  &DEVC XB= -2.95,2.95,0,0, 1.4, 1.4, QUANTITY='PDPA',PROP_ID='pdpa_w00'
    ,POINTS=60,ID='w00_0.5m'/
138.  &DEVC XB= -2.95,2.95,0,0, 0.9, 0.9, QUANTITY='PDPA',PROP_ID='pdpa_w00'
    ,POINTS=60,ID='w00_1.0m'/
139.  &DEVC XB= -2.95,2.95,0,0, 0.4, 0.4, QUANTITY='PDPA',PROP_ID='pdpa_w00'
    ,POINTS=60,ID='w00_1.5m'/
140.  &DEVC XB= -2.95,2.95,0,0,-0.1,-0.1, QUANTITY='PDPA',PROP_ID='pdpa_w00'
    ,POINTS=60,ID='w00_2.0m'/
141.
142.
143.
144.  &DEVC XB= -2.95,2.95,0,0, 1.4, 1.4, QUANTITY='PDPA',PROP_ID='pdpa_f'
    ,POINTS=60,ID='f_0.5m'/
145.  &DEVC XB= -2.95,2.95,0,0, 0.9, 0.9, QUANTITY='PDPA',PROP_ID='pdpa_f'
    ,POINTS=60,ID='f_1.0m'/
146.  &DEVC XB= -2.95,2.95,0,0, 0.4, 0.4, QUANTITY='PDPA',PROP_ID='pdpa_f'
    ,POINTS=60,ID='f_1.5m'/
147.  &DEVC XB= -2.95,2.95,0,0,-0.1,-0.1, QUANTITY='PDPA',PROP_ID='pdpa_f'
    ,POINTS=60,ID='f_2.0m'/
148.
149.
150.  *end fds script
151.  &TAIL/
152.
```

Appendix B : Sprinkler 2 bar with fire polydisperse spray

```
!!! General configuration
*creating the header and title
&HEAD CHID= 'sprinkler_Fire_2bar_poly_fire', TITLE= 'fire suppression'/

!!! Computational domain
*computational domain from Joachim experiment
&MESH  IJK= 60,60,40, XB=-3,3,-3,3,-2,2, / *number of meshes is 20 in all sides

*simulation end time
&TIME  T_END= 100. / *the total simulationtime
&RADI RADIATION=F/
&MISC HUMIDITY=100/
*to invoke water vapor (liquid) properties define Species_ID
&SPEC ID ='WATER VAPOR' /

*define device location, orientation and activation delay
&DEVC ID='Spr_1',
  XYZ =0,0,1.9,
  ORIENTATION=0,0,-1,
  PROP_ID ='K-11',
  QUANTITY='TIME',
  SETPOINT =0 /

*defining nozzle properties
*https://components.semcomaritime.com/wp-content/uploads/SemSafe.pdf,
*(offset, k_factor, operating_pressure and droplet_velocity
*from Joachim's experimental reference 2021)
&PROP ID='K-11',
  QUANTITY='SPRINKLER LINK TEMPERATURE',
  PART_ID ='water drops',
  OFFSET =0.30,
  K_FACTOR=58.8,
  OPERATING_PRESSURE =2,
  ORIFICE_DIAMETER=0.0096
  SPRAY_ANGLE =0.,55.,
  PARTICLES_PER_SECOND =40000,
  SPRAY_PATTERN_SHAPE='UNIFORM',
   /*flow rate in L/min

&PART ID='water drops'
  SPEC_ID = 'WATER VAPOR',
  DIAMETER=419,
  GAMMA_D=2.4,
  CHECK_DISTRIBUTION=.TRUE./

!!!activating fire block
*creating obstruction for the fire
&OBST XB=-0.40,0.40,-0.40,0.40,-1.5,-2.0/

*define fuel, heat of combustion in KJ/kg, soot yield is fraction of fuel converted into
soot.
&REAC ID ='PROPANE',
  SOOT_YIELD =0.01,
  CO_YIELD=0.02,
  HEAT_OF_COMBUSTION =46460,
  CRITICAL_FLAME_TEMPERATURE =1267/

*fire activation through HRRPUA
&SURF ID='fire', HRRPUA = 4000/

*placing a vent plane for fire
&VENT XB=-0.40,0.40,-0.40,0.40,-1.5,-1.5, SURF_ID='fire',/


!!!declaring geometery
*mesh boundary MB
```

```
66.
67. &VENT MB='XMIN', SURF_ID='OPEN'/*BC open for left
68. &VENT MB='XMAX', SURF_ID='OPEN'/*BC open for right
69. &VENT MB='YMIN', SURF_ID='OPEN'/*BC open for front
70. &VENT MB='YMAX', SURF_ID='OPEN'/*BC open for back
71.
72. &SLCF PBY=-0.01, QUANTITY='U-VELOCITY',CELL_CENTERED=T/
73. &SLCF PBY=-0.01, QUANTITY='W-VELOCITY',CELL_CENTERED=T/
74. &SLCF PBY=-0.01, QUANTITY='PARTICLE FLUX Z', PART_ID = 'water drops',CELL_CENTERED=T /
75. &SLCF PBY=-0.01,QUANTITY='MASS FRACTION',SPEC_ID='WATER VAPOR',CELL_CENTERED=T /
76. &SLCF PBY=-0.01,QUANTITY='MPUV', PART_ID='water drops',CELL_CENTERED=T /
77.
78. &BNDF QUANTITY='AMPUA',PART_ID='water drops'/
79.
80. &PROP ID='pdpa_n',
81.       PART_ID='water drops',
82.       QUANTITY='NUMBER CONCENTRATION',
83.       PDPA_RADIUS=0.05,
84.       PDPA_START=5,
85.       PDPA_END=250.0 /
86.
87. &PROP ID='pdpa_d32',
88.       PART_ID='water drops',
89.       QUANTITY='DIAMETER',
90.       PDPA_RADIUS=0.012,
91.       PDPA_START=5,
92.       PDPA_END=250.0,
93.       PDPA_M=3,
94.       PDPA_N=2
95.       /
96.
97. &PROP ID='pdpa_w00',
98.       PART_ID='water drops',
99.       QUANTITY='W-VELOCITY',
100.        PDPA_RADIUS=0.012,
101.        PDPA_START=5,
102.        PDPA_END=250.0,
103.        PDPA_M=0,
104.        PDPA_N=0
105.       /
106.
107.
108.  &PROP ID='pdpa_f',
109.        PART_ID='water drops',
110.        QUANTITY='PARTICLE FLUX Z',
111.        PDPA_RADIUS=0.012,
112.        PDPA_START=5,
113.        PDPA_END=250.0 /
114.
115.  !!! activating the thermocouple block
116.  *adding device thermocouple for measuring the temperature at various points
117.  &DEVC ID='TEMP1', XYZ=0.8,0.8,1.4, QUANTITY='THERMOCOUPLE' /
118.  &DEVC ID='TEMP2', XYZ=0.8,0.8,0.9, QUANTITY='THERMOCOUPLE' /
119.  &DEVC ID='TEMP3', XYZ=0.8,0.8,0.4, QUANTITY='THERMOCOUPLE' /
120.  &DEVC ID='TEMP4', XYZ=0.8,0.8,-0.1, QUANTITY='THERMOCOUPLE' /
121.
122.
123.  &DEVC ID='Mass',  XB=-3.0,3.0,-3.0,3.0,-2.0,-2.0, IOR=3, QUANTITY='AMPUA',
    PART_ID='water drops', STATISTICS='SURFACE INTEGRAL'  /
124.
125.  &DEVC XB= -2.95,2.95,0,0, 1.4, 1.4, QUANTITY='PDPA',PROP_ID='pdpa_n'
    ,POINTS=60,ID='n_0.5m'/
126.  &DEVC XB= -2.95,2.95,0,0, 0.9, 0.9, QUANTITY='PDPA',PROP_ID='pdpa_n'
    ,POINTS=60,ID='n_1.0m'/
127.  &DEVC XB= -2.95,2.95,0,0, 0.4, 0.4, QUANTITY='PDPA',PROP_ID='pdpa_n'
    ,POINTS=60,ID='n_1.5m'/
128.  &DEVC XB= -2.95,2.95,0,0,-0.1,-0.1, QUANTITY='PDPA',PROP_ID='pdpa_n'
    ,POINTS=60,ID='n_2.0m'/
129.
```

```
130.  &DEVC XB= -2.95,2.95,0,0, 1.4, 1.4, QUANTITY='PDPA',PROP_ID='pdpa_d32'
    ,POINTS=60,ID='d32_0.5m'/
131.  &DEVC XB= -2.95,2.95,0,0, 0.9, 0.9, QUANTITY='PDPA',PROP_ID='pdpa_d32'
    ,POINTS=60,ID='d32_1.0m'/
132.  &DEVC XB= -2.95,2.95,0,0, 0.4, 0.4, QUANTITY='PDPA',PROP_ID='pdpa_d32'
    ,POINTS=60,ID='d32_1.5m'/
133.  &DEVC XB= -2.95,2.95,0,0,-0.1,-0.1, QUANTITY='PDPA',PROP_ID='pdpa_d32'
    ,POINTS=60,ID='d32_2.0m'/
134.
135.
136.
137.  &DEVC XB= -2.95,2.95,0,0, 1.4, 1.4, QUANTITY='PDPA',PROP_ID='pdpa_w00'
    ,POINTS=60,ID='w00_0.5m'/
138.  &DEVC XB= -2.95,2.95,0,0, 0.9, 0.9, QUANTITY='PDPA',PROP_ID='pdpa_w00'
    ,POINTS=60,ID='w00_1.0m'/
139.  &DEVC XB= -2.95,2.95,0,0, 0.4, 0.4, QUANTITY='PDPA',PROP_ID='pdpa_w00'
    ,POINTS=60,ID='w00_1.5m'/
140.  &DEVC XB= -2.95,2.95,0,0,-0.1,-0.1, QUANTITY='PDPA',PROP_ID='pdpa_w00'
    ,POINTS=60,ID='w00_2.0m'/
141.
142.
143.
144.  &DEVC XB= -2.95,2.95,0,0, 1.4, 1.4, QUANTITY='PDPA',PROP_ID='pdpa_f'
    ,POINTS=60,ID='f_0.5m'/
145.  &DEVC XB= -2.95,2.95,0,0, 0.9, 0.9, QUANTITY='PDPA',PROP_ID='pdpa_f'
    ,POINTS=60,ID='f_1.0m'/
146.  &DEVC XB= -2.95,2.95,0,0, 0.4, 0.4, QUANTITY='PDPA',PROP_ID='pdpa_f'
    ,POINTS=60,ID='f_1.5m'/
147.  &DEVC XB= -2.95,2.95,0,0,-0.1,-0.1, QUANTITY='PDPA',PROP_ID='pdpa_f'
    ,POINTS=60,ID='f_2.0m'/
148.
149.
150.
151.  *end fds script
152.  &TAIL/
153.
```